905

GENERAL EVALUATION OF CURRENT CONCRETE PAVEMENT PERFORMANCE IN MICHIGAN

JOINTED CONCRETE PAVEMENT DETERIORATION CONSIDERED AS A PROBABILITY PROCESS

MICHIGAN DEPARTMENT OF STATE HIGHWAYS

GENERAL EVALUATION OF CURRENT CONCRETE PAVEMENT PERFORMANCE IN MICHIGAN

JOINTED CONCRETE PAVEMENT DETERIORATION CONSIDERED AS A PROBABILITY PROCESS

L. F. Holbrook
Wen-Hou Kuo

Final Report on a Highway Planning and Research
Investigation conducted in cooperation with the
U.S. Department of Transportation, Federal Highway Administration

Research Laboratory Section
Testing and Research Division
Research Project 69 F-110
Research Report No. R-905

Michigan State Highway and Transportation Commission
E. V. Erickson, Chairman; Charles H. Hewitt,
Vice-Chairman, Carl V. Pellonpaa, Peter B. Fletcher
John P. Woodford, Director
Lansing, March 1974

-DEDICATION-

This report is dedicated to the memory of Ms. Virginia M. Seely, whose fastidious workmanship contributed substantially to these investigations.

ABSTRACT

A large variety of techniques were used to measure and predict jointed concrete pavement structural performance for 128 projects with up to 15 years of performance history. Factor analysis, a statistical method designed to group correlated performance variables such as spalls, cracks, corner breaks, etc., into a smaller number of clusters thereby simplifying analysis, reduced 19 field survey performance variables to 14. This reduction was not considered sufficient to warrant further analysis with causal variables, nor to provide a generalized measure of pavement performance. Thus, the expectation that survey variables could be combined into one or two indices of performance was abandoned. The reason for the failure of factor analysis is that projects subject to some kind of deterioration, such as corner breaks or centerline spalls, may not be as subject to other kinds of deterioration, such as transverse cracks or blowups. While there is frequently correlation between these variables, it is not extensive enough to warrant the general performance index approach.

As a consequence of these findings, it was decided to explore pavement performance with selected performance variables found to have a high frequency of occurrence in the pavement condition surveys. Transverse cracking was chosen as the subject of five pilot performance models which were designed to predict crack incidence probability for any point in time up to 15 years of service. Eight traffic and passing lanes (four projects) for which historical roadway traffic counts were available were examined, with average daily traffic count providing the only input to differentiate lane cracking performance. The Markov chain approach gave the best correlations with field data and thus was generalized into a form suitable not only for transverse cracking, but joint performance as well. This generalization took the form of a theoretical development solving systems of partial differential equations.

Mathematical models developed from Markov chain assumptions were then fitted to actual field transverse crack and joint deterioration data from 43 postwar jointed concrete construction projects for which 5, 10, and 15-year condition surveys were available. In most cases, the models' fit were excellent; suggesting that they could be used for prediction of future pavement condition.

Because blowups are a serious hazard and maintenance problem, this state of joint deterioration was singled out for special analysis. In particular, 5 and 10-year survey data, together with crude information on coarse aggregate composition, were used to predict future blowup occurrence.

Since the projects selected had 15-year surveys, the prediction could be compared with what actually occurred. These comparisons showed generally good agreement between actual and predicted experience, although it was not always clear from the surveys if a patched or reconstructed joint had in fact experienced a blowup. It was concluded, nonetheless, that probability modeling could be used to identify projects that will have serious joint problems by 15 years, even though few joints have been replaced or patched by the time of the 10-year condition survey.

Not all 128 projects were modeled with these techniques since only 43 had the 15-year service history considered necessary for good performance modeling. The remaining projects did have 5 and 10-year field surveys which provided a basis for evaluation, if not prediction. These performance evaluations, together with similar evaluations of the other 43 projects, provided sufficient data to satisfy most of the proposal's objectives. In particular, it was found that joint performance of Michigan's highways has not changed significantly from the 1946 through 1961 construction years. While there has been differences between years, there has been no substantial trend towards better or poorer performance even though later projects have experienced greater traffic volumes and salting.

Of the materials, environment, and construction variables available for analysis, only the coarse aggregate source seemed to have a significant bearing on joint performance. Projects constructed with either essentially carbonate-free aggregates (0 to 10 percent CO_3) or high carbonate gravels (80 to 100 percent CO_3) performed considerably better than all other aggregates. All other aggregates (100 percent pure crushed limestone and the other gravel-carbonate mixes) gave both good and poor performance. No geographical or usage variable, such as traffic volume, could be found to explain the extremely large performance variances for these materials. One thing is clear, however; joint performance of projects built with either carbonate-free or carbonate-rich gravels is uniformly good in Michigan -- at least up to 15 years of service life.

No variable other than traffic volume could be found to explain differences in transverse cracking between projects. Original soil conditions were examined and classified into five categories of base quality. Absolutely no correlation could be found between these soil ratings and cracking rate. The implication is that soil importation and compaction procedures are capable of rectifing original soil deficiencies.

CONTENTS

PREFACE

This report is addressed to two kinds of reader: the applied statistician or engineer who has a special interest in the methods of modeling jointed concrete pavement deterioration from either a random process or a general index point of view; and the manager who is interested in knowing if pavement performance can be predicted and if so, from what causal variables. The first individual is directed to Sections I, III, and IV. These sections detail a kind of research history as assumptions and techniques evolved. Some of the problems the applied statistician meets come out in full relief in these sections. For example, all quantitative models require assumptions; however, one frequently does not know which ones to make, e.g., is future slab cracking independent of prior cracking? Moreover, one often has several alternative methods of analysis at his disposal. Which of these, in the absence of trials with actual data, will provide the most accurate and far reaching results? Finally, data -- especially routine field data -- are frequently not collected with precise investigatory analysis in mind. The purposes for which these data are collected range from special non-scientific interests, to general information as input to management policy. Furthermore, more extensive or precise data, as in the cases of aggregate composition and traffic volumes, would be too costly for these purposes. The result, from a post hoc research perspective, is that these relatively low grade data not only make the detection of underlying relationships difficult, but compromise the predictive value of models exploiting these relationships.

The second individual, who is concerned with using research results for decision purposes, will be most interested in Section II and some parts of V and VI. While there is technical material in some of these sections, this can be bypassed so that full attention can be focused on results. In particular, it is shown in Section V that early joint performance history can be used to predict later deterioration, such as blowups, with a suprising degree of accuracy. It is shown in Section VI that the likelihood of transverse cracking is related to the accumulated crack count, and that each construction project reaches its own critical crack-per-slab number for which additional cracking is most likely. The extent to which past, present, and future performance can be modeled with a minimum of parameters is illustrated by graphs in these sections and in the Appendix. These graphs should be of particular value to managers interested in the extent to which maintenance problems can be anticipated.

In Section II the original objectives of the study are discussed. These were:

1. To determine if concrete pavements constructed between 1954 and 1964 are performing as well or better than those constructed in the previous period of 1946 through 1953.

2. To determine the effect of changes in design and construction on performance. These include the substitution of sawing for a preformed bituminous strip for forming the plane-of-weakness for centerline joints, the reduction in joint spacing from 99 ft to 71 ft 2 in., and the joint performance differences resulting from the use of hot-pour rubber-asphalt, two-component cold pours, and preformed neoprene joint seals.

3. To extend the previous study of the causal effect of commercial traffic and the quality of the coarse aggregate (soft, non-durable content) on pavement performance.

With regard to these objectives, the data and measurement techniques of this study support the following conclusions:

1. The joint performance of projects constructed between 1954 and 1961 is slightly better than that of those constructed between 1946 and 1953. The difference is not, however, considered statistically significant.

2. The construction changes referred to in Objective 2 did not affect enough projects for which condition surveys were available. Most changes occurred in the '60's, hence there was not enough performance history available at the time of analysis to adequately explore these variables. It was found after considerable experience with survey data that at least 10, and preferably 15, years of service are necessary to differentiate project joint performance.

3. An earlier study (MDSHT Research Report R-711) found that both traffic and coarse aggregate affected general performance as defined by that study. The additional projects available for the present study bear out the connection of aggregate source with performance and, to some extent, traffic volume. They show that low carbonate gravels and high carbonate gravels never produced poor joint performance. However, carbonate-gravel mixtures in more-or-less equal proportions produced both good and poor joint performance. In Report R-711 it was assumed that percent deleterious, in particular percent of soft, non-durable particles, in these gravel-carbonate mixes was responsible for the generally below average performance of pro-

jects built with these aggregates. This relationship was not maintained with the larger data set of the present study. This may be due to imperfect data (only a very small sample is tested for deleterious materials) or it may be that percent soft, non-durables is not related to our particular measure of joint performance.

Also of interest is the variable performance of the pure crushed limestones. While high carbonate gravels in our sample never performed poorly, crushed limestones behaved about like the gravel-carbonate mixes: some delivered excellent performance, others very poor. No environmental or usage cause could be found to explain these differences.

In Report R-711 traffic appeared to be a factor in general performance. However, the larger data set herein examined supports this conclusion only on a traffic-passing lane comparison basis even though low traffic projects perform slightly better than high traffic projects on the average. Moreover, the major performance difference is realized only in transverse cracking, not joint performance. It may be that joint performance is not seriously affected by differences in traffic volumes, or that our ADT figures are not sufficiently accurate to detect these differences.

INTRODUCTION

The work described in this report is the result of a research program carried out by the Research Laboratory of the Michigan Department of State Highways and Transportation in cooperation with the Federal Highway Administration. The contents of this report reflect the views of the authors who are responsible for the facts and the accuracy of the data presented herein. The contents do not necessarily reflect the official views or policies of the Federal Highway Administration. This report does not constitute a standard, specification, or regulation.

This research project was conceived as a two fold program; to confirm, if possible, the findings of previous research (1), and to explore methods of modeling jointed concrete pavement deterioration so that future condition could be predicted. Confirmation of previous findings would take the form of a successful reduction of 19 condition survey variables to a general performance index. If this were possible, one could speak unambiguously of a project's condition and use this measure as a dependent variable in the search for causes of deterioration.

The factor analysis techniques provide methods of reducing a large set of variables to a smaller more manageable set which, in turn, can be used to generate a general condition index. Earlier research (1) suggested that correlations among survey variables were high enough to warrant the factor analytic approach. The present study continues this inquiry with additional data that became available through Michigan's on-going condition survey program.

The second purpose -- to find a successful modeling technique so that deterioration can be estimated over time -- depends on the results of the performance index investigation. If a satisfactory performance index could be found, then there are a number of methods available which might model the performance index as a time process. If a general performance index could not be found, performance could still be modeled as a time process but it would have to be the performance of a selected survey variable such as transverse cracking. Hence a time process model would apply only to one aspect of deterioration, leaving the other aspects to be ignored or modeled separately. What one would probably do in this case is to select several important survey variables and develop a time process model for each one.

Once either a general performance index or selected survey variables have been modeled, it should then be possible to search for environmental or construction variables that correlate with the model's parameters. This search is facilitated if there is only a single model (i.e., a general performance index has been found) and if the time process model has few parameters (Fig. 1). A large number of fitting parameters tend to be intercorrelated, and compensate for one another in statistical estimation procedures. This, in general, relaxes relationships with causal independent variables. For this reason, it will be the intent of the present study to develop time process models with the smallest number of parameters consistent with a good fit to field data.

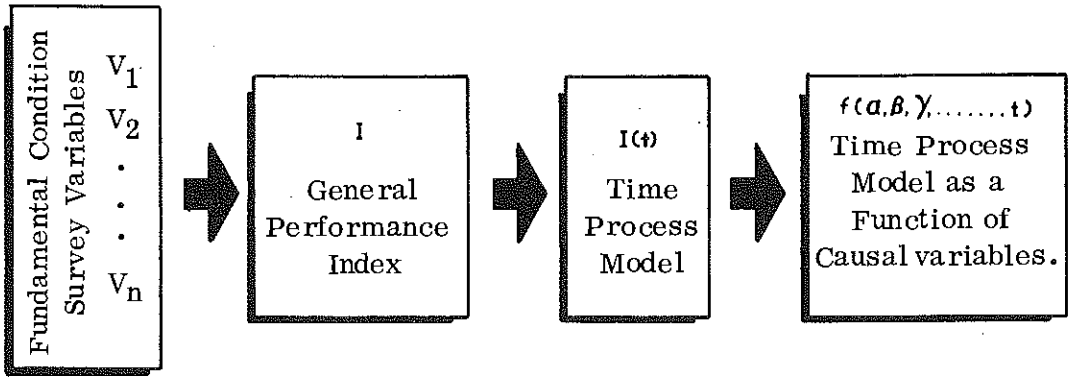

Figure 1. Ideal Pavement Performance Modeling Procedure.

I

THE FACTOR ANALYSIS APPROACH TO A GENERAL PERFORMANCE INDEX

Each of three observations (at 5, 10, and 15 years) on the 19 survey variables (Fig. 2) was entered as a basic variable so that a correlation matrix of 3 x 19 = 57 variables, each with 47 observations from 47 construction projects, could be formed. Generally, the between-year intercorrelations for each variable were very high: 0.60 to 0.90. However, three variables (blowups, resurfacing, and mudjacking) did not show this pattern. This is not surprising since blowups do not occur at 5 years, and rarely at 10, and resurfacing follows the same pattern. Moreover, mudjacking is used to correct for roadbed settlement, usually occurring early in the pavement's service life.

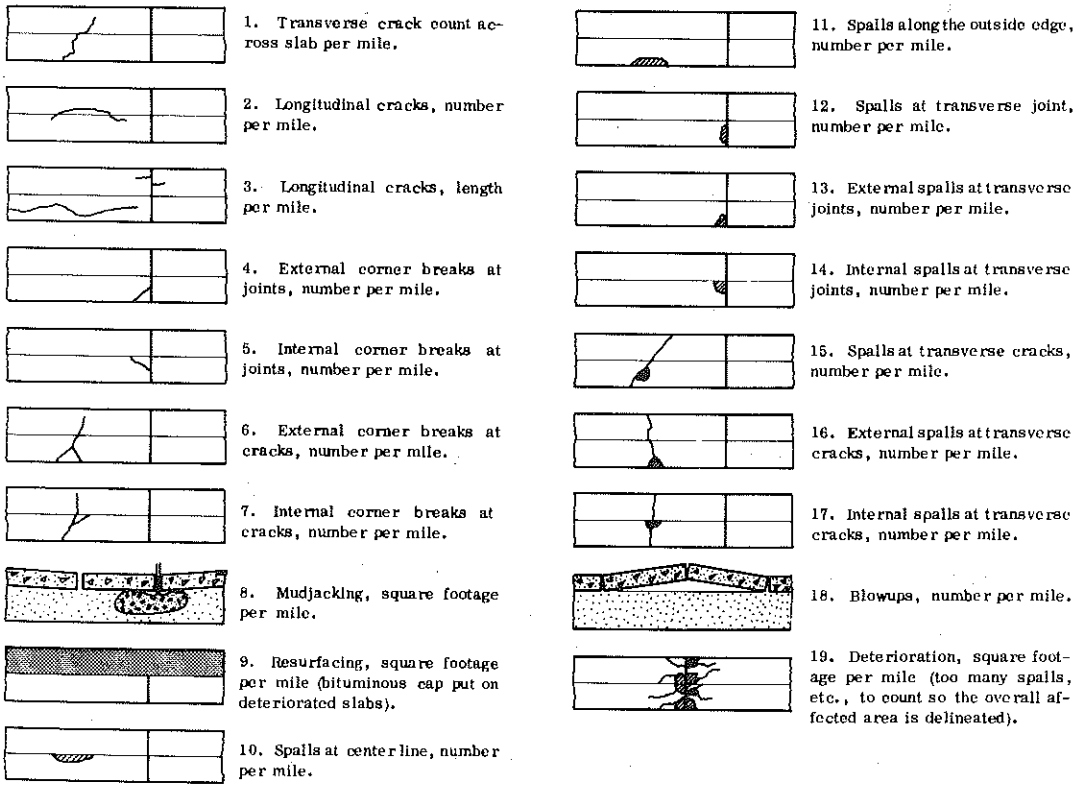

Figure 2. Graphical representation of pavement condition survey variables.

Because most correlations among years for the same variable were high, it was decided to pool the 5, 10, and 15-year data. Examination of the correlation matrix revealed that in some cases the correlations for 5, 10, and 15-year data with the multiple group composite (factor) followed either a sharp increasing or decreasing trend; e.g., 0.30, 0.60, 0.80, or 0.80, 0.60, 0.30, thus suggesting time order effects. In all cases of high 5-year correlations followed by lower 10 and 15-year correlations it was

found that the 5-year data were clearly not bivariate normal. For an example of this, see Figure 3.

The inordinate deterioration of a single project (shown as 'Project A' in Fig. 3) causes a high, but unreliable and probably not meaningful, correlation. One solution to this problem is to rank order the data. However, this destroys precisely the interval scale information which is of interest. In the present analysis, the problem was left unsolved.

The 57 variables were factor analyzed with highest r's on diagonal with a Kiel-Wrigley criterion of one. This showed very high loadings of the 5, 10, and 15-year data for a number of variables on at least one of the first four factors. In other words, some of the 57 variables reduced more or less to four groups or clusters. Furthermore, those variables which shared the same factor (in terms of high correlations: above +0.60) seemed logically related. Nine variables defined clear groups as shown below:

Group I
- Spalls at transverse joints, externally
- Spalls at transverse joints, internally

Group II
- Spalls at transverse cracks
- Spalls at transverse cracks, externally
- Spalls at transverse cracks, internally

Group III
- Corner breaks at transverse joints, externally
- Corner breaks at transverse joints, internally

Group IV
- Longitudinal cracks, number
- Longitudinal cracks, length

The intercorrelations within groups are given in Table 1.

TABLE 1
VARIABLE INTERCORRELATIONS WITHIN GROUP

Group	5 Years	10 Years	15 Years
I	0.58	0.66	0.84
II	0.44, 0.80, 0.40	0.66, 0.61, 0.43	0.80, 0.78, 0.65
III	0.64	0.65	0.73
IV	0.79	0.65	0.71

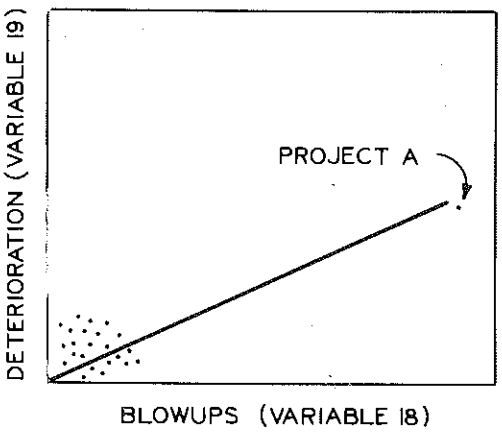

Figure 3. Example of spurious correlation between survey variables.

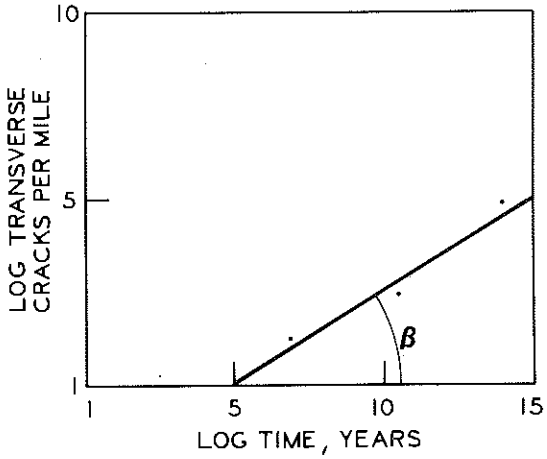

Figure 4. Linearization of transverse crack growth over time.

At this point, 56 additional projects that had 5 and 10-year surveys only, became available. However, the above factor analysis procedure could not be used directly since these 56 projects would not figure in any of the 15-year correlations. Not only was some device needed to bypass this problem, but some method of extracting the time factor was needed if a time independent index was to be achieved. It was noted that performance variables generally were linear over time in a log-log coordinate system (Fig. 4). This suggested a power law formulation:

$$P = \lambda T^{\beta}$$

where:

P = any of the performance variables

T = time in years

λ, β = fitting parameters

Since it was desired that performance difference be reflected in only one parameter, β was determined by least squares for each variable using all 103 projects. Using β as a constant, λ's were determined by least squares for each project. This procedure was carried out for each of the 19 survey variables.

The λ's thus formed a 19 x 103 matrix which was then converted into a 19 x 19 correlation matrix. Examination of this matrix revealed the same high correlations among the variables grouped using the 5, 10, and 15-year data. However, there were no additional high correlations among the other

variables so the matrix was considered to be of rank 14. In other words, nine survey variables reduced to four groups, and the remaining ten variables did not combine or group whatsoever.

Multiple Regression

Since the 14 variables from the factor analysis solution are considered to form a rank of 14 set, no further reduction would seem feasible. Therefore, if one is to relate causal (C) to performance (P) variables, he must consider each of 14 variables as potential dependent variables for multiple regressions on the causal variables:

$$\hat{P}_1 = \hat{\beta}_{10} + \hat{\beta}_{11}C_1 + \hat{\beta}_{12}C_2 + \ldots\ldots\ldots\ldots\ldots + \hat{\beta}_{1k}C_k$$

$$\hat{P}_2 = \hat{\beta}_{20} + \hat{\beta}_{21}C_1 + \hat{\beta}_{22}C_2 + \ldots\ldots\ldots\ldots\ldots + \hat{\beta}_{2k}C_k$$

$$\vdots \quad \vdots \quad \vdots \quad \vdots \qquad\qquad\qquad\qquad \vdots$$

$$\hat{P}_{14} = \hat{\beta}_{14,0} + \hat{\beta}_{14,1}C_1 + \hat{\beta}_{14,2}C_2 + \ldots\ldots\ldots\ldots + \hat{\beta}_{14,k}C_k$$

This rather long list of equations must replace the hoped-for general index (factor) of performance to be predicted by the causal variables. Unfortunately, the hoped-for reduction of variables was not nearly as substantial as found in MDSHT Report R-711 using fewer construction projects. Therefore, it was considered that a general performance index using these variables was not realistic in light of their resistance to grouping. Moreover, the 14 groups which could be formed would result in 14 indices for each time period (5, 10, or 15 years) and 14 x 3 = 42 multiple regression equations -- too many for general performance evaluation. Aside from inconvenicnce, the large number of indices would not afford reliable estimates of future performance. Therefore, a different approach using selected non-grouped basic variables moving over time had to be developed.

II

EVALUATION OF PAVEMENT PERFORMANCE AND CAUSAL FACTORS

Performance Index

Since the general index approach did not appear feasible, it was decided to explore performance of important fundamental variables or some logical combination of them. Of special interest are joints, since their repair can be costly and inconvenient. The problem, then, is to define a reasonable measure of joint performance in terms of one or more survey variables.

One might suppose that a good measure of joint deterioration would be spall count. However, as the number of spalls increases they tend to merge; consequently, more advanced deterioration may have a lower spall count than earlier deterioration. Also, the worst state of deterioration, namely the blowup, is qualitatively different from a spall and hence does not form a logical point on a spall scale of deterioration. This is so even though in a statistical sense spalls are precursors of blowups. Examination of Figure 5 reveals that if the joint is divided into five equal transverse regions, future blowup probability is clearly related to the total number of regions experiencing spall activity. In order to measure all types of joint deterioration in proportion to their seriousness, a more comprehensive scaling method had to be developed. Consequently, it was decided to measure joint deterioration as the percent of the total transverse joint length affected by any kind of surveyed concrete failure. To facilitate measurement and mathematical modeling, these percentages were grouped into four categories, or states, as follows:

0 to 25 percent	- defines State I
26 to 50 percent	- defines State II
51 to 75 percent	- defines State III
76 to 100 percent	- defines State IV

State I turns out to consist mostly of either no spalls or a few external corner spalls, while State IV consists mostly of blowups -- rarely would a joint be spalled 76 to 100 percent of its transverse length without blowing up. Usually, State IV joints were observed as full slab width patches at the time of survey which, by their extent and character, strongly suggested the prior occurrence of a blowup. Using these definitions of joint deterioration, each joint could be classified and its progression from state to state charted with each subsequent condition survey.

As discussed earlier, in evaluating a project's performance, particularly if one is looking for causes of deterioration, it is helpful if pavement condition can be summarized by a single index or performance measure.

The above definitions of joint condition allow characterization of each joint's condition, but this is too large and varied a body of information to work with if one is evaluating such causal variables as traffic volume, aggregate sources, weather conditions, etc. These variables apply to all or most slabs in a project. Hence, joint condition was averaged for each project. This average is called the "expected state" E(s), of the project.

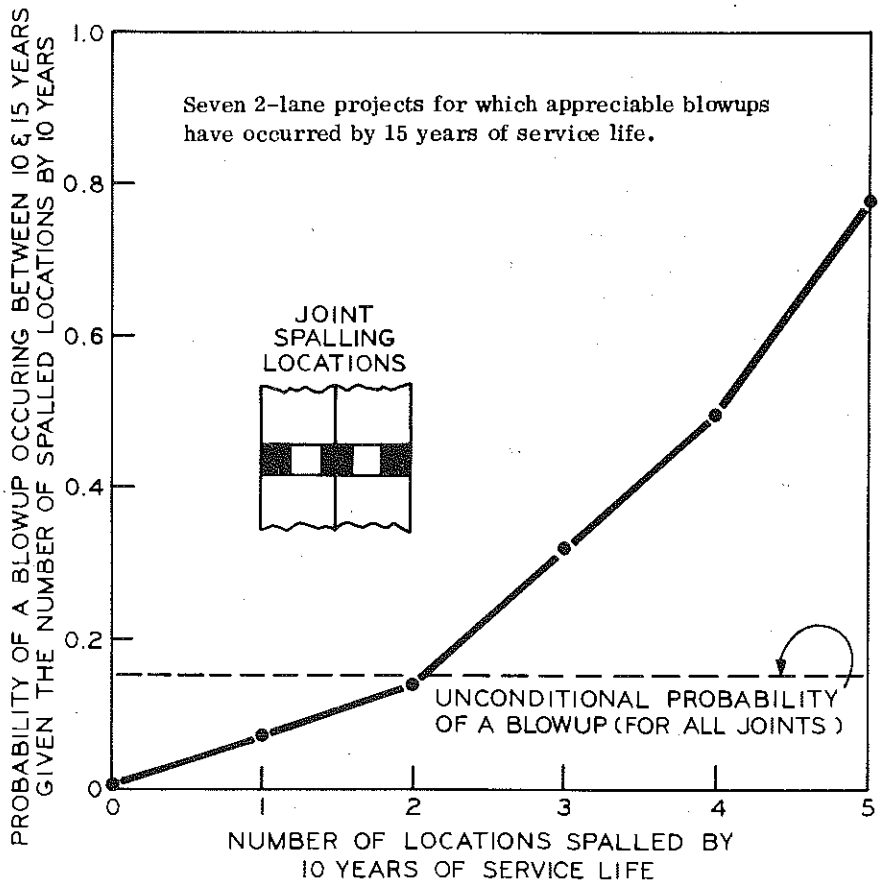

Figure 5. Probability of a blowup as a function of joint spalling.

The expected state can be computed for each condition survey, thereby providing a joint performance index history. Forty-three projects had 5, 10, and 15-year surveys, and 85 had only 5 and 10-year surveys. In order that all projects could be used, logistic[1] performance trend curves were fitted to the expected state data and a logistic curve parameter, δ, was

---

A logistic curve was necessary because 'expected state' is bounded between 1.0 and 4.0.

used to regulate the growth of deterioration over time (Fig. 6). Thus, each of the 128 projects could be evaluated by a single deterioration growth parameter by simply regressing expected state on time, using the logistic function. The Appendix shows fitted logistic functions for the 43 projects for which 5, 10, and 15-year survey data were available -- in general, the fit is quite good.

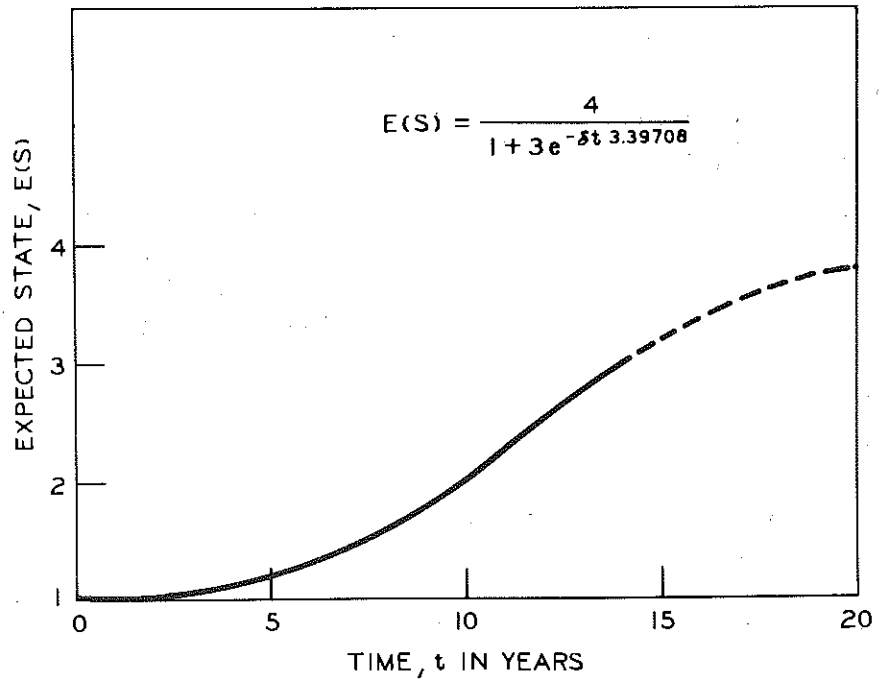

Figure 6. Growth of average joint deterioration over time.

Interestingly, the distribution of δ for the 128 projects very closely follows the exponential form as shown in Figure 7. Thus, a large number of projects have very small δ's, i.e., they show a low deterioration rate. Higher δ values, indicating greater deterioration rates, are found less frequently, and very high δ's (extremely high deterioration rates) are rarely found.

Joint Performance Change Over Time

The first objective of this study was to determine if performance was associated with construction year. In particular, we wished to know if recent projects (1954 to 1961) performed better than earlier ones (1946 to 1953). The fact is that they did perform slightly better, but not signifi-

cantly so (Fig. 8). Even though the difference in performance distributions is slight, it must be remembered that projects built during the later period experienced more traffic and heavier calcium chloride application by their tenth year of service than those from the earlier period. Thus, later projects performed as well despite more inclement conditions. This is not to say that later surveys, such as at 20 years, would not show greater deterioration for the more recent projects. A plot of δ by year group is shown in Figure 9.

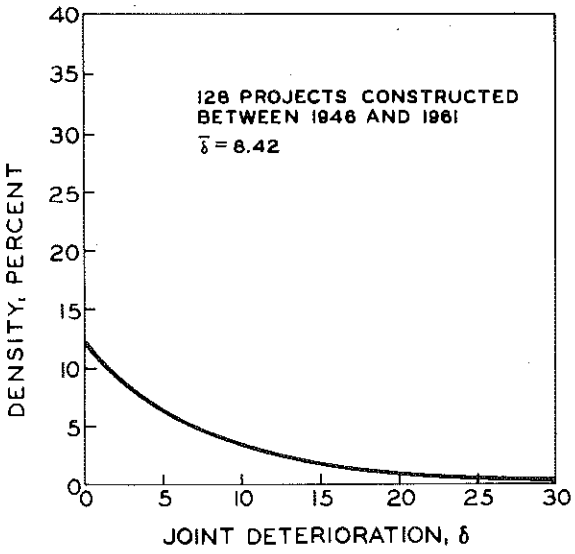

Figure 7. Frequency distribution of joint deterioration for all projects examined during the 1946-1961 construction period.

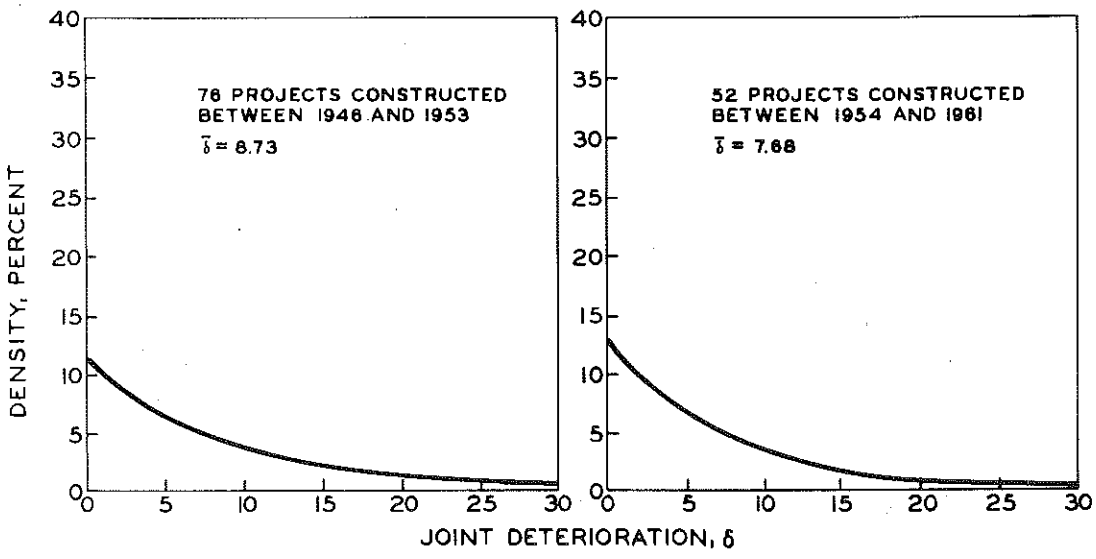

Figure 8. Frequency distributions of joint deterioration for two post-war construction periods.

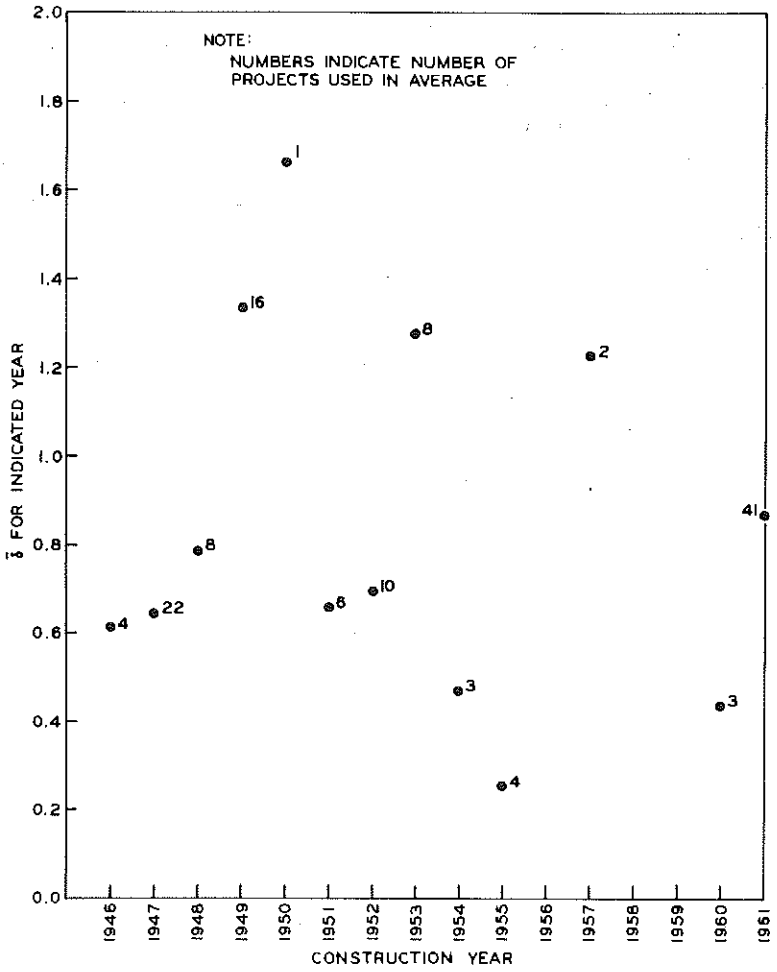

Figure 9. Average project performance for each construction year with at least a 10-year service history.

A second objective was to examine possible effects of construction changes on performance. Unfortunately, changes in slab length and joint seal were generally implemented in the mid to late '60's, and we will have to wait until projects constructed in this period have had at least 10-year survey data available. This is because very little joint deterioration can be detected by condition surveys in the first 10 years of service life. It is expected that as these surveys become available, comparisons of joint seals, slab lengths, etc., will be made using the same performance measure, δ, developed in this study.

A third objective was to confirm earlier findings implicating such variables as traffic volume and percent soft, non-durable materials in the coarse

aggregate in accelerated deterioration (1). As far as joints are concerned, traffic volumes did not correlate well with performance for the 128 projects studied (Fig. 10). In this figure, projects having average ADT below and above 2,000 show very little difference in performance distributions. Hence, we must conclude that either traffic is not an important variable in joint performance up to about 10 to 15 years, or that our data, including the sample itself, are not adequate for detecting whatever effect may exist.

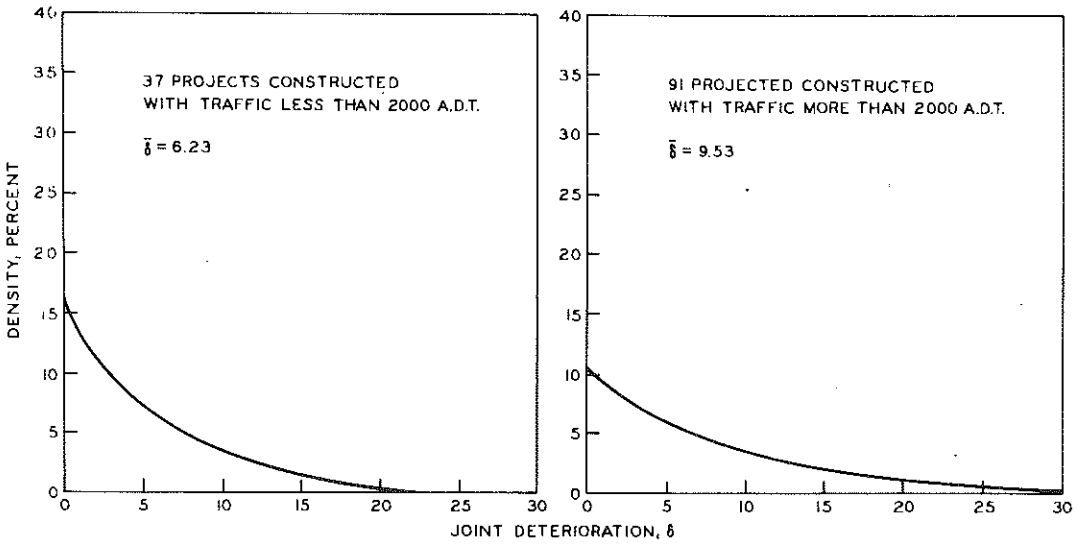

Figure 10. Frequency distributions for low and high traffic volumes.

When projects ' δ 's are arranged according to coarse aggregate composition, however, we found a strong segregation of joint performance (Fig. 11). Projects built with either very low or very high carbonate gravels always performed well. Aggregates composed of from 10 to 80 percent carbonates gave variable performance as did the crushed limestones. For these materials, no other variable could be found which explained the wide performance differences. In Research Report R-711, it was assumed that percent soft, non-durable materials in the coarse aggregate was a performance factor since there was some evidence that high soft, non-durable contents were associated with poor performance. The larger data set of this study does not support the earlier observation; percent soft, non-durables data, taken from aggregate inspection records, do not correlate in the larger sample with joint performance (or δ as herein defined). It may be, of course, that these field sample data are not sufficiently accurate for our purposes. Therefore, at this time we must conclude that the best predictor of joint performance is coarse aggregate classification based on geo-

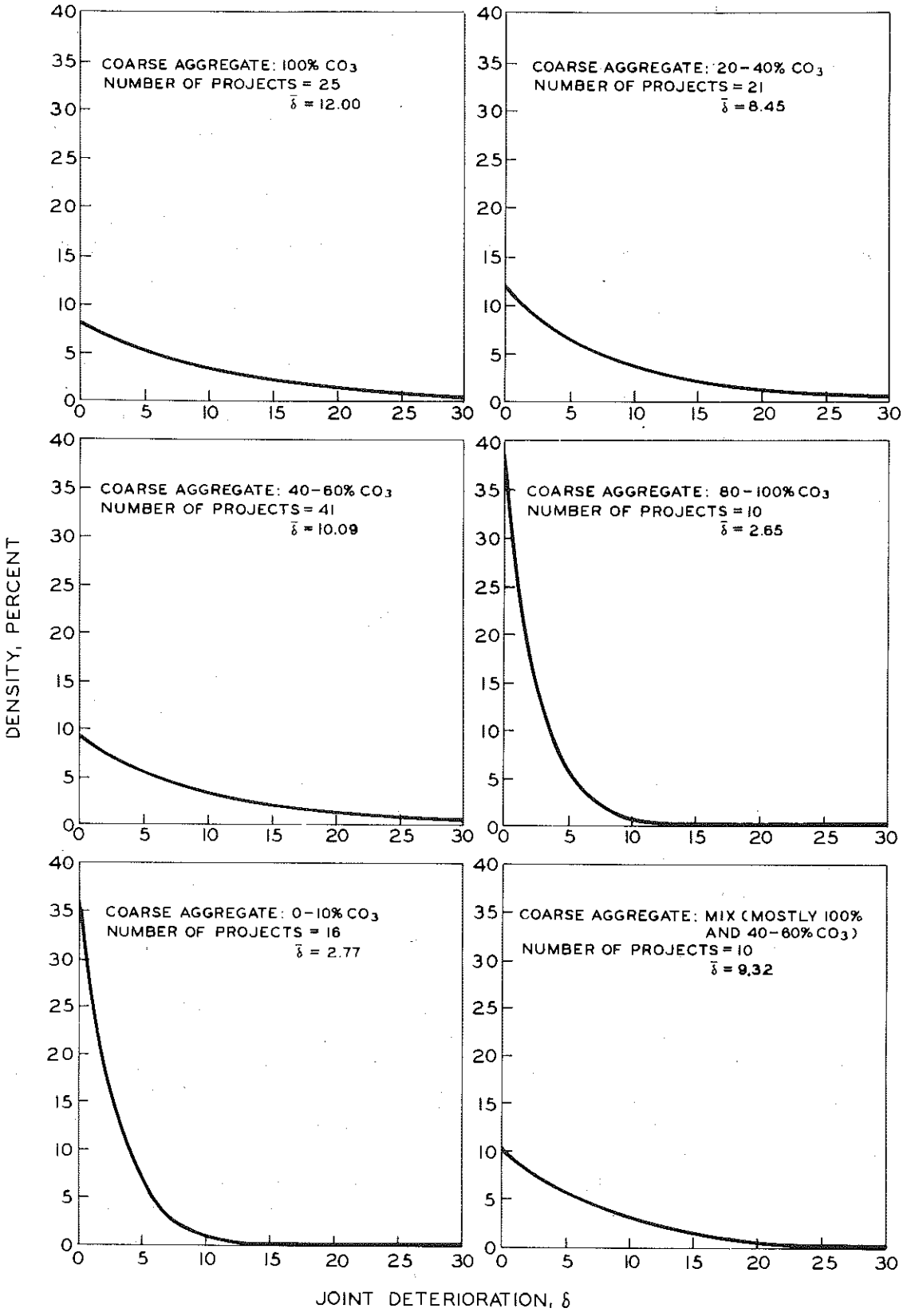

Figure 11. Frequency distributions of various categories of coarse aggregate carbonate content.

logical knowledge of carbonate proportions. For the middle carbonate groups, as well as crushed limestone, we found no way of predicting future joint performance.

It was also of interest to compare two-lane project joint performance with that of four-lane projects -- particularly since four-lane roadway in Michigan constructed after 1956 was generally part of the Interstate system, or built to those specifications. Figure 12 shows the joint performance distributions for 1946 through 1961 two-lane and four-lane roadways. As can be seen, our performance measure cannot detect a significant difference between the two roadway types.

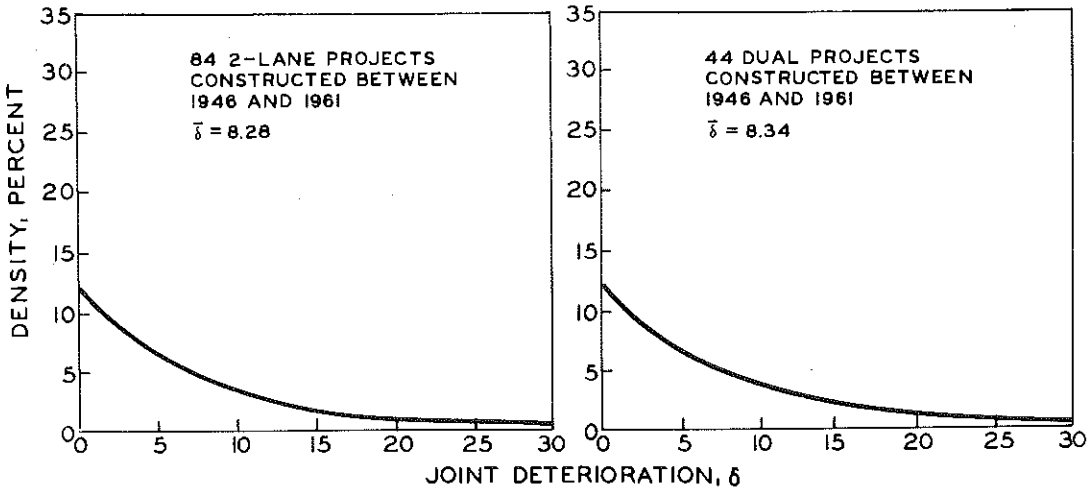

Figure 12. Frequency distributions of joint deterioration for dual and single lane roadways.

As far as transverse cracking is concerned, it is assumed that traffic loading in conjunction with base and subbase conditions is a large factor in performance differences. Differences in traffic and passing lane cracking bears out this assumption (Section III). However, general ADT figures taken for all 128 projects do not. Also of interest is the finding that our soil quality classification (1 to 5, based on drainage in situ) did not relate to cracking at any time up to 15 years of service. Presumably, soil upgrading, together with base requirements, improves drainage conditions to a point where crack incidence cannot be predicted from original soil information alone. On the other hand, projects differed widely in terms of crack incidence, suggesting that these upgrading procedures vary considerably in execution. Considering that loading appears not to be a strong factor, and that both good and poor original soils produce both good and poor pavement cracking histories, we suspect that other factors associated with construction practices are responsible for the variability of crack occurrence.

III

FIVE PRELIMINARY PROBABILITY MODELS OF TRANSVERSE CRACKING

Transverse cracking in concrete pavement is the kind of fundamental highway performance variable which may be amenable to finite state probability modeling. It is especially tempting as a performance variable because it can be easily measured and occurs with sufficiently high frequency to ensure statistical legitimacy. These virtues are not generally found with the other fundamental survey variables. It is the purpose of this Section to explore alternate methods of crack modeling from a probabilistic - time process point of view. The crack distributions in terms of crack count per 100-ft slab, measured in Michigan at the 5, 10, and 15-year service periods, are undoubtedly related to many 'causal' variables such as concrete aggregates, soil base, and traffic volume even though we have found it difficult to pin down these relationships. Because of data quantity and reliability, traffic volume was singled out as the only subject of these models. The data used came from the traffic and passing lanes of four divided freeways for which early traffic figures, as well as 5, 10, and 15-year crack tabulations, were available. This is because only dual expressway provides the opportunity to examine differences in traffic loading while all other variables are held constant. A small sample of eight lanes was used in order that a sizable number of models could be compared without requiring excessive computation.

While traffic volume histories are available for these projects, they do not provide ideal input data since they resulted from only one 24-hr sample per project (two lanes) per year. Moreover, they represent total roadway volumes so that one must apportion by some formula the roadway totals into the respective traffic and passing lane sub-volumes. Therefore, the probability models will not be free of systematic error introduced by the background causes that mediate the effects of traffic loading, nor will they be free of the random error introduced by undersized and probably biased traffic samples. These difficulties notwithstanding, it was decided to compare alternate methods of predicting transverse crack distributions, based on the available data.

Since each model will be 'driven' by only traffic volume it was necessary to develop some means of dividing the total roadway volume into the traffic and passing lane subtotals. One can gain insight into the lane allocation problem by thinking of traffic density in three stages:

Stage I - Low Total Roadway Volume. Most vehicles use the traffic lane since there is little need to pass. If T_p and T_t represent passing and traffic lane volumes, respectively, $\frac{\Delta T_p}{\Delta T_t}$ will be low; i.e., an incremental increase in traffic lane volume will not result in much increase in passing lane volume.

Stage II - Moderate Total Roadway Volume. At this stage, the increased volume in the traffic lane will result in much greater passing frequency, hence increased usage of the passing lane. Therefore, $\frac{\Delta T_p}{\Delta T_t}$ will be higher than in Stage I.

Stage III - High Total Roadway Volume. At this stage, the saturated traffic lane has already caused frequent passing; consequently, the passing lane is approaching saturation as well. Therefore, the passing lane becomes a less attractive alternative and $\frac{\Delta T_p}{\Delta T_t}$ will be somewhat lower than in Stage II (Fig. 13).

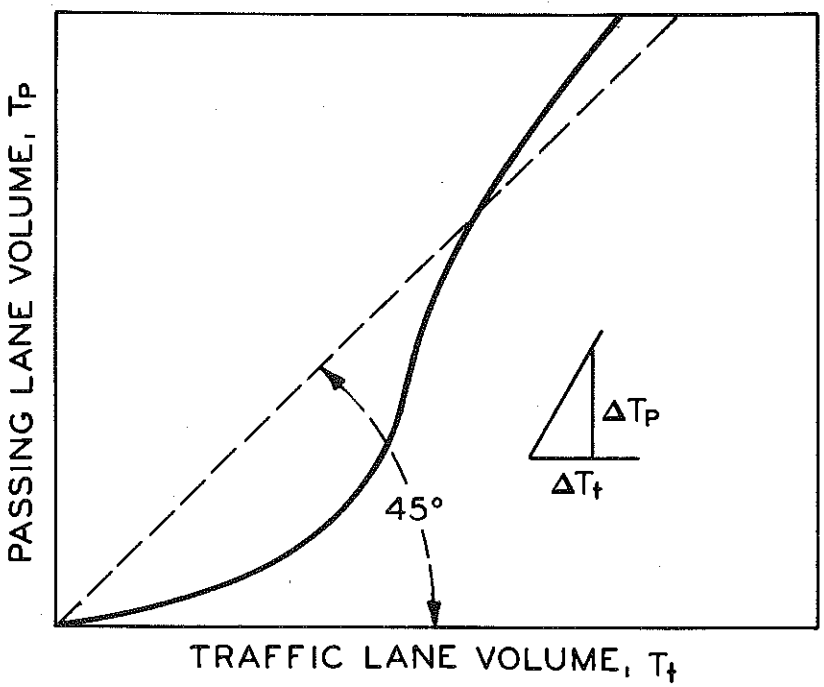

Figure 13. Idealized passing lane growth rate function.

The above considerations suggest that $\frac{\Delta T_p}{\Delta T_t}$ should follow a growth curve (2) for which T_t is the dependent variable; or in terms of a differential equation:

$$\frac{dT_p}{dT_t} = \frac{A}{1+Be^{-CT_t}} - \frac{A}{1+B}$$

The second term is necessary to insure that $\frac{dT_p}{dT_t} = 0$, when $T_t = 0$. There

is evidence (3) that when the traffic lane is saturated, the passing lane usage approaches a point of carrying up to 50 percent more volume due to the somewhat greater speed of vehicles in this lane. Using this estimate, one can shape the growth curve as follows:

$$\frac{dT_p}{dT_t} \longrightarrow 1.5 \text{ as } T_t \longrightarrow \infty$$

That implies that:

$A - \frac{A}{1+B} \longrightarrow 1.5$ or for practical purposes, when T_t is very large,

$$A = \frac{1.5\,(1+B)}{B}$$

Thus,

$$\frac{dT_p}{dT_t} = \frac{1.5(1+B)}{B}\left(\frac{1}{1+Be^{-CT_t}} - \frac{1}{1+B}\right) = \frac{1.5}{B}\left(\frac{1+B}{1+Be^{-CT_t}} - 1\right)$$

So that,

$$T_p = \frac{1.5\,(1+B)}{B}\int \frac{dT_t}{1+Be^{-CT_t}} - \frac{1.5}{B}\int dT_t \quad \text{and}$$

$$T_p = \frac{1.5\,(1+B)}{B}\left(\frac{-1}{C}\,\ell n\left|\frac{e^{-CT_t}}{1+Be^{-CT_t}}\right|\right) - \frac{1.5T_t}{B} + k$$

where k is the integration constant.

When $T_t = 0$, $T_p = 0$, so that,

$$\frac{1.5\,(1+B)}{B}\left(\frac{-1}{C}\,\ell n\left|\frac{1}{1+B}\right|\right) + k = 0 \quad \text{and,}$$

$$k = \frac{1.5(1+B)}{B}\left(\frac{1}{C}\,\ell n\left|\frac{1}{1+B}\right|\right)$$

Therefore,

$$T_p = \frac{1.5(1+B)}{B}\left[\frac{1}{C}\,\ell n\left(\frac{1+Be^{-CT_t}}{e^{-CT_p}}\right)\left(\frac{1}{1+B}\right)\right] - \frac{1.5T_t}{B}$$

$$T_p = \frac{1.5}{B}\left(\frac{1+B}{C}\,\ell n\left|\frac{e^{-CT_t}+B}{1+B}\right|\right) - T_t \qquad (1)$$

By using T_p and T_t data taken simultaneously, it would ordinarily be possible to estimate the fitting parameters B and C by regression techniques. In the present case, however, Eq. (1) cannot be put in linear form, and some method of non-linear least squares must be used. Systematic substitution of values for B and C produced an approximate minimum for the squared error expression:

$$S^2 = \sum_{i=1}^{n} \left\{ T_{pi} - \frac{1.5}{B} \left[\frac{1+B}{C} \ln \frac{e^{CT_{ti}+B}}{1+B} - T_{ti} \right] \right\}^2$$

at $B = 1.10$, and $C = 0.17$, using data obtained graphically from ref (3).

With approximate values of B and C established, the relation $T_p = f(T_t)$ can be generated graphically. From this function, the relations $T_p = g(T_p + T_t)$ and $T_t = h(T_p + T_t)$ can be obtained as shown in Figure 14. This graph was used to decompose total roadway volumes into traffic and passing lane sub-volumes.

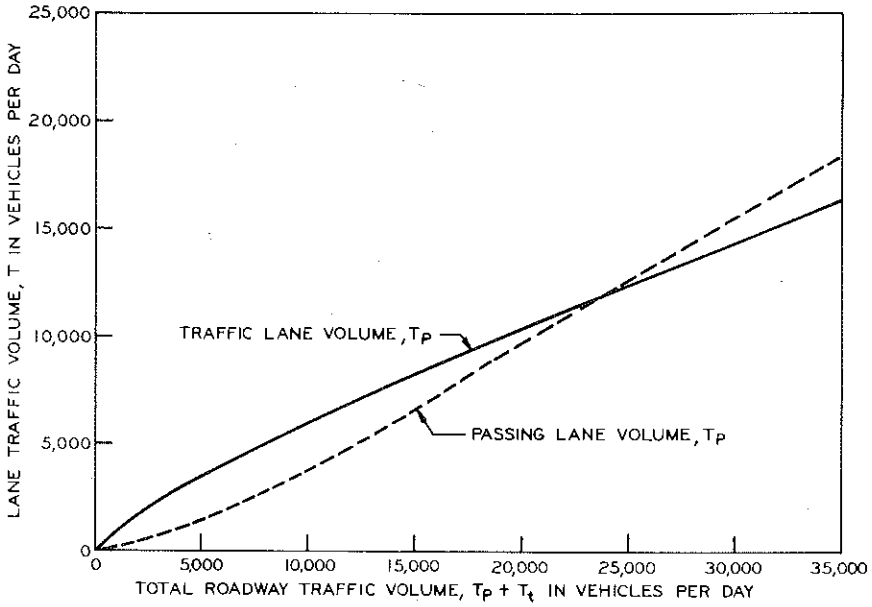

Figure 14. Theoretical relationship between traffic and passing lane daily traffic volumes.

Transverse Crack Growth Over Time

As would be expected, the average number of transverse cracks per slab increases sharply during early service life. The form of this increase can be considered linear, at least for the 15-year service period shown in

Figure 15. The average number of cracks per slab (λ) for nearly all lanes shown in Figure 15 appear approximately linear over time (t); i.e., of the form $\lambda_i = \phi_i t$ where i indexes the construction project. However, the lanes exhibit substantially different crack growth rates or slopes (ϕ_i). These slopes range from about 0.03 to 0.30 cracks per year. The differences in cracking rate are presumed to be due to differences in construction materials, soil base, construction practices, and traffic volumes. Since the cracking models under consideration are intentionally limited to traffic as the only input variable, the rates indicated as slopes in Figure 15 were correlated with average daily traffic volumes for the eight lanes examined (Fig. 16). The log-log coordinates of Figure 16 suggest a power law relationship of the form:

$$\phi_i = \theta_i T_i^{\theta_2}$$

where ϕ_i is the cracking rate for the i-th project over time, T_i is the average daily traffic volume for the i-th project measured after 5 years of service, and θ_i and θ_2 are fitting parameters. Ordinary least squares using this equation form provides the following estimation equation

$$\phi_i = 0.00125 T_i^{0.63} \quad \text{so that,} \quad \lambda_i = 0.00125 T_i^{0.63} t$$

Using this formula, one can estimate the average number of cracks per slab to be expected at time t providing that a reliable 5-year daily traffic figure T_i is available.

It may be desirable, where possible, to incorporate into the cracking models the general observation that traffic volume tends to increase over the service life of each project. Investigation showed that this assumption was true for each project considered in this analysis. The average trend suggests about a 2.6-fold traffic increase from the 5th to the 15th year of service. Thus, if one is to predict the 15-year crack distribution using a 5-year traffic survey, he would find that over the intervening 10 years, daily traffic volume typically increased from T to $2.6T$. For the first N-th portion of this 10-year period, the increase would be $\frac{2.6T}{N}$ assuming linear growth.

One way of broadening the analysis to allow for the traffic increase over time is merely to average the initial (5 year) and final $\left(T + \frac{2.6T}{N}\right)$ traffic volumes for the period under consideration. This approach is somewhat complicated by the fact that the period itself may be a variable (as in the Markov models) the value of which is not initially known. This problem was

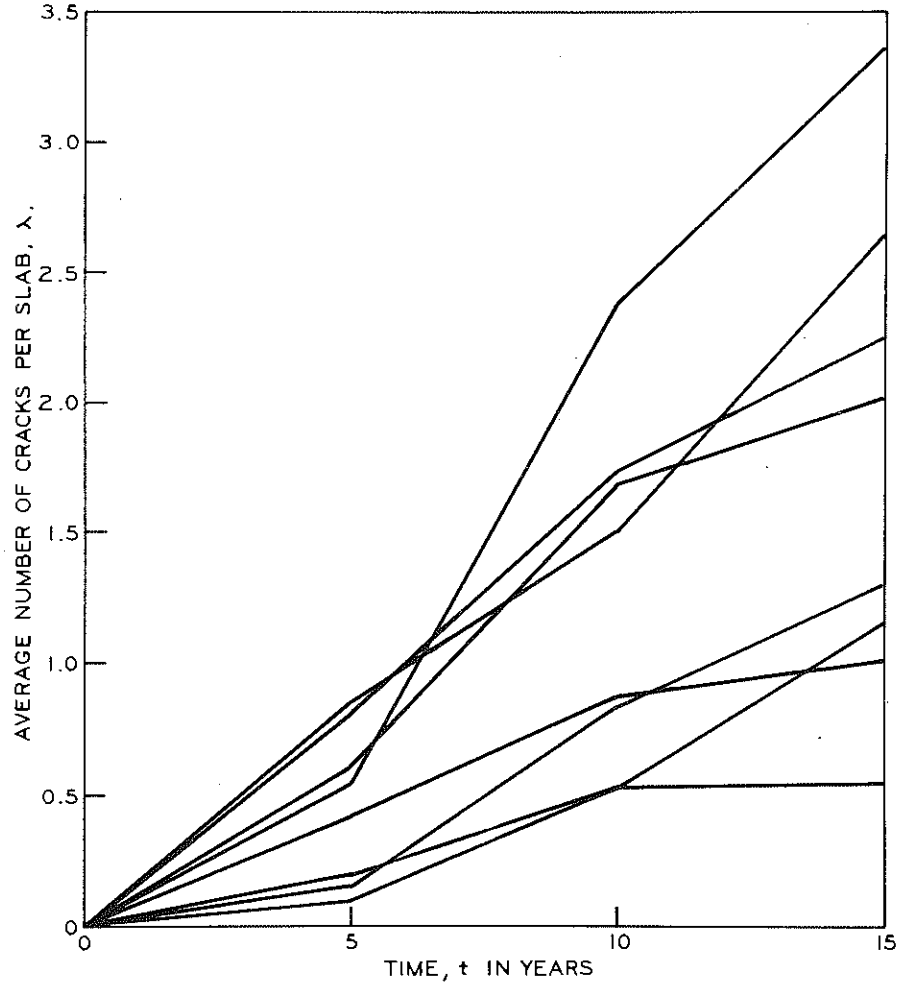

Figure 15. Growth of transverse cracks over time.

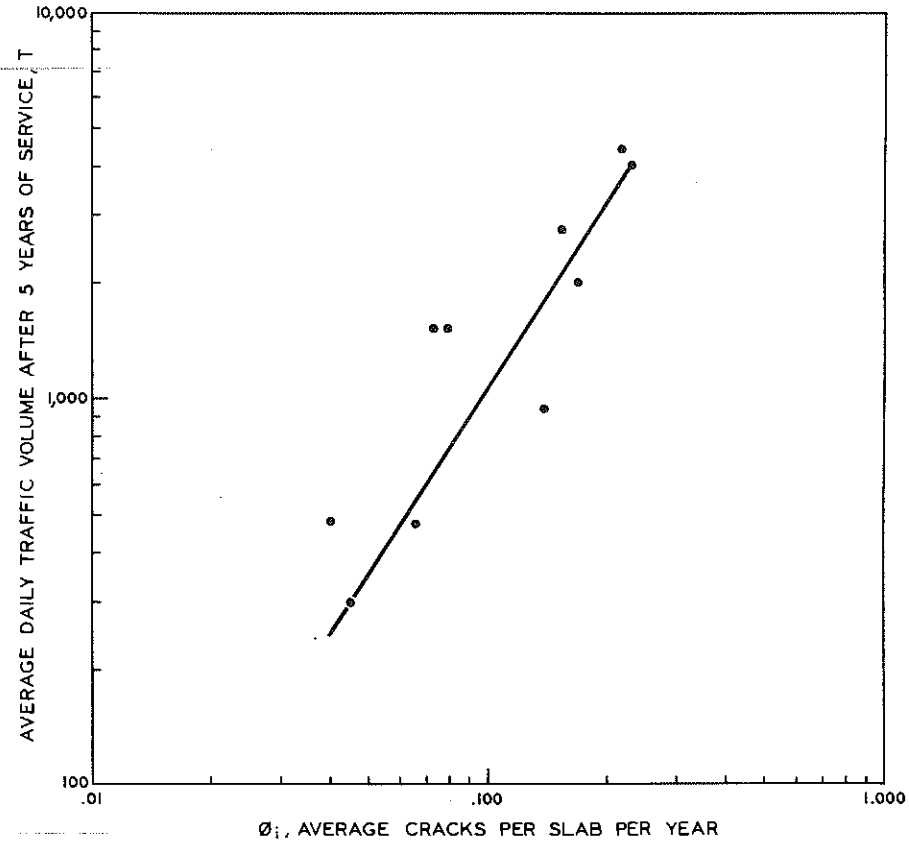

Figure 16. Relationship between transverse cracks and traffic volume.

worked out for each model in turn. Whenever this latter refinement was incorporated into a model, it was based on a correction factor composed of initial and final averaging for each period as follows: If T is the 5-year traffic volume, then $2.6T$ will be the increase in volume over the next 10 years. For the first N-th portion of the 10-year period, the volume will increase $\frac{2.6T}{N}$. Hence, the total volume at the end of the first N-th period will be $T + \frac{2.6T}{N}$. The average based on the beginning and ending volumes for this same period will then be $\frac{T+(T+\frac{2.6T}{N})}{2} = T(1+\frac{1.3}{N})$. For model number V, this will be further developed to provide for traffic volumes in the second N-th period, etc.

Model I - Markov Chain for Small Time Periods

For this model, the Markov transition matrix (4) $\mathbf{M}$ represents a roughly stationary (Fig. 17) finite state, discrete time process of sufficiently short duration to preclude the possibility of more than one additional crack appearing in the transition interval N. That is:

$$P_{ij} = \begin{cases} \epsilon_i \text{ for } j = i+1 \\ 1-\epsilon_i \text{ for } j = i \\ 0 \text{ for all other } j \end{cases}$$

It is also assumed that the occurrence of cracks prior to the transition period reduces the probability of additional cracking. Moreover, the extent of reduction is proportional to the number of cracks already present at the onset of the transition period. It seems reasonable that the retarding influence of prior cracking on additional cracking should build gradually and ultimately prevent further cracking beyond a 'saturation' point which defines the cracking limit for slabs of given dimensions, quality, and support. In formal terms:

$$\epsilon_i = \frac{T}{10^5}\left[1+\frac{1.3}{N}\right]F_i \qquad (2)$$

Where T is the 5-year average daily traffic. The factor 10^5 is necessary to reduce the magnitude of T to a very small value $(\sim 0.05 \max)$; and F_i is the reduction factor required if stress relaxation due to prior cracking is significant. F_i is developed as follows: Since F_i should be a maximum when the number of prior cracks is zero, and probably declines at an in-

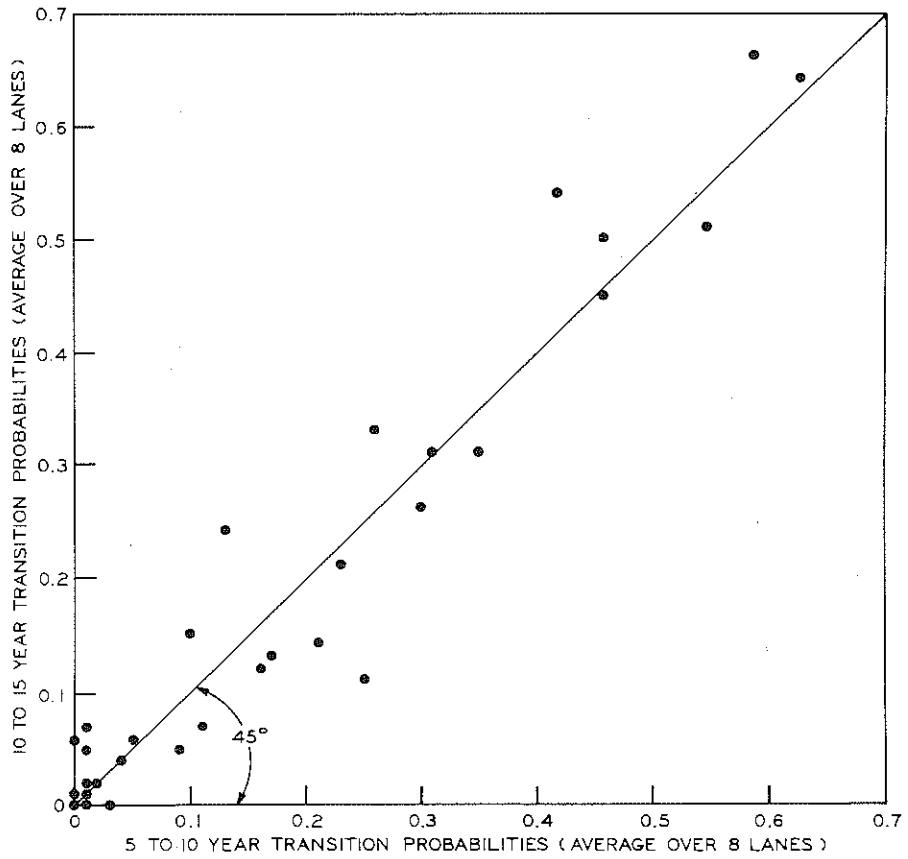

Figure 17. Relationship between 5 - 10 and 10 - 15-year crack transition probabilities.

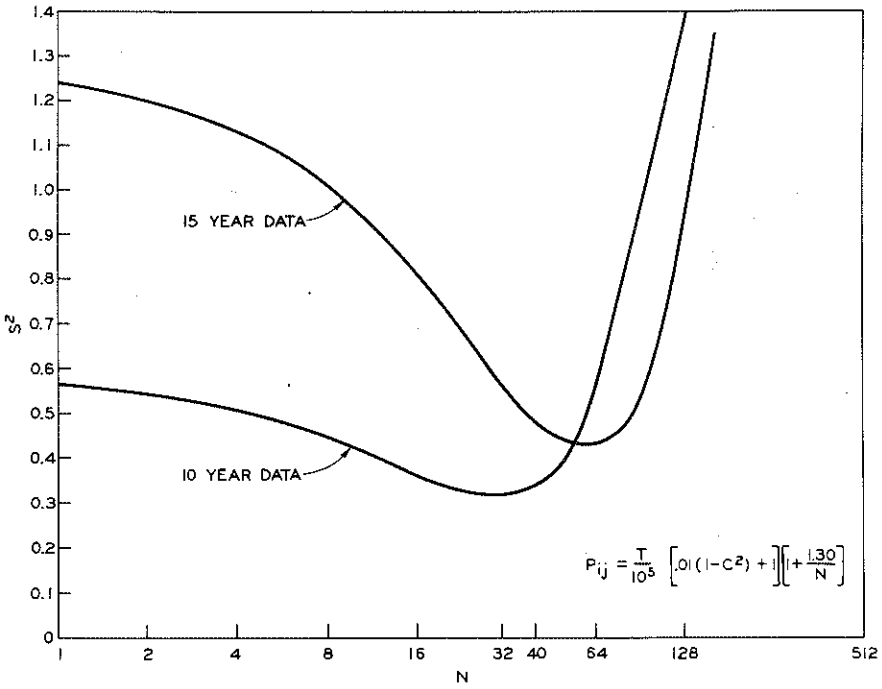

Figure 18. Squared error minimization procedure for various transition periods.

creasing rate as the number of prior cracks increases, a simple second-order relationship is postulated:

$$F_i = \lambda - \beta(i+1)^2$$

where λ and β are fitting parameters and i is the transition matrix column location containing F_i. As initial conditions, it is required that $F_i = 1$, when $i = 0$, therefore:

$$\lambda = \beta + 1$$
$$F_i = \beta(1 - C^2) + 1 \qquad \text{and}$$

Eq (2) now becomes:

$$\epsilon_i = \frac{T}{10^5}\left[\beta(1-C^2)+1\right]\left[1+\frac{1.3}{N}\right] \qquad \text{and}$$

the Markov process in matrix form will be:

$$SQM^N = \hat{F}$$

where S is a scalar representing the number of slabs in the i-th lane, and:

$$M = \begin{pmatrix} 1-\epsilon_0 & \epsilon_0 & 0 & \cdots & 0 \\ 0 & 1-\epsilon_1 & \epsilon_1 & \cdots & 0 \\ \cdots & \cdots & \cdots & \cdots & \cdots \\ \cdots & \cdots & \cdots & \cdots & \cdots \\ 0 & 0 & \cdots & 1-\epsilon_{k-1} & \epsilon_{k-1} \\ 0 & 0 & \cdots & 0 & 1 \end{pmatrix}$$

$q_0, q_1, \ldots, q_k$ are the 5-year initial state probabilities, and $\hat{f}_0, \hat{f}_1, \ldots, \hat{f}_k$ are predicted 10 and 15-year final state probabilities. Notice that the transition matrix is upper triangular since crack count cannot decrease, hence the probability of going to a lower state (fewer cracks) is always zero.

As N increases, probabilities decrease in the left portion and increase in the right portion of the transition matrix until in the limit, the N-step matrix becomes ergodic, i.e. non-changing. Because all row probabilities must add to 1.0, the ergodic state of the N-th power of the transition matrix will be in the limit:

$$M^N \to \begin{pmatrix} 0 & 0 & 0 & \cdots & 1 \\ 0 & 0 & 0 & \cdots & 1 \\ \cdots & \cdots & \cdots & \cdots & \cdots \\ 0 & 0 & 0 & \cdots & 1 \end{pmatrix} \qquad N \to \infty$$

However, long before this condition, a minimum S^2 will have been reached for both the 10 and 15-year data. S^2, of course, is equal to:

$$\sum_{i=1}^{m} \sum_{j=1}^{k} \left[f_{ij} - \hat{f}_{ij} \right]^2$$

where f_{ij} is the observed 10 or 15-year probability of j cracks occurring in a random slab of the i-th lane. Because S^2 is presumed to have a minimum value for some N, it can be used as a criterion for estimating the value of N which best satisfies the assumptions of the model. Consequently, for each incremented value of β, M was successively squared until a minimum S^2 was established (Fig. 18). When a value of β was found which resulted in the lowest minimum S^2, it was used together with the 5-year Poisson-generated probabilities to provide 10 and 15-year slab count estimates for crack categories 0 through 5.[2]

The S^2 criterion using 15-year data resulted in an N of about 64, or a crack transition period of $\frac{10}{64} \times 12 = 1.88$ months. The same criterion applied to 10-year data resulted in an N of about 32, which provides the same transition period estimate. Therefore, one concludes that the assumptions of this model hold best for about a two-month transition period. Results of this model together with the other four will be presented at the end of this section.

Model II - Markov Chain for Large Time Periods

Model I specified that non-zero crack occurrence probabilities could exist for only zero or one crack occurring during the transition interval. This specification can be relaxed, provided that the remaining probabilities in each row can be generated by some rule. This provision allows for longer transition time periods during which more than one crack can occur. One may then postulate that each row in the transition matrix defines a condition governing future cracking for which a Poisson distribution of additional cracks is appropriate. Thus, in row zero, where no prior cracking is assumed, the occurrence of additional cracks would follow the Poisson distribution with parameter λ_0. In row one, where one prior crack is assumed, the stress condition of the slab has possibly been ameliorated by

[2] For all Markov models considered, $q_1, q_2, \ldots, q_6$ were generated assuming a Poisson distribution. The Poisson parameter, λ, was estimated from the previously discussed relationship:

$$\lambda_j = 0.00125 T_j^{0.63} \text{ setting } t \text{ equal to } 5.0$$

the single crack to the extent that the occurrence of additional cracks follows the Poisson distribution with parameter λ_1, where λ_1 may be less than λ_0. This treatment can be extended to all rows in the transition matrix. Moreover, the provision of flexible Poisson parameters in each row can be used to test the assumption that the stress relaxation due to prior cracks lessens the probability of further cracking. If this were a viable assumption, one would find that λ_i systematically decreases as $i \to s$, the crack saturation number.

Examination of Figure 19 shows that there is some decrease in the expected number of cracks as the number of prior cracks increases (as indicated by row number). Thus, we have:

$$P_{ik} = \frac{\lambda_i^{(k-r)} e^{-\lambda_i}}{(k-r)}$$

and

$$P_{ik} \to 0 \text{ as } i \to s$$

where P_{ik} is the conditional probability of going from i to k cracks in the transition period, and λ_i is the expected number of cracks for the transition period given that i have occurred previously. The expression $(K-r)$ rather than k is necessary to ensure that each row represents the distribution of additional cracks, that is, k cannot be less than i. Now, λ_i can be estimated by the log-log regressions of conditional λ_i's on traffic (T) so that the transition matrix appears as:[3]

$$M = \begin{pmatrix} \frac{\lambda_0^0 e^{-\lambda_0}}{0!} & \frac{\lambda_0^1 e^{-\lambda_0}}{1!} & \frac{\lambda_0^2 e^{-\lambda_0}}{2!} & \cdots & \frac{\lambda_0^k e^{-\lambda_0}}{k!} \\ 0 & \frac{\lambda_1^0 e^{-\lambda_1}}{0!} & \frac{\lambda_1^1 e^{-\lambda_1}}{1!} & \cdots & \frac{\lambda_1^{k-1} e^{-\lambda_1}}{(k-1)!} \\ \cdots & \cdots & \cdots & \cdots & \cdots \\ 0 & 0 & \cdots & \cdots & 1 \end{pmatrix}$$

where $\lambda_i = a_i T^{\beta_i}$, thus, the 10-year crack distributions would be row vectors estimated from:

$$F_{10,i} = S_i \; Q_i \; M_i$$

and,

the 15-year distributions from:

$$F_{15,i} = S_i \; Q_i \; M_i$$

---

[3] Ten and 15-year data were combined because of the stationarity assumption.

where $\mathbf{Q}_i$ is the row vector of 5-year probabilities for the i-th lane and $\mathbf{M}_i$ is the transition matrix for the i-th lane.

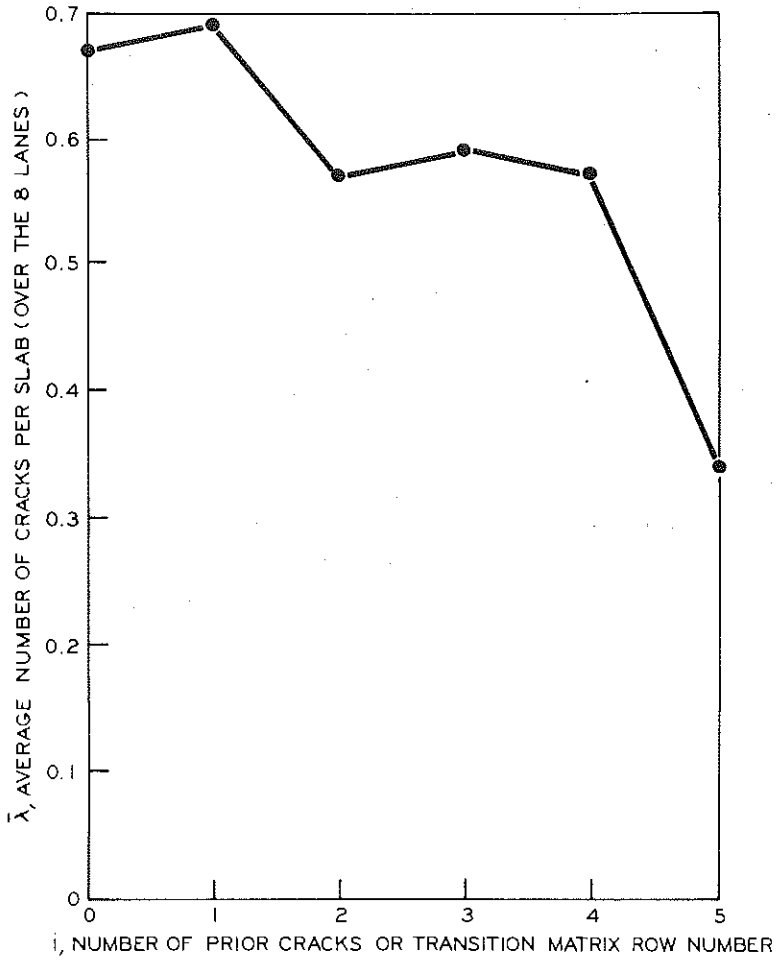

Figure 19. Relationship between extent of prior cracking and expected crack count at the end of the transition interval.

Model III - The Poisson Process

In contradistinction to the assumptions of Models I and II, one can assume that transverse cracking occurs independently of previous cracking history. Thus, if a slab has k cracks at time t, the probability of a crack appearing at time $t+\Delta t$ is the same as if there were no cracks at t. Embodying this assumption in a probability model is tantamount to denying that prior cracking relieves enough stress to lessen the extent of future

cracking. The Poisson distribution is developed using the independence assumption. Its general form, as discussed earlier is:

$$P(k)_i = \frac{\lambda_i^k e^{-\lambda_i}}{k!}$$

where $P(k)_i$ can be interpreted as the probability of k cracks occurring in the i-th lane where the expected number of cracks is λ_i. In this form, the distribution does not explicitly take account of time, i.e., it is not a 'process.' Recalling that λ_i can be estimated by,

$$\lambda_i = 0.00125 T_i^{0.63 t}$$

substitution converts the general Poisson model into the Poisson process:

$$P_k(t)_i = \frac{(0.00125 T_i^{0.63 t})^k e^{-0.00125 T_i^{0.63 t}}}{k!}$$

where $P_k(t)_i$ is the probability of observing k cracks in the i-th lane by time t. Using this simple model, one can estimate crack distributions for any time up to 15 years using only 5-year traffic data.

Model IV - Erlang Distribution (4)

Suppose that for a sufficiently small period of time, cracks follow the discrete form of the exponential distribution; i.e.,

$$P_{ij} = N\theta \int_i^j e^{-N\theta x} dx = e^{-N\theta i} - e^{-N\theta j}$$

where P_{ij} is the probability of between i and j cracks occurring during the period, and both i and j are integers such that $j \geq i$. In this distribution, N is the expected number of cracks for the period and can be estimated from traffic data as was done for the preceding models. Applications of the exponential distribution assume that the length of time between cracks is independent of when this time interval occurs.

The crack distributions for a longer period of time, such as 5 to 10 years, will be the net result of cracking which occurs during each of the N basic periods for which the exponential distribution holds. If these periods can all be represented by identical exponential distributions, i.e., N is common to each period, the final distribution at 10 or 15 years of service will be the Erlang distribution for which the density function is:

$$f(x) = \frac{(N\theta)^N x^{N-1} e^{-N\theta x}}{(N-1)!} \qquad x \geq 0$$

The principal unknown is N, the number of periods which must be added together. This model does not make provision for changing probabilities as the crack count accumulates, nor does it make provision for increases in expected cracking due to the upward secular trend in traffic volumes.

The easiest way to generate the exponential distributions required is to produce rectangularly distributed random numbers X_m and transform to exponentially distributed random numbers by $X'_m = -\frac{\ell n X_m}{N\theta}$. Since $\frac{1}{N\theta}$ is also the expected value, λ of each exponential distribution, it can be estimated from

$$\hat{\lambda} = 0.00125 T^{0.63}$$

If we define the period length measured from the 5-year survey as $t_{15} = \frac{10}{N}$ for the 15-year prediction, and $t_{10} = \frac{5}{N}$ for the 10-year prediction, we have:

$$X'_m = \frac{-0.0125}{N} \left\{ T \left[1 + \frac{1.30}{N} \right]^{0.63} \right\} \ell n \, X_m \qquad (3)$$

for the 10-year data, and

$$X'_m = \frac{-0.00625}{N} \left\{ T \left[1 + \frac{0.65}{N} \right]^{0.63} \right\} \ell n \, X_m \qquad (4)$$

for the 15-year data. These formulas assume an average traffic figure composed of the initial and final volumes for each period.

One-hundred values for X'_m according to Eqs. (3) and (4) were generated for $N = 1, 2, \ldots, 15$ for both the 10 and 15-year predictions. X'_m random variables were then added together to form the appropriate sums $\sum_{i=1}^{n} X'_m$. As with Model I, a value of N was sought which minimized S^2 for each survey period.

Model V - Summed Exponential Distributions with Flexible Parameters

The assumption of equal expected values for each basic exponential distribution is probably overly restrictive when one considers that λ may decrease as the number of cracks per slab approaches saturation (a phenomenon that would affect the distributions belonging to the later periods). Also, as previously noted, traffic volume increases over time so that the later periods might experience more cracking due to this cause. These opposing factors probably have a joint result that makes the equal distri-

bution assumption unrealistic. For Model V, this assumption was relaxed so that one no longer would expect an Erlang distribution by the time 10 or 15 years have passed.

In order to accommodate the secular trend in traffic increase, the following formulas were developed:

$$X'_m = \frac{-0.0125}{N} \left\{ T \left[1 + \frac{1.30(2i-n)}{N} \right]^{0.63} \right\} \ln X_m$$

for the 15-year data, and

$$X'_m = \frac{-0.00625}{N} \left\{ T \left[1 + \frac{0.65(2i-1)}{N} \right]^{0.63} \right\} \ln X_m$$

for the 10-year data, where $i = 1, 2, \ldots, N$ are used to expand the 5-year traffic volume according to the sequence number of each period. The X'_m were added together as in Model IV and again minimum S^2 was the criterion upon which N was selected.

All models are compared in Table 2 using the same highway projects for both 10 and 15-year field survey data.

TABLE 2
MINIMUM S^2 FOR ALL 8 LANES

Model	10 Years	15 Years
I - Markov Chain permitting only 0 or 1 crack per transition period	0.32	0.43
II - Markov Chain with Poisson rows	0.73	0.48
III - Poisson process	0.53	0.56
IV - Erlang distribution	0.58*	0.48*
V - Sum of dissimilar exponential distributions	0.58*	0.48*

*Both Models IV and V achieved minimum S^2 for $N = 1$.

For the 15-year comparisons, all models did about equally well, with Model I giving the smallest S^2. For more short-run predictions, i.e., for 10-year cracking, there was enough spread in S^2 between models to permit some relative evaluation. Models IV and V gave identical S^2 values because

the minimum S^2 occurred for N = 1 in both cases, even though Model V achieved smaller S^2 values in general. It is presumed that for longer duration predictions, e.g., to the 20 or 25-year survey times, optimal N's greater than 1 would be found for these models.

Technically, Model I achieves the smallest S^2 for both time periods, and is, therefore, presented with field data in Figure 20. These plots of actual vs. predicted slab counts for crack categories 0 through 6 show that Model I appears to work well for both 10 and 15-year predictions for some lanes but not for others. The reasons for this could be the paucity of traffic volume data or that traffic is not a principal variable in transverse crack formation. It is also possible, of course, that we have oversimplified the cracking process in our model selections. As mentioned earlier, both the 10 and 15-year crack probabilities are generated from only a single 24-hr total traffic count for each project. These figures were further broken down into lane volumes by the method developed in this report. The extent to which the resultant volumes do not faithfully represent the traffic history of each lane will, of course, be reflected in crack distribution prediction error for both the 10 and 15-year performance surveys. Further, it should be recalled that traffic volume was the only input variable considered in these analyses. No doubt materials and soils are not only relevant, but play a large part in determining the cracking patterns of these highways. Nevertheless, work with Model I looked promising, and it was decided to pursue this type of model with all construction projects for which 5, 10, and 15-year survey data were available. The main problem with Model I was the indeterminent nature of the transition interval. While the eight lanes together yielded an optimal time span of about two months, it is doubtful that a large body of data containing 30 to 40 construction projects would produce an optimal transition period value which would be close to ideal for each project. Therefore, the following in-depth studies of joints and transverse cracks are based on the assumption of continuous time, finite state, Markov processes. Furthermore, it was considered that existing traffic volume figures alone were too weak to constitute a predictor variable; therefore, it was decided that other variables must be considered if causal predictions are to be made.

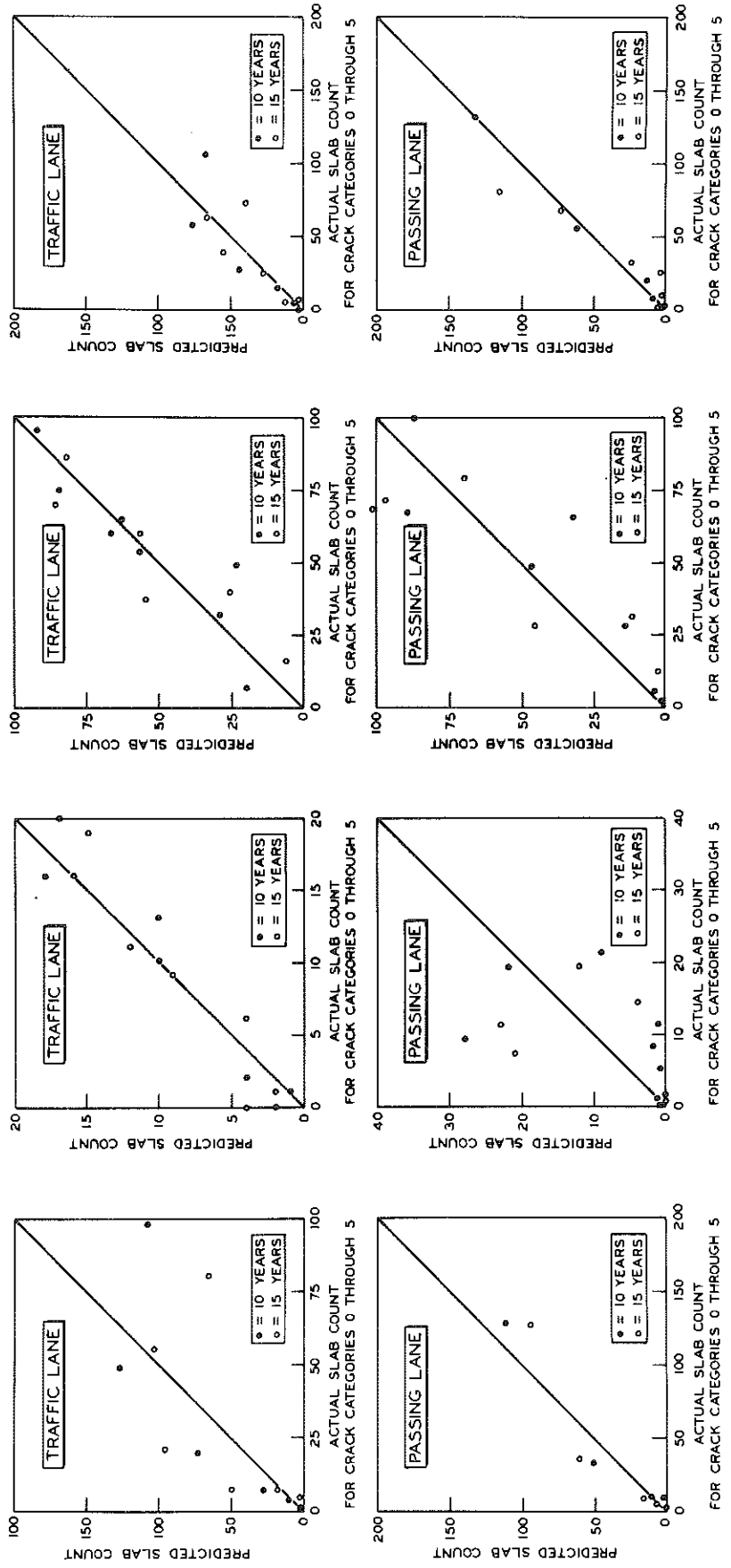

Figure 20. Actual vs. predicted slab count in six crack categories.

IV

THEORETICAL DEVELOPMENT OF PROBABILITY MODELS IN CONTINUOUS TIME

If we denote $P_{ij}(\tau,t)$ the conditional probability that the system at time t is in state E_j, given that at a previous instant τ the system was at state E_i, then crucial to the concept of a time non-homogeneous Markov chain are the following two assumptions (5).

(A) For every state E_n there exists a continuous function $\lambda_n(t) \geq 0$ such that as $h \longrightarrow 0$,

$$\frac{1 - P_{nn}(t,t+h)}{h} \longrightarrow \lambda_n(t)$$

uniformly in t.

(B) To every pair of states E_j, E_k with $j \neq k$ there corresponds transition probabilities $P_{jk}(t)$ such that as $h \longrightarrow 0$,

$$\frac{P_{jk}(t,t+h)}{h} \longrightarrow \lambda_j(t)\, P_{jk}(t)$$

uniformly in t and uniformly with respect to j for each fixed k. The $P_{jk}(t)$ are continuous in t, and for every fixed t, j, $\sum_k P_{jk}(t) = 1$ and $P_{jj}(t) = 0$. The probabilistic interpretation of assumption (A) is as follows: if at time t the system is in state E_n, then the probability that during $(t, t+h)$ a change occurs in $\lambda_n(t) + O(h)$. The $P_{jk}(t)$ in assumption (B) can be interpreted as the conditional probability that, if a change from E_j occurs during $(t, t+h)$, this change takes the system from E_j to E_k. The graphic interpretation of assumption (B) can be seen in Figure 21.

Assumptions (A) and (B) lead to the following forward differential equation:

$$\frac{\partial P_{ik}(\tau,t)}{\partial t} = -\lambda_k(t) P_{ik}(\tau,t) + \sum_{j \neq k} P_{ij}(\tau,t)\, \lambda_j(t)\, P_{jk}(t) \tag{1}$$

In joint deterioration and slab cracking processes it is reasonable to specify that a joint or slab cannot progress to an advanced state of deterioration without passing through each intervening state. We note also that it is impossible for joints or cracks to pass from a given state to a lower state; namely, we shall assume that:

$$P_{ik}(t) = \begin{cases} 1 & \text{if } k = i+1 \\ 0 & \text{otherwise} \end{cases} \tag{2}$$

Furthermore, a simple formulation which fits graphical plots of the data is:

$$\lambda_k(t) = a_k t^{\phi}, \quad a_k \geq 0 \tag{3}$$

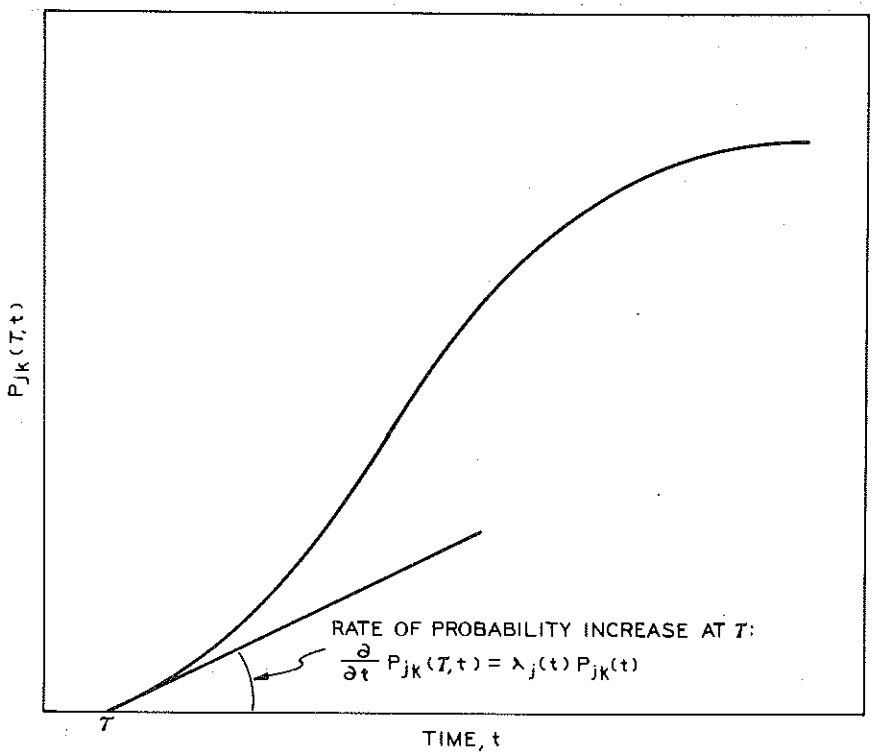

Figure 21. Growth of transition probability over time.

Where the a_k's are scaling coefficients and ϕ is a parameter which indicates the degree of time non-homogeneity. Note that if $\phi = 0$, the process is time homogeneous.

Applying Eq. (2) and letting $i = k$ in Eq. (1) we obtain,

$$\frac{\partial P_{ii}(\tau,t)}{\partial t} = -\lambda_i(t) P_{ii}(\tau,t) \tag{4}$$

which, together with the initial condition $P_{ii}(\tau,\tau) = 1$ gives the following result:

$$P_{ii}(\tau,t) = e^{-a_i h(\tau,t)}, \quad t \geq \tau \geq 0, \quad I = 1 \ldots N-1 \tag{5}$$

where N is the largest state in the system and

$$h(\tau,t) = \frac{t^{\phi+1} - \tau^{\phi+1}}{\phi+1} \tag{6}$$

It is clear that $P_{NN}(\tau,t) = 1$, for $t \geq \tau \geq 0$. Now, letting $k = i+1$ in Eq. (1) we obtain,

$$\frac{\partial P_{i,i+1}(\tau,t)}{\partial t} = -\lambda_{i+1}(t) P_{i,i+1}(\tau,t) + \lambda_i(t) P_{ii}(\tau,t) \tag{7}$$

Applying Eq. (5) to Eq. (7) and using the initial condition $P_{ij}(\tau,\tau) = 0$ for $i \neq j$ we see that for every $t \geq \tau \geq 0$ and $i = 1,\ldots,N-2$,

$$P_{i,i+1}(\tau,t) = \begin{cases} \dfrac{a_i}{a_{i+1}-a_i} e^{-a_i h(\tau,t)} + \dfrac{a_i}{a_i - a_{i+1}} e^{-a_i h(\tau,t)} & , a_i \neq a_{i+1} \\ a_i h(t) e^{-a_i h(\tau,t)} & , a_i = a_{i+1} \end{cases} \tag{8}$$

where $h(\tau,t)$ was defined in Eq. (6).

Similarly, letting $k = i + 2$ in Eq. (1) and so on (by induction) we obtain the following system of solutions of Eq. (1):

Case 1: All a_i's are distinct:

$$\begin{cases} P_{ii}(\tau,t) = e^{-a_i h(\tau,t)}, \quad t \geq \tau \geq 0, \; i = 1,\ldots,N-1 \\ P_{in}(\tau,t) = \displaystyle\sum_{j=i}^{n} \frac{a_j}{a_n} \left(\prod_{\substack{k=i \\ k \neq j}}^{n} \frac{a_k}{a_k - a_j} \right) e^{-a_j h(\tau,t)}, \quad N > n > i \geq 1, \; t \geq \tau \geq 0 \end{cases} \tag{9}$$

where $h(\tau,t)$ was defined in Eq. (6).

Case 2: Some a_i's are equal:

The solution of Eq. (1) in this case will be the limiting form of Eq. (9). For example, if $a_\ell = a_m = a_p$, $i \leq \ell, m, p \leq n$, then the solution of Eq. (1) takes the following form:

$$\begin{cases} P_{ii}(\tau,t) = e^{-a_i j(\tau,t)}, \quad t \geq \tau, \; i = 1,\ldots,N-1 \\ P_{in}(\tau,t) = \lim\limits_{\substack{a_p \to a_\ell \\ a_m \to a_\ell}} \displaystyle\sum_{j=1}^{n} \frac{a_j}{a_n} \left(\prod_{\substack{k=i \\ k \neq j}}^{n} \frac{a_k}{a_k - a_j} \right) e^{-a_j h(\tau,t)}, \quad N > n > i \geq 1 \end{cases} \tag{10}$$

These systems of Eq. (9) (and Eq. (10)) will be used, together with field data, to estimate parameters a_i and ϕ.

V

APPLICATIONS TO JOINT PERFORMANCE

The Problem

Because joint deterioration is a serious problem from both a roughness and maintenance standpoint, it is desirable to model, for predictive purposes, the deterioration process. A successful model would hopefully forecast such problem occurrences as blowups, and thereby afford an opportunity for preventive maintenance. It is unlikely that the large number of variables that affect joint deterioration would be tractable enough to allow an extract (deterministic) formulation of the problem. Under such circumstances, one often resorts to the prediction of probabilities, provided he can reasonably define states for the process. This type of predictive model is called stochastic, and often fits the real world quite well. In the case of joint deterioration, the first problem encountered in developing the model occurred in the measurement of deterioration, as discussed in Sections I and II.

Using the definitions of joint deterioration specified in Section II, a probability model was developed using only the 43 projects which had 5, 10, and 15-year surveys. This smaller set of projects was used rather than the full 128 because it was felt that 15 years of service was necessary to bring out reliable differences in project performance. To be sure, the model could be applied to all projects as long as one survey was available; however, for model development purposes, the longer histories of the 43 project set were considered to be a great advantage.

Development of the Model

It seems reasonable to assume that only the state of current joint deterioration determines the probability of progression to the next higher state. This is tantamount to assuming that the time history of deterioration is irrelevant as far as future behavior is concerned -- all one needs to know is the present slab state and the probabilities of further deterioration associated with each other state. From a stochastic process point of view, this assumption of lack of system memory is called the "Markov property" and, if applicable, suggests that the deterioration process may be considered as a Markov chain (7, 8, 9).

Putting the differential equations suggested by Eq. (7) Section IV into matrix form we have:

$$\frac{\partial}{\partial t}\,\mathbf{P}(\tau,t) = \mathbf{P}(\tau,t)\,\mathbf{A}(t) \qquad (1)$$

where:[4]

$$\mathbf{P}(\tau,t) = \left[P_{ij}(\tau,t)\right]_{ij} \quad \text{and} \quad \mathbf{A}(t) = \left[\lambda_{ij}(t)\right]_{ij}$$

If the $\lambda_{ij}(t)$ are constant for all time, the process will be time homogeneous. If the $\lambda_{ij}(t)$ change over time, the process will be time non-homogeneous. Because joints, like other physical structures, "age," it seems unlikely that joint deterioration would be time homogeneous. In fact, we found by using the chi-square test, that of 43 projects there were only seven projects accepted as time homogeneous at the 0.05 significance level. Examining these seven projects closely, we see that all seven show very little deterioration at 15 years of service life. It is clear that projects with little or no deterioration will not change enough to suggest time non-homogeneity. However, because the majority of projects could not be considered time homogeneous, we believe that even very good performing projects will become time non-homogeneous for longer service periods. Thus, we feel justified in using the time non-homogeneous Markov process for these data and feel that this assumption is warranted for any probability modeling of joint deterioration.

Notice, also, that it is impossible for joints to pass from a given state to a lower state. This requires that the matrices $\mathbf{P}(\tau,t)$ and $\mathbf{A}(t)$ be upper triangular -- a feature which makes it possible to solve the system of differential equations generated by Eq. (1). Now let us assume that in the case of joint deterioration it is reasonable to specify that a joint cannot progress to an advanced state of deterioration without passing through each preceding state. Consequently, all transition probability rates for which $j > i+1$ must be zero. Thus, $\mathbf{A}(t)$ now becomes:

$$\mathbf{A}(t) = \begin{bmatrix} -\lambda_{12}(t) & \lambda_{12}(t) & 0 & \cdots & 0 \\ 0 & -\lambda_{23}(t) & \lambda_{23}(t) & \cdots & 0 \\ \cdots & \cdots & \cdots & \cdots & \cdots \\ 0 & \cdots & \cdots & \cdots & 0 \end{bmatrix} \tag{2}$$

since $\sum_k \lambda_{jk}(t) = 0$ as discussed earlier. Because it was decided to classify joint condition into four classes, Eq. (2) is limited to a 4 x 4 matrix. All of these considerations define a special case of Eq. (1) which

---

[4] Note that λ_{ii} and λ_{ij}, $i \neq j$; correspond to λ_i and $\lambda_i P_{ij}$ of Section IV.

generates the following system of differential equations:

$$\frac{\partial}{\partial t} P_{11}(\tau, t) = -P_{11}(\tau, t)\, \lambda_{12}(t)$$

$$\frac{\partial}{\partial t} P_{12}(\tau, t) = P_{11}(\tau, t)\, \lambda_{12}(t) - P_{12}(\tau, t)\, \lambda_{23}(t)$$

$$\frac{\partial}{\partial t} P_{22}(\tau, t) = -P_{22}(\tau, t)\, \lambda_{23}(t)$$

$$\frac{\partial}{\partial t} P_{23}(\tau, t) = P_{22}(\tau, t)\, \lambda_{23}(t) - P_{23}(\tau, t)\, \lambda_{34}(t)$$

$$\frac{\partial}{\partial t} P_{33}(\tau, t) = -P_{33}(\tau, t)\, \lambda_{34}(t)$$

$$\frac{\partial}{\partial t} P_{13}(\tau, t) = P_{12}(\tau, t)\, \lambda_{23}(t) - P_{13}(\tau, t)\, \lambda_{34}(t)$$

The $P_{j4}(\tau, t)$ are known since $\sum_k P_{jk} = 1$

The preceding development does not specify the way in which the transition rates, $\lambda_{i,i+1}(t)$ vary with time. As mentioned before, aging very likely increases the probability that a joint in a given state of deterioration will pass to a higher state for the same time interval. Therefore, it would seem plausible that the $\lambda_{i,i+1}(t)$ would increase with time. A simple formulation that fits graphical plots of the data is:

$$\lambda_{12}(t) = \alpha t^{\phi} \tag{3a}$$

$$\lambda_{23}(t) = \beta t^{\phi} \tag{3b}$$

$$\lambda_{34}(t) = \gamma t^{\phi} \tag{3c}$$

where α, β, γ are scaling coefficients and ϕ is a parameter which indicates the degree of time non-homogeneity. Note that if $\phi = 0$ the process is time homogeneous, and if $\phi \neq 0$ the process is time non-homogeneous. Furthermore, we would expect that $\alpha > \beta > \gamma$ since a joint already in a highly deteriorated state can be expected to decay more rapidly to the next higher state. This specification of $\lambda_{i,i+1}(t)$ together with the initial conditions $P_{11}(\tau,\tau) = P_{22}(\tau,\tau) = P_{33}(\tau,\tau) = 1$ yield the following solutions to the system of equations when $\alpha \neq \beta \neq \gamma$:

$$P_{ii}(\tau, t) = e^{-\theta_i \int_{\tau}^{t} x^{\phi} dx} = e^{-\theta_i h(\tau, t)}, \quad i = 1, 2, 3$$

where: $\theta_1 = \alpha$, $\theta_2 = \beta$, $\theta_3 = \gamma$ and $h(\tau, t)$ was defined in Eq. (6) of

Section IV. Also:

$$P_{12}(\tau,t) = c_1(\tau)\, e^{\int_{\tau}^{t} x\Phi\, dx} + \text{particular solution},$$

which when solved gives:

$$P_{12}(\tau,t)\begin{cases} \frac{\alpha}{\beta-\alpha}\left[e^{-\alpha h(\tau,t)} - e^{-\beta h(\tau,t)}\right] & \text{if } \alpha \neq \beta \\ \alpha h(\tau,t)\, e^{-\alpha h(\tau,t)} & \text{if } \alpha = \beta \end{cases}$$

Similarly,

$$P_{12}(\tau,t)\begin{cases} \frac{\beta}{\alpha-\beta}\left[e^{-\beta h(\tau,t)} - e^{-\gamma h(\tau,t)}\right] & \text{if } \beta \neq \gamma \\ \beta h(\tau,t)\, e^{-\beta h(\tau,t)} & \text{if } \beta = \gamma \end{cases}$$

and,

$$P_{13}(\tau,t)\begin{cases} \alpha\beta\left\{\frac{e^{-\alpha h(\tau,t)}}{(\beta-\alpha)(\gamma-\alpha)} + \frac{e^{-\beta h(\tau,t)}}{(\gamma-\beta)(\alpha-\beta)} + \frac{e^{-\gamma h(\tau,t)}}{(\beta-\gamma)(\alpha-\gamma)}\right\} & \text{if } \alpha \neq \beta \neq \gamma \\ \alpha^2\left\{\frac{h(\tau,t)}{\gamma-\alpha} e^{-\alpha h(\tau,t)} + \frac{1}{(\gamma-\alpha)^2}\left[e^{-\gamma h(\tau,t)} - e^{-\alpha h(\tau,t)}\right]\right\} & \text{if } \alpha = \beta \neq \gamma \\ \alpha\beta\left\{\frac{h(\tau,t)}{\beta-\alpha} e^{-\alpha h(\tau,t)} + \frac{1}{(\beta-\alpha)^2}\left[e^{-\beta h(\tau,t)} - e^{-\alpha h(\tau,t)}\right]\right\} & \text{if } \alpha = \gamma \neq \beta \\ \alpha\beta\left\{\frac{h(\tau,t)}{\alpha-\beta} e^{-\beta h(\tau,t)} + \frac{1}{(\alpha-\beta)^2}\left[e^{-\alpha h(\tau,t)} - e^{-\beta h(\tau,t)}\right]\right\} & \text{if } \alpha \neq \beta = \gamma \\ \frac{(\alpha h(\tau,t))^2}{2!} e^{-\alpha h(\tau,t)} & \text{if } \alpha = \beta = \gamma \end{cases}$$

Estimation of Parameters

The problem now arises as to how to estimate α, β, γ and Φ. Since the expressions for $P_{ii}(\tau,t)$ and $P_{ij}(\tau,t)$ are non-linear, classical least squares techniques are not helpful. In the present case, a computer optimization procedure, using a modification of the steepest descent method was used (10, 11, 12). The procedure minimized the expression where the $P_{ij}(\tau,t)$ were proportions computed directly from the survey data. Additionally, each residual was weighted in proportion to the number of joints entering into the probability determination.

Results with Field Data

An attempt was made to estimate the model's four parameters by the non-linear least squares procedure for all the 43 construction projects surveyed at 5, 10, and 15-year intervals. Except for a small number of extremely good performing projects for which there was no appreciable deterioration at 15 years, estimates for α, β, γ, , and ϕ converged rapidly. In all cases the model's fit was within $S^2 = 0.10$ for the four probabilities x three survey years x 43 projects = 516 data points (Figs. 22 through 25). Examples of state probability history curves for several particularly good and poor performing projects are shown in Figures 26 and 27. Figure 28 shows the expected (average) state histories for the same two projects. Note that the probabilities for States II and III of the poor performing projects peak at about 11 and 13 years and then decline. This is because joints are not entering States II and III as fast as they are leaving these states for State IV. State IV, being a terminal or absorbing state, naturally accumulates joints with time until all joints are finally in this state. Similar graphs for all projects are included in the Appendix.

It is also interesting to note that $\hat{\alpha} < \hat{\beta} < \hat{\gamma}$ as expected. Thus, a joint is more likely to deteriorate to the next highest state if it is already in a deteriorated condition. Distributions of $\hat{\beta}/\hat{\alpha}$ and $\hat{\gamma}/\hat{\alpha}$ are shown in Figure 29. Since $\hat{\gamma}$ was generally greater than $\hat{\alpha}$ or $\hat{\beta}$, one would presume that State III joints would be the ones most likely to progress to State IV. Therefore, if a State IV (mostly blowups) prediction is desired, a good strategy would be to look for joints in State III. Because the model will predict the probability of a State IV condition given the State III condition for any elapsed time, one can compute State IV probability curves once α, β, γ and ϕ have been estimated from earlier performance data (or possibly environmental and materials variables). Figure 30 shows, for an arbitrary construction project, the cumulative probability of State IV occurring given that the joint was in State III at the selected τ times of 1, 11, and 15 years. Notice the rapid rate of increase in probability as τ increases. For example, if a joint is in State III at 1 year $(\tau = 1)$, it takes just over 12 years before the occurrence of State IV has reached a probability of 0.50. However, if the joint is in State III at 11 years $(\tau = 11)$, in only three years time the probable occurrence of State IV will have reached 0.50. These curves will not give good forecasts of blowup probability unless α, β, γ and ϕ are reliably estimated from early performance data for each project itself, or from a group of relevant causal variables, or both.

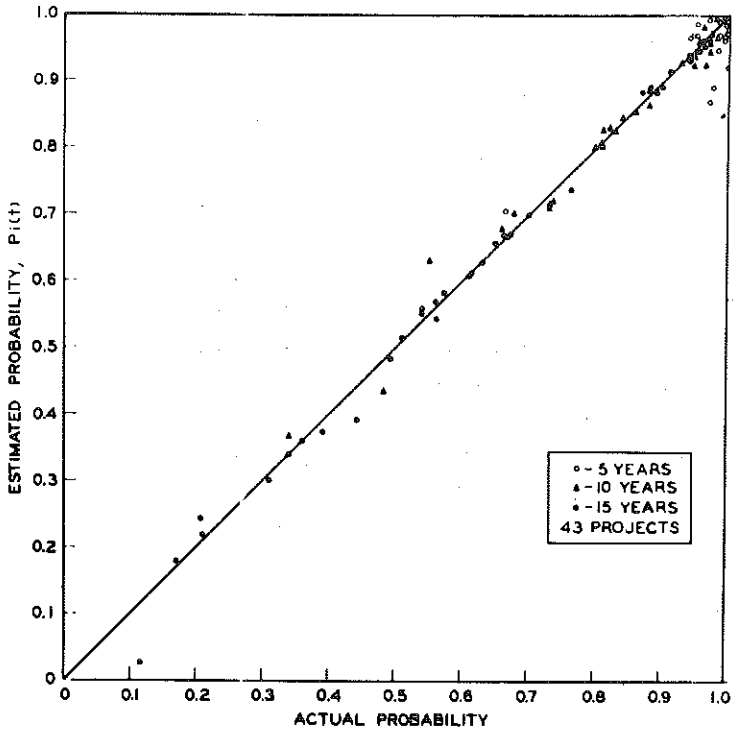

Figure 22. Actual vs. predicted probabilities for joint transition $P_{11}(o,t)$.

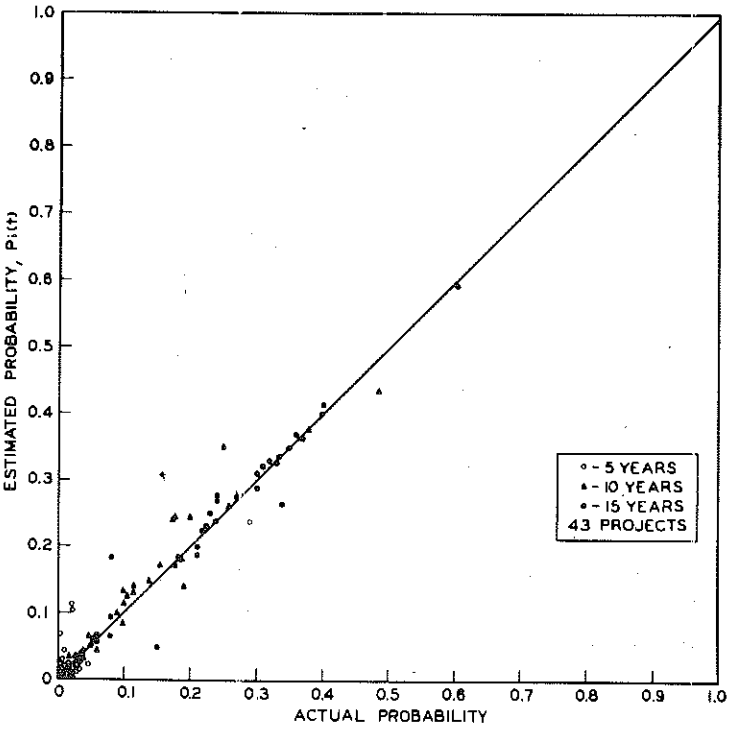

Figure 23. Actual vs. predicted probabilities for joint transition $P_{12}(o,t)$.

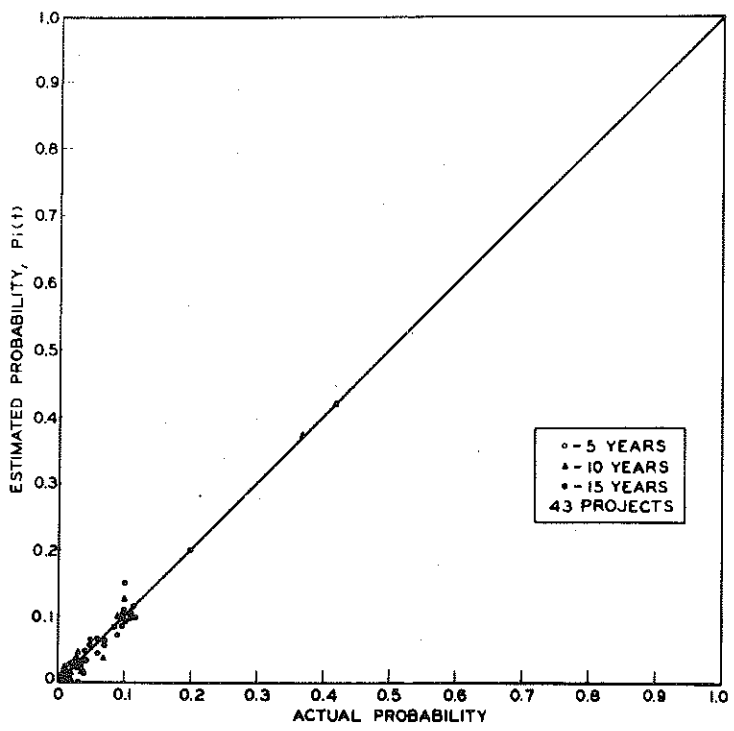

Figure 24. Actual vs. predicted probabilities for joint transition $P_{13}(o,t)$.

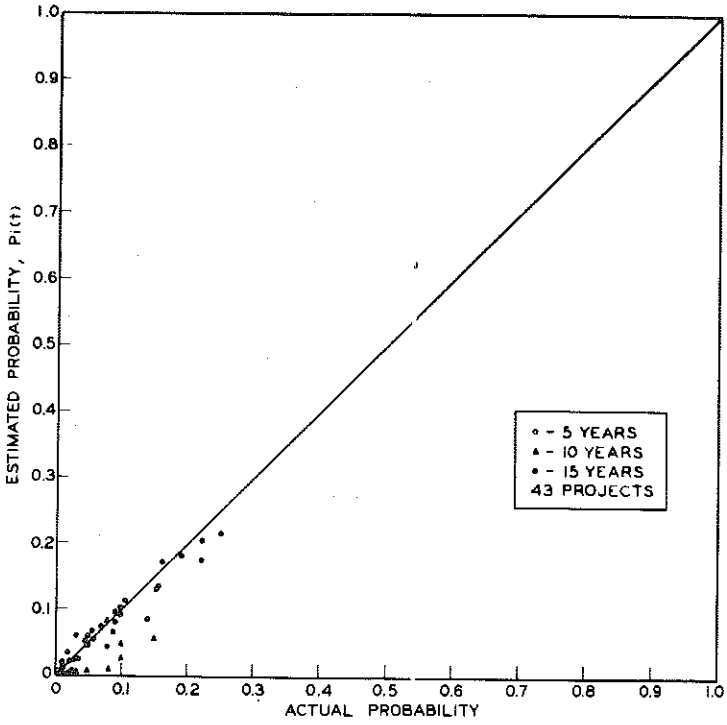

Figure 25. Actual vs. predicted probabilities for joint transition $P_{14}(o,t)$.

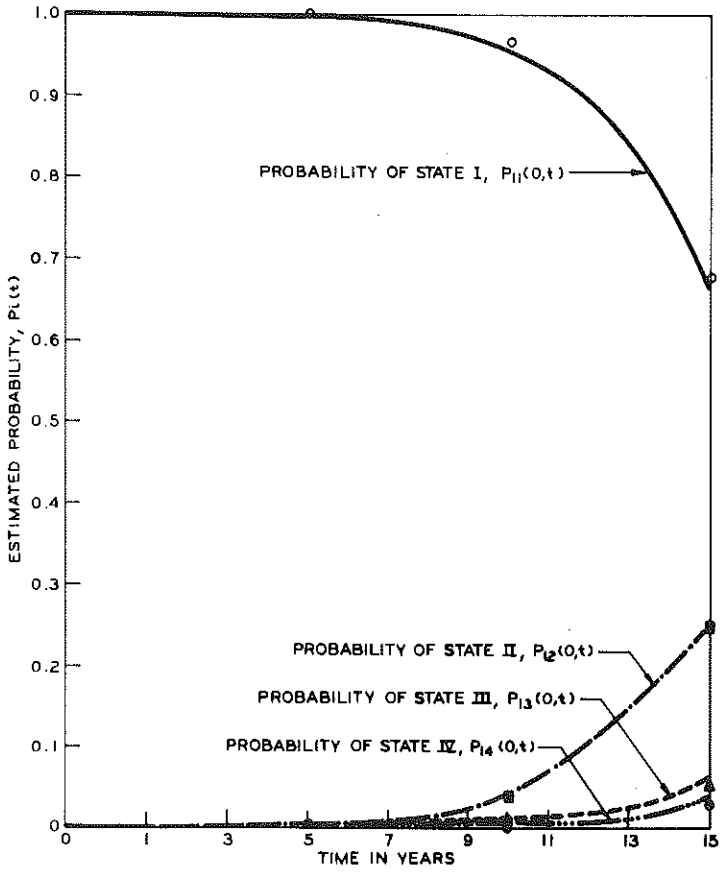

Figure 26. Time history of various transition probabilities for a relatively good project.

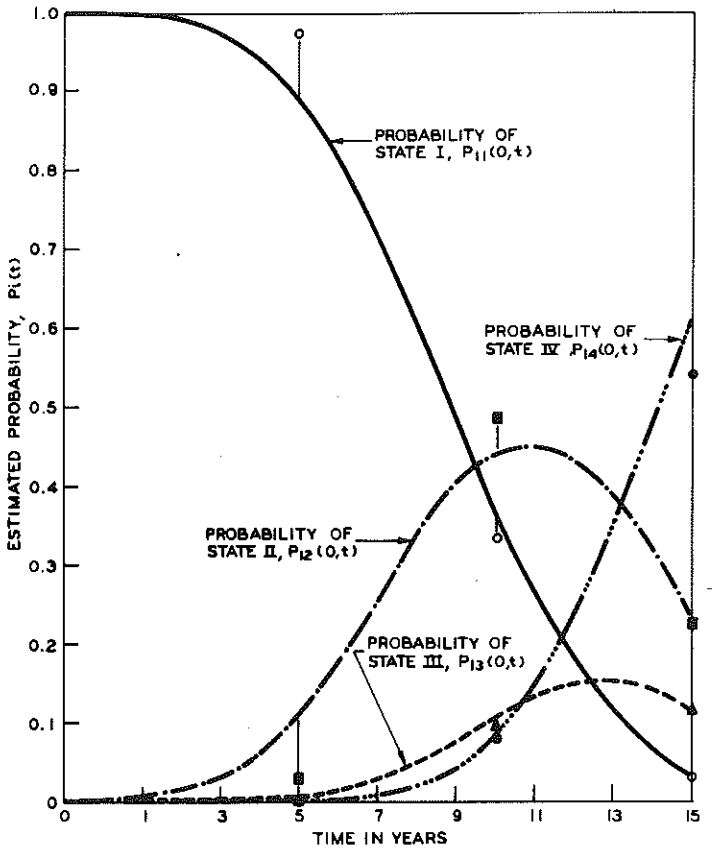

Figure 27. Time history of various transition probabilities for a relatively poor project.

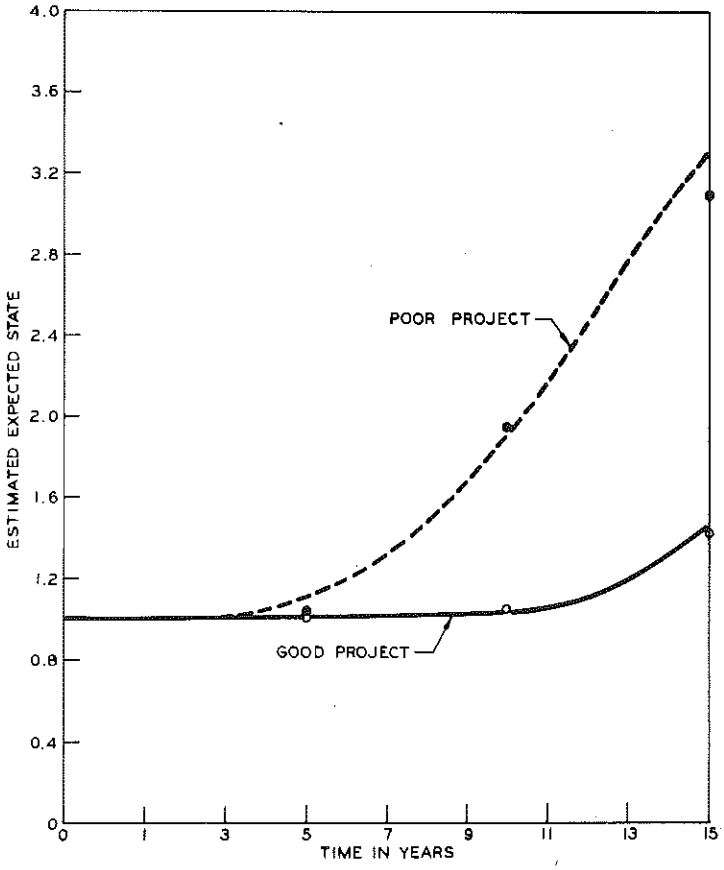

Figure 28. Growth of actual and estimated expected state over time.

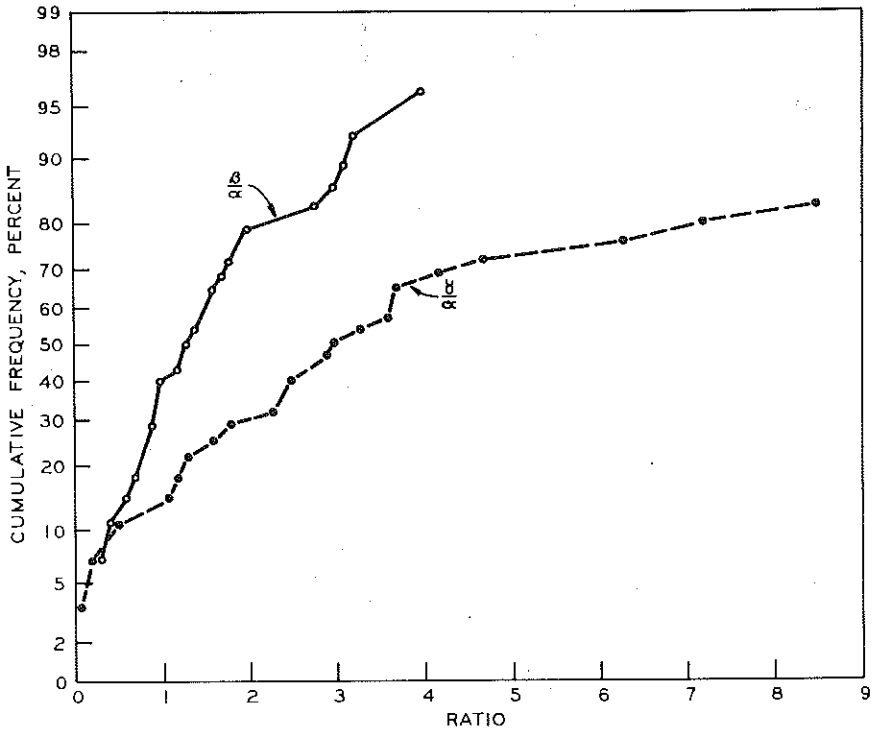

Figure 29. Cumulative distributions for β/α and γ/α ratios.

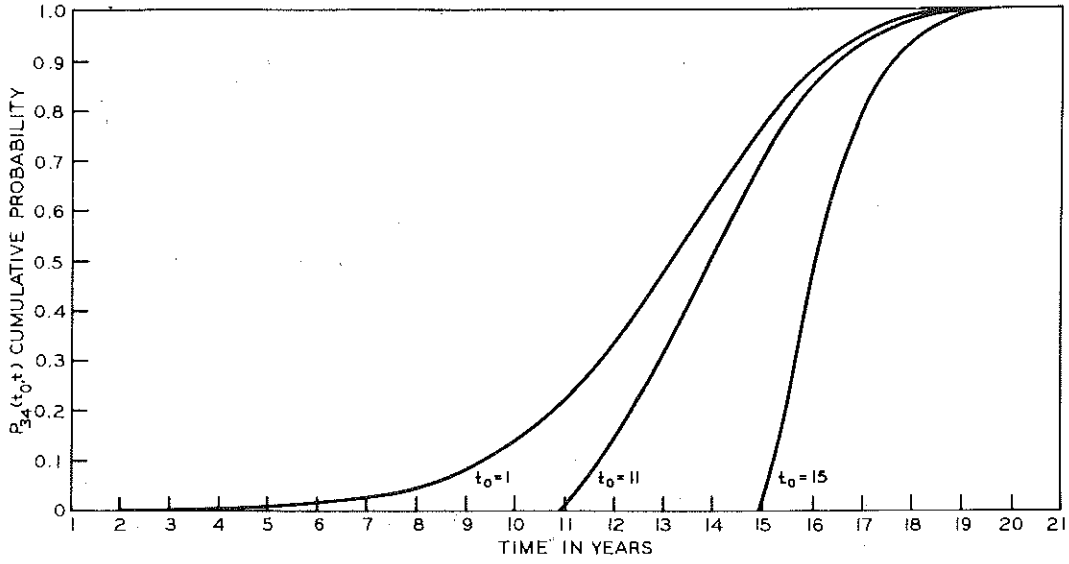

Figure 30. Example of transition probability growth $P_{34}(t_0,t)$ over time.

As discussed earlier, ϕ is a measure of the time non-homogeneity of the process. Figure 31 shows the frequency distribution of $\hat{\phi}$ for the 43 projects for which ϕ was estimable. Notice that $\hat{\phi}$ varies from about 0.20 to 5.83, with a median value of about 2.3. Thus, our hypothesis concerning time non-homogeneity is tenable, particularly since most $\hat{\phi}$ are significantly greater than 0 (α level = 0.05, as tested by a linearized t-test).

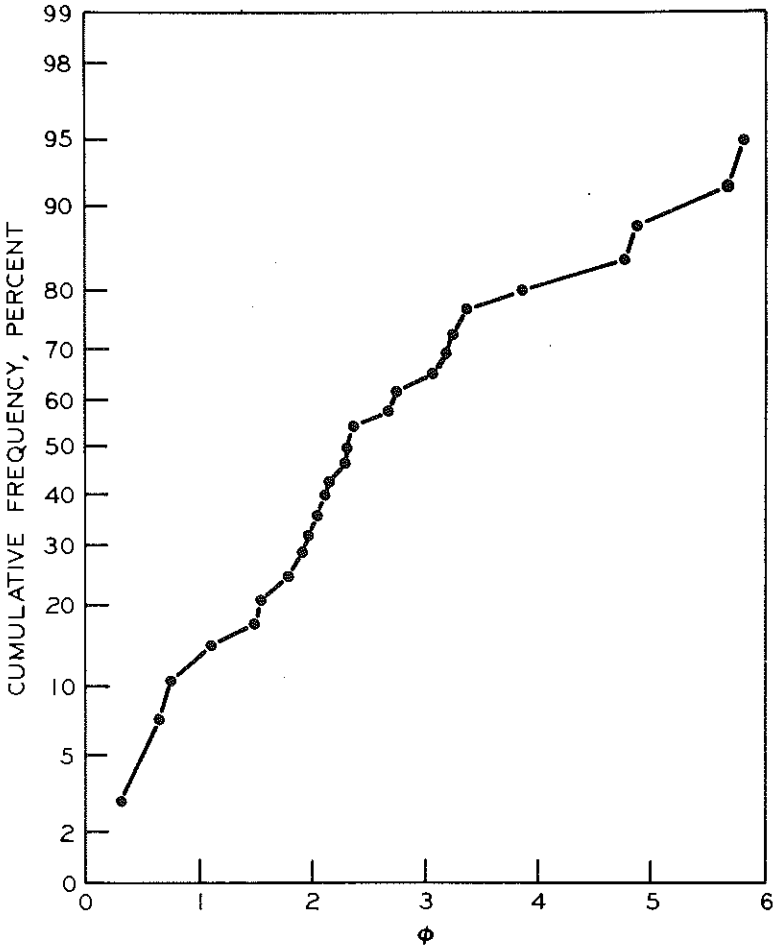

Figure 31. Cumulative distribution of parameter ϕ

Correlation with Causal Data

Because both traffic and percent soft, non-durable materials in the coarse aggregate have been implicated in structural deterioration (1, 6), these potential causal variables were examined in relation to each project's

performance. A new variable, temperature, was also included because it was thought that very high summer temperatures could hasten joint deterioration, particularly the passage into State IV which, of course, is primarily blowups. The temperature variable was developed on the basis of the total number of days between 1956 and 1963 when the maximum temperature exceeded 90 F, as measured by the nearest U.S. weather station. Thus, a trichotomous variable was defined as:

0: total days between 0 and 40 F
1: total days between 41 and 80 F
2: total days between 81 and 120 F

Similarly, the traffic variable was defined as:

0: ADT between 0 and 2,000, averaged over the same period
1: ADT greater than 2,000, averaged over the same period

Previous research (1) showed that percent soft, non-durable material in the coarse aggregate tended to be associated with general pavement deterioration (an index based on all slab and joint performance variables, not joints alone). Efforts were made in the present study to explore the effects of soft, non-durable material on joint deterioration. However, only a few records of soft, non-durable material percentages could be found for the projects of this period. Consequently, a more primitive basis of estimation had to be used. It was noted (1) that percent soft, non-durable material was highest for those aggregates that were composed of non-quarried limestones and gravels in about equal proportions. Moreover, soft, non-durable particles tended to be absent from aggregates containing either a high percentage of gravel or limestone. Extreme examples would be pure silicious rock and crushed dolomite. Therefore, based on overall pit estimates of percent limestone, the following materials variable was defined:

0: either 0 to 10 percent carbonate, or 80 to 100 percent carbonate in the pit, exclusing crushed limestone
1: between 10 and 80 percent carbonate in pit, or crushed limestone

Thus, projects constructed from pits containing relatively homogeneous gravels were assigned a value of 0, and those constructed from pits containing gravel-limestone mixes or crushed limestones were assigned a value of 1. Admittedly, this is a very crude measure; however, in the absence of better data it did differentiate projects on the basis of a materials variable previously found to be important. All the variables showed correlation with expected state, E(s); however, since in Michigan these causal variables

turn out to be highly intercorrelated, one cannot easily judge which variables are important. The only relevant statistical procedures which take account of independent variable intercorrelations and make decisions of the inclusion or exclusion of these variables, are the stepwise multiple regression techniques. These techniques accept only those variables that make a 'significant' contribution to the extimation of the dependent variable in the context of the other independent variables.

In the present case, the dependent variable could be either α, β, γ or ϕ. This is too many parameters for an unambiguous analysis. Moreover, where only 5 and 10-year data were used to predict 15-year performance, using four independent parameters, the results were somewhat unstable. However, it was noted that the four parameters were not independent, but rather highly correlated with ϕ.[5]

$$\alpha = \exp\left(-\frac{\phi + 0.7481}{0.3638}\right)$$

$$\beta = \exp\left(-\frac{\phi + 0.6118}{0.3629}\right)$$

$$\gamma = \exp\left(-\frac{\phi - 0.3318}{0.3013}\right)$$

When functions reflecting these correlations were used (thereby requiring the optimization of only a single parameter) the 15-year predictions settled down statistically and facilitated the single parameter estimation sought.

Thus, the problem was to predict ϕ from potentially causal variables so that future performance could be estimated. The ideal model would enable performance predictions to be made only from causal data at any time during or before the service life. However, it was not felt that the causal data were good enough by themselves to adequately satisfy this goal (traffic data were based on only one 24-hour sample per year, and percent carbonates were estimated from very general geological knowledge and experience with each pit). Therefore, it was decided to also include early performance as an additional independent variable. Since many projects do not show much joint deterioration before 10 years, this period was used as

---

[5] The introduction of these relationships complicates the interpretation of ϕ as a measure of time homogeneity.

a basis for post 10-year predictions. The general form entered into the stepwise regression procedure was then,

$$\hat{\phi} = \beta_1 \phi + \beta_2 M + \beta_3 V + \beta_4 T + \beta_5$$

where: $\hat{\phi}$ = each project's single performance parameter based on 5, 10, and 15-year data.

ϕ = the same as $\hat{\phi}$ except that it is based on 5 and 10-year data only

M = the 0, 1 materials variable

V = the 0, 1 traffic variable

T = the 0, 1, 2, temperature variable

$\beta_1 \ldots\ldots \beta_5$ = fitting coefficients

The stepwise procedure accepted ϕ as the best predictor of $\hat{\phi}$. However, significant improvement in prediction was possible when M was entered in addition to ϕ, while T and V provided no significant improvement over ϕ and M. Also, slightly better results were obtained with log $\hat{\phi}$. Therefore, the traffic and temperature variables were rejected and ϕ and materials were retained in the following equation:

$$\log \hat{\phi} = \beta_1 \log \phi + \beta_2 M + \beta_3$$

where: $\beta_1 = 1.11$

$\beta_2 = -0.56$

$\beta_3 = 0.42$

The multiple correlation coefficient ρ was 0.96 for the above specification using 43 projects, suggesting that 5 and 10-year performance, together with some knowledge of coarse aggregate type, is sufficient to estimate a single performance parameter characterizing the first 15 years of service life (Fig. 32).

Of particular interest, is the prediction of 15-year State IV probabilities from 5 and 10-year data. This is because State IV is primarily blowups. Figure 32 also shows State IV predictions for which the multiple correlation is 0.87. Thus, it should be possible to predict the proportion of joints in

State IV at 15 years from knowledge of the coarse aggregate pit composition and the 5 and 10-year condition survey data. This is important since virtually no blowups occur by 10 years, so that one cannot extrapolate later blowup problems from earlier blowup occurrence alone. The model, however, provides a basis for blowup prediction even though few, if any, blowups have occurred by the time of the prediction. An interesting case is provided by Project 44-33-C2. This project exhibited good joint performance at 5 years with all of the 120 joints in State I, except for three in State II. By 10 years, some joints showed a fair amount of spalling, and 10 were in State IV, including four known blowups. By 15 years, spalling had increased sharply, and 68 joints, including 26 known blowups, were in State IV. Based on the first 10 year's performance, and materials knowledge, the model predicted that by 15 years 59 joints would have passed into State IV. This particular project also had a 20-year survey. By 20 years, 89 joints were in State IV. It is presumed that most were blown, but the exact number could not be determined since all 89 were replaced with concrete or bituminous patches by the time of the survey. The model's 20-year estimate of State IV joints based on only 10 years survey experience and materials data was 84, or 5 less than that which actually occurred 10 years hence. However, since 15 to 20-year field experience was not generally available and could not be used in the determination of $\hat{\phi}$, it is not recommended that 20-year forecasts be made from this model. When 20 year experience becomes available, it can of course, be incorporated into the model. Complete joint condition frequency distributions for 15 years of service based on only 10-year experience are presented in the Appendix. However, a general idea of the model's fit can be obtained from Figure 33 which shows the 15-year expected (average) state, again based on 10-year data and materials information. As can be observed from Figure 33, most projects' expected states are predicted fairly well with an overall correlation of 0.93.

Relationship Between ϕ and δ

In Section II, the performance of each of 128 projects was summarized by the index, δ. This parameter, it will be recalled, governed the rate of logistic growth of expected state or average joint condition. In the present section, 43 projects were examined under the specification of a Markov process and joint performance parameters ϕ, α, β and γ were developed. Because these parameters were intercorrelated α, β and γ were estimated as functions of ϕ for final analysis with the model. The question now arises as to the possibility of a relationship between ϕ and δ. If ϕ can be estimated from δ, then one need not go through the elaborate procedures of optimization of conditional probabilities used in this section. Rather, one need only compute the average or expected

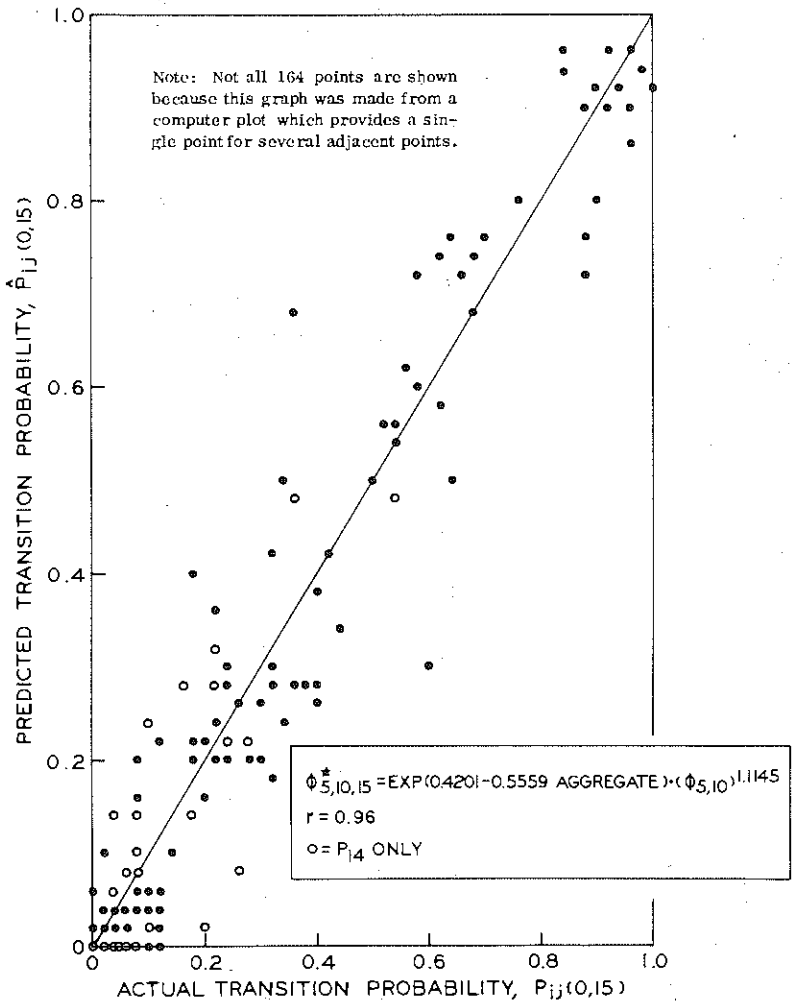

Figure 32. Actual vs. predicted transition probability using ϕ * only.

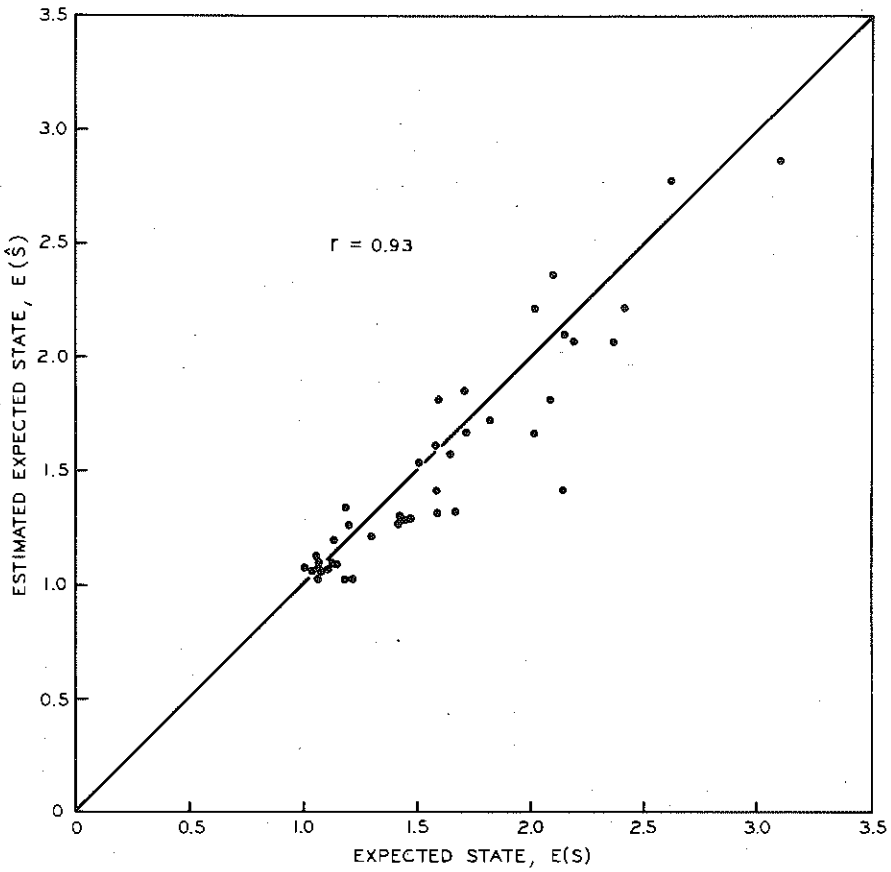

Figure 33. Relationship between actual and predicted state using ϕ * only.

state of each project for the time periods surveyed and fit the logistic growth function. This procedure also implies that the process of joint deterioration is similar for all projects -- all one needs to know is the expected state at several time intervals to generate all conditional probabilities including those pertaining to State IV (blowups). Thus, the logistic growth of average state (δ) determines the passage patterns of all states and can be used to predict future frequencies of these states.

The relationship between ϕ and δ is shown in Figure 34. Notice that the fit is quite good for the function used. If one made use of this relationship, he would forecast joint behavior as shown in Figure 35.

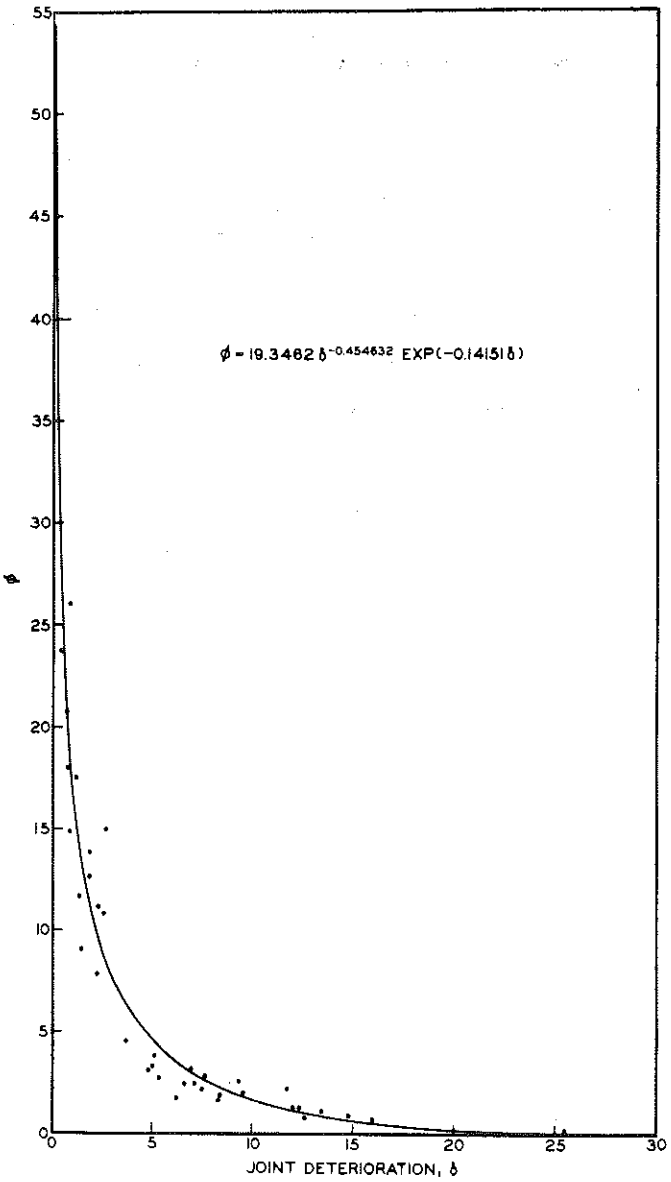

Figure 34. Relationship between ϕ and δ

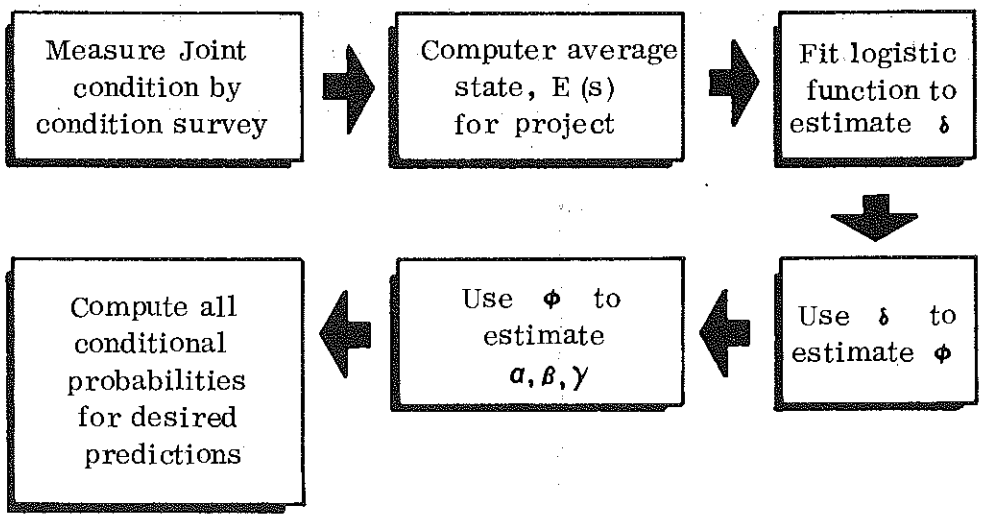

Figure 35. Simplified Procedure for Predicting Joint Deterioration.

VI

APPLICATIONS TO TRANSVERSE CRACKING

The experience gained in modeling joint deterioration facilitated the application of similar modeling procedures to transverse slab cracking. The cracking model was both more complex and more simple. Rather than a limited number of states, such as the four determined for joint deterioration, we find that there is no theoretical limit to the number of transverse cracks per slab. Thus, the transition matrix could have an infinite dimension. In practice, however, one rarely encounters more than 15 transverse cracks per slab, at least during the first 15 years of service life[6].

State 1: no transverse cracks in a slab
State 2: one transverse crack in a slab
. . . . . .
State 16: 15 or more transverse cracks in a slab

Using these definitions, the model form was that of Section IV with N = 16.

The cracking process was simpler than the joint deterioration process in the sense that a crack is an obvious, easily measured deterioration variable. Unlike joint deterioration, cracking did not require the mixing of fundamental survey variables (such as corner spalls, patching, corner breaks, etc.) to provide a deterioration variable amenable to sensible measurement[7]. Therefore, the crack model's predictions could easily be interpreted since it treats only one simple fundamental survey variable.

The development of Section IV requires n + 1 parameters (one for each state, plus one to regulate time non-homogeneity). This requirement clearly would "over parameterize" the crack model since 16 parameters would be required. This circumstance would not only make optimization difficult, but would seriously impair parameter reliability and, consequently, any future interpretation or causal analysis. Moreover, it stands to reason that at least the 16 state parameters would be related. The general nature of

---

[6] For a crack to be counted as a transverse crack, it had to be within a 45-degree angle to the transverse dimension and be at least 5 ft long. Thus, cracks that did not completely traverse the slab width were counted as full cracks.

[7] Recall that sensible measurement was not possible with fundamental joint survey variables such as spalls because: 1) different types of deterioration affected the same joints (spalling, patching, corner breaks, etc.), and, 2) as spalls enlarged with time they tended to merge, thus decreasing their number. Thus, spall count does not make sense as a deterioration measure since unlike deterioration it does not monotonically increase with time.

this relationship can be reasoned as follows. When a slab is constructed, it is automatically in State 1 (no cracks). It takes some time before settlement, traffic, frost heave (if any), etc., affect crack formation. Therefore, the probability of passing from State 1 to State 2 is low. More important, a State 1 slab surviving a number of years will probably continue in this state since its uncracked survival suggests that base and subbase soil conditions are good enough to allow the slab to withstand whatever traffic loading it encounters. However, once a slab has passed from State 1 to State 2 by cracking once, the implication is that further cracking is more likely to occur since conditions sufficient to allow at least one crack must already exist. Therefore, passage from State 2 to State 3 may be more probable than passage from State 1 to State 2. Nevertheless, the former probability will still be fairly low because settlement, etc., is still occurring. After some time, settlement effectively stops and the slab becomes so cracked that loading stress is essentially relieved; the average distance between cracks being only a few feet. At this point, the slab is more or less crack saturated and the probability of further cracking decreases to a point where an additional crack is very improbable. The general quantitative relationship of state transition probabilities, if the above reasoning is correct, should look something like the function in Figure 36.

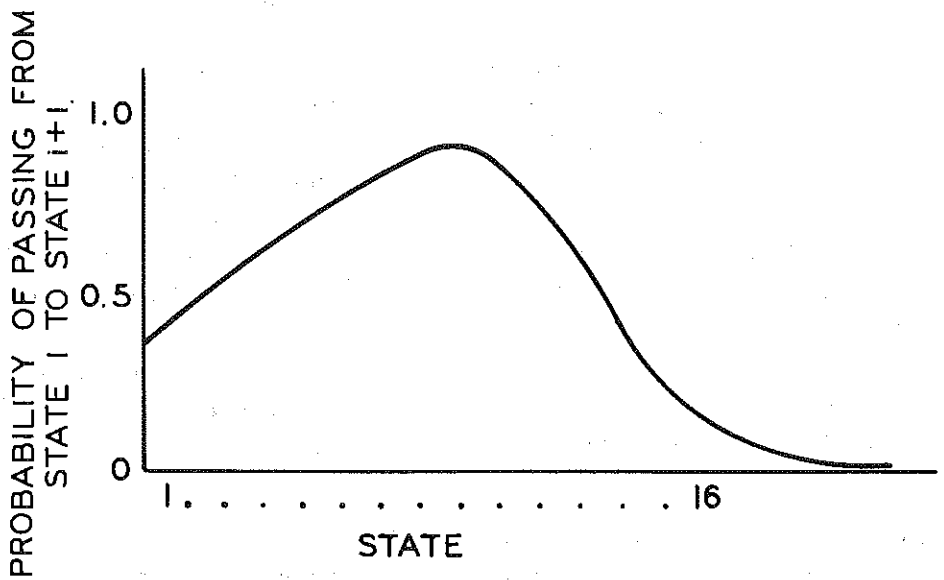

Figure 36. Hypothesized transverse crack transition function.

Formal provision for this reasoning was built into the model by specifying a polynomial of the form:

$$a_i = (a_i^2 + b_i + c)^2$$

With this form, the relationship between the states suggested by Figure 36 is possible, as well as simpler forms such as a constant or straight line. Notice that squaring the entire expression guarantees that the function will never be negative; i.e., that the probability transition rates are always positive. This must be so, since negative probabilities are not defined. Optimization of the crack model was now possible with a reduced set of parameters (from 16 to 4).

After optimizing most of the 43 projects, it became apparent that the majority of polynomials turned out to be of the expected form; that is, with state transition probabilities rising to a maximum value after which they decrease sharply and approach zero. Closer examination of these polynomials, which we shall call "transition polynomials," revealed that all of them were closely symmetric and could be well approximated with a bell-shaped curve[8]. Thus, the transition polynomial typically turned out as shown in Figure 37, with the maximum transition probability often occurring around States 4 or 5.

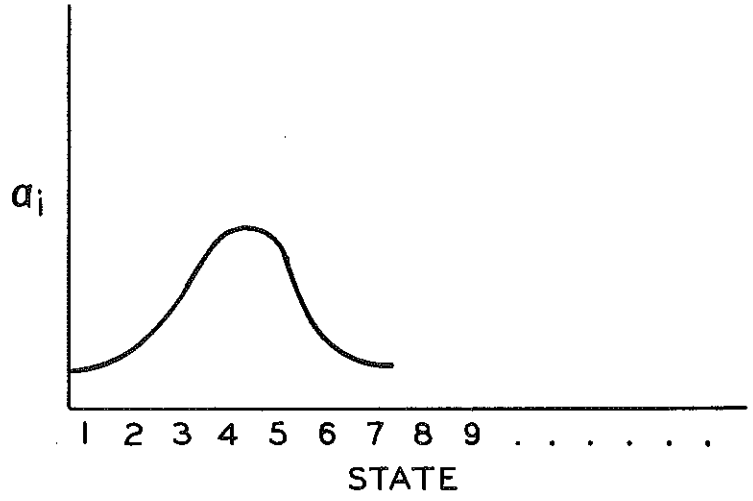

Figure 37. Experimentally derived transverse crack transition function.

[8] The term "bell-shaped," rather than "normal," is used here to avoid confusion with the normal density function which, of course, the transition polynomial is not.

Re-optimization of the 43 projects with the bell-shaped curve specification provided as good results as the polynomial optimization and also provided the additional benefit of more meaningful parameters[9]. Results of the bell curve optimization are shown for each project in the Appendix. It is not understood why this particular form specifies the behavior of the crack state transitions; hence, further examination of these curves in connection with construction and environmental variables is required. However, it can be said that slabs in a low state (such as 1, 2, or 3) have a relatively good chance of remaining in that state for a specified time interval; slabs in an intermediate state (4, 5, or 6) are unstable and have a relatively good chance of cracking further within this interval; and slabs in a high state (such as 7, 8, or over) will probably not crack again for some time. In other words, slabs that are either not cracked or slightly cracked are somewhat stable; slabs that are moderately cracked are unstable, and slabs that are highly cracked again tend toward stability. Also, projects exhibiting the bell-shaped curve for probability transition rates had what can be termed a 'critical state,' designated as State C. This state was the most unstable; hence the most short-lived. Thus, slabs with the critical number of cracks will probably crack again before any other slabs in the project. The critical crack number for each project is plotted as a function of time in the Appendix.

There are various ways of evaluating the model's fit to survey data. Included in the Appendix are:

1) The probabilities of all or selected states over time. Because presentation of all 16 states would be cumbersome, States 1 and C are presented. The behavior of State 1 is interesting since it specifies the probability of a slab remaining uncracked as service life progresses.

2) The actual and fitted crack distributions at some point in time, such as 15 years.

3) The plot of actual vs. estimated probabilities for all states of all survey times for each project. This gives perhaps the best feeling for the model's ability to reproduce field experience. As can be seen from these plots, the model does very well for many projects, moderately well for some, and only fairly well for a small number.

---

[9] The polynomial coefficients are not easily interpreted, whereas the bell curve parameters (mean and standard deviations) are easily related to the curve's form and to interpretation. For example, the mean designates the most unstable state.

4) Expected average number of cracks vs. time for the three survey years. The expected state indicates the number of cracks per slab, which on the average one would expect to find for any survey time. As can be seen from these graphs, the model traces most crack histories quite well. These histories are extrapolated beyond 15 years, and when 20-year survey data become available these predictions can be evaluated.

5) The actual expected state vs. the predicted expected state for years for which any slabs remain uncracked. The fit in this case will not be as good as in the other plots since for some plotted probabilities, such as P_{ij} (10, 15), the probability of going from one crack at 10 years to j cracks at 15 years is based on a small number of slabs and is, therefore, not very reliable. All project plots of these probabilities and expected states are presented in Figures 38 and 39. As can be seen from these plots, most probabilities are reasonably well estimated. Most probabilities which are poorly estimated are based on a very small number of slabs in State 1 (no cracks) at times other than t = 0, such as t = 5, or t = 10. These probabilities could be expected to be unreliable.

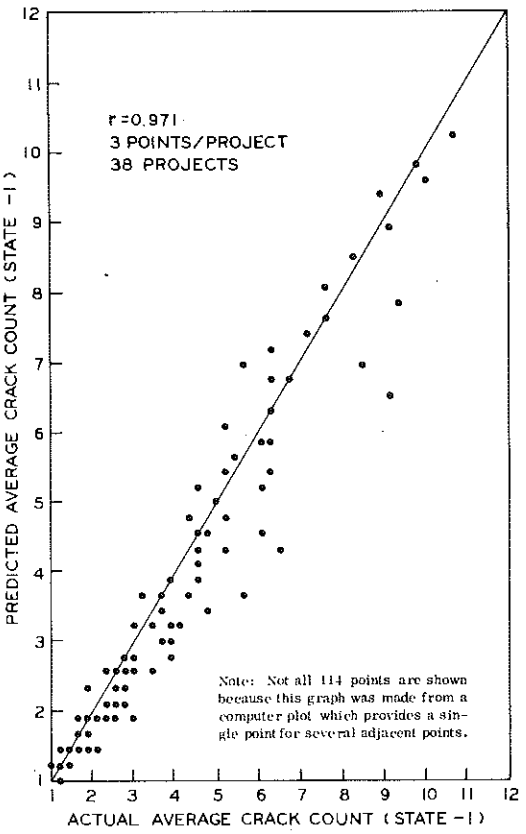

Figure 38. Actual vs. predicted average crack counts.

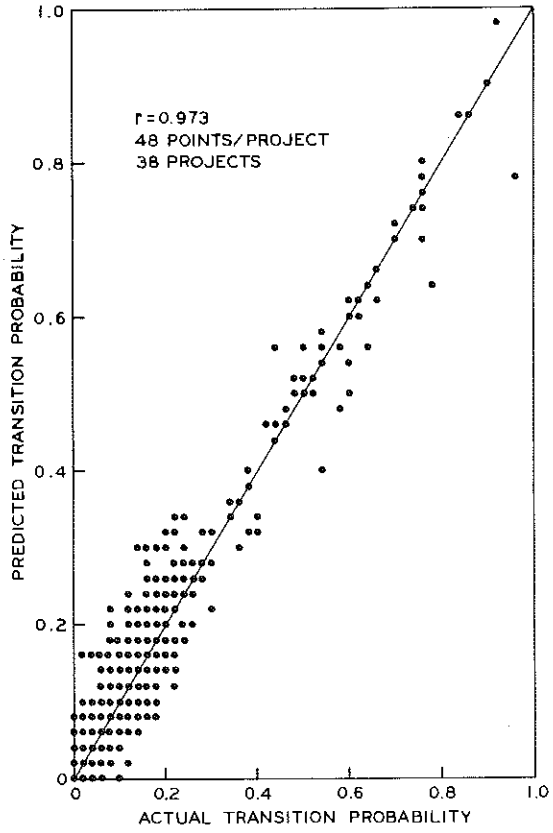

Figure 39. Actual vs. predicted crack transition probabilities.

Serial Correlation of Slab Cracking

An interesting feature of jointed pavement performance variables is that they occur in slabs that are ordered -- deterioration in any given slab can be related to deterioration in slabs either adjacent or some specified distance away. Thus, one can consider slab performance in the light of the performance of neighboring slabs. Specifically, slab crack count for each of the three survey periods was correlated with neighboring slab counts. This correlation was then plotted as a function of slab separation (serial correlation). These plots, presented in the Appendix, show that cracking incidence in neighboring slabs (up to about three slabs removed) tends to be similar for most projects. However, slabs tend to crack independently of one another if separated by greater distances. Thus, considering that slabs in this study are about 100 ft long, similar cracking behavior tends to characterize slabs spanning about 300 ft, but no further. This may be the typical length of local base and subbase conditions. Some projects, on the other hand, show the same serial correlation for all distances, thereby suggesting that soil conditions are uniform and not subject to variation sufficient to result in differential cracking behavior.

CONCLUSIONS
AND
RECOMMENDATIONS

CONCLUSIONS

1) The 19 condition survey variables discussed in Section I are not intercorrelated enough to warrant combining them into a general index of pavement performance. While some projects show a high incidence of nearly all survey variables, many do not. Thus, a project that experiences a high incidence of blowups may not show excessive transverse cracking, etc. While some forms of spalling are well correlated with blowups, for example, the general index approach would require stronger relationships among the remaining variables.

2) For a divided freeway, it is possible to develop a method which allocates roadway traffic volumes to traffic and passing lane sub-volumes, depending on the overall average daily traffic. These volumes, in turn, can be used to generate a variety of transverse cracking models which predict crack accumulation for any time up to 15 years of service. The model which seems to fit the data best is the so-called "Markov Chain," using a state transition period of about two months.

3) When joint performance is considered separately, it is possible to model and predict deterioration using continuous time Markov chain methods. This method assumes that a measure of joint performance is available. In the present study it was the total percent of transverse joint length affected by the relevant survey variables (interior and exterior spalls, deterioration, blowups, etc.). These percentages can be grouped into classes or states (0 to 25 percent, 26 to 50 percent, etc.) and the proportion of joints in each state can be well predicted provided early survey data are available. In the present study, 5 and 10-year survey data were used to predict future performance. The 15-year performance predictions often were remarkably close to actual 15-year survey findings. It is concluded that this technique can be used to identify projects which will undergo serious joint deterioration, including blowups.

4) Causes of joint deterioration are difficult to identify from the historical data available. Traffic, temperature, construction year, and coarse aggregate types were examined in an effort to find correlations. The only variable that was not rejected was coarse aggregate type. It was found that pits containing relatively pure natural aggregates, with very low or very high carbonate gravels, were associated with good joint performance. On the other hand, pits containing gravel-limestone mixes or pure crushed limestones were associated with both poor and good joint performance. Inclusion of this finding in the joint performance prediction model improved the predictions materially.

5) It is possible to model (again, by continuous time Markov methods) transverse cracking. The fit with field data is good and future cracking behavior can be estimated. The particular model used in this study identifies a critical crack number or state for each slab. A slab with this number of cracks is the one most likely to crack again. Slabs which have either less or more cracks than the critical number are less likely to crack again. The critical number is usually between three and five, depending on the project. The critical number does not seem to be related to original soil conditions.

6) Slab cracking behavior tends to be similar for groups of up to three contiguous slabs. This suggests that local base and subbase conditions are similar up to 300 ft, but dissimilar beyond this distance.

7) Original soil conditions based on regional evaluations do not correlate with any kind of pavement performance herein examined. Based on these data, one would conclude that local upgrading of conditions through importing granular soils usually rectifies subbase deficiencies to the extent that transverse cracking cannot be predicted from soil boring information.

8) Michigan's joint performance does not appear to have significantly changed since the post-war period. This conclusion holds for projects constructed through 1963. Technically, there is a slight improvement despite increased loading and salting over the 1946 - 1963 construction period.

RECOMMENDATIONS

1) For most condition survey variables, nothing much happens during the first 5 years. By 10 years, however, some projects begin to show substantial deterioration. Therefore, we recommend that the 5-year condition survey be eliminated in favor of a 7, 8, or even 10-year survey. Thus, more information could be obtained from an 8, 12, and 16-year survey program than from the 5, 10, and 15-year program now in effect in Michigan.

2) We recommend that careful attention be given to acceptance testing programs designed for coarse aggregate pits known to contain gravel-limestone mixes in roughly a 50/50 proportion. These sources are likely to contain large amounts of deleterious materials, and projects constructed from these sources do not generally exhibit as good joint performance as those constructed from either high or low carbonate gravel sources. In particular, we recommend that the extent of aggregate sampling for deleterious material detection purposes be based on the gravel-limestone proportion known to characterize each aggregate source. If this were done, sampling and testing efforts could be distributed such as to maximize the possibility of poor material detection.

3) We recommend that early survey information (such as that obtained from 5 and 10-year field examinations) be used to estimate future joint performance. If this is facilitated with models developed in this report, good estimates can be made of 15-year performance. These estimates could then be used to alert maintenance personnel as to potential joint problems such as blowups. The joint model will allow projects to be rank ordered in terms of anticipated joint problems and attention can be given to the top priority projects in the form of preventive maintenance such as joint reconstruction.

4) We recommend that this same performance estimation program be used to focus attention on problem projects so that additional condition surveys can be made. Thus, if a project's 15-year expected condition was good, a 15-year survey could be delayed. However, if the expected condition was poor, additional surveys could be made. This type of program would have the effect of concentrating survey efforts on those projects which experience the highest incidence of deterioration.

5) We recommend that future research on pavement performance take account of our favorable findings with the continuous time Markov chain. The assumptions of this model seem reasonable and good results have been obtained with it. We would suggest, however, that future research with this model make use of more states than the four we used for joint condition. If we were to redo the problem, we would consider perhaps 10 states, including a zero-percent deterioration state.

REFERENCES

1. Oehler, L. T., Holbrook, L. F., "Performance of Michigan's Postwar Concrete Pavements," Research Report R-711, Michigan Department of State Highways and Transportation, 1969.

2. Pielou, E. C., An Introduction to Mathematical Ecology, Wiley-Interscience, 1969, pp. 19-32.

3. Heathington, K. W., Tutt, P. R., "Traffic Volume Characteristics of Urban Freeways," Transportation Engineering Journal of ASCE, Vol. 97, Feb. 1971, pp. 105-116.

4. Hillier, F. S., and Lieberman, G. J., Introduction to Operations Research, Holden-Day, 1967, p. 302.

5. Feller, William, An Introduction to Probability Theory and its Applications (Vol. I), John Wiley, 1950, Chapt. 17.

6. Holbrook, L. F., "An Examination of Concrete Pavement Structural Performance," Highway Research Record 311, Highway Research Board, 1970.

7. Clarke, B. A., Disney, Ralph L., Probability and Random Processes for Engineers and Scientists, John Wiley, 1970.

8. Karlin, Samuel, A First Course in Stochastic Processes, Academic Press, 1969.

9. Parzem, Emanuel, Stochastic Processes, Holden-Day, 1962.

10. Dye, J. L., Nicely, V. A., "A General Purpose Curve Fitting Program for Class and Research Use," Journal of Chemical Education, Vol. 48, p. 443, 1971.

11. Draper, N., Smith, H., Applied Regression Analysis, John Wiley, 1966.

12. Aoki, Masanoa, Introduction to Optimization Techniques, MacMillan, 1971.

APPENDIX

NOTES ON INTERPRETING THE APPENDIX

In Chapters V and VI we discussed how joint deterioration and transverse crack survey data was transformed into the so-called "transition probability," $P_{ij}(\tau, t)$ defined in Chapter IV. The model developed in Chapter IV was then used to estimate the actual transition probabilities. The results of this fitting procedure have been explained verbally and graphically in Chapters V and VI. For the convenience of the reader, we now detail these results in the following sample appendix. The results for all 43 projects are available in a separate appendix on request.

Each of the projects presented, has 11 figures. Figures 1 through 7 pertain to transverse cracking (Chapter VI) and Figures 8 through 11 pertain to joint performance (Chapter V). Figure 1 shows how well the model fit the actual transverse crack data. If the model fit the data perfectly, every joint would fall on the 45 degree line shown in Figure 1. Each point represents the probability of a specific number of cracks at either the 5, 10, or 15-year survey time. Figure 2 follows from Figure 1 by the process of averaging. That is to say, each point in Figure 2 represents the average crack count to be expected at 5, 10, and 15 years given no cracks initially, or the average crack count to be expected at 10 or 15 years given the crack count at 5 or 10 years. The graph shows the relationship between the model's prediction of average state and the average state obtained from the survey data.

Using the optimal parameters obtained from the model, we computed and plotted in Figure 3 the estimated (theoretical) transition probability $P_{11}(0, t)$ and $P_{1c}(0, t)$. In this figure, the solid line specifies the probability that a slab will remain uncracked after t years. The dotted line specifies the probability that a slab will reach the critical number of cracks after t years. It will be recalled that the critical number occurs when the probability of further cracking is greatest.

Figure 4 shows the trend of the estimated expected (average) state over time. The points in this figure represent the actual data. Again, this figure partially demonstrates how well the model fits the actual survey data.

Figure 5 shows the actual (bars) and estimated (curve) transition probability of the various states for the three survey periods. As we mentioned in Chapter VI, the cracking transition rate is well characterized by a bell-shaped curve.

The curve in Figure 6 is optimal for the corresponding project and shows the relative likelihood of further cracking for each state (crack count). The critical state corresponds to the peak of each curve.

Figure 7, serial correlation, shows how cracking in any given slab can be related to cracking in slabs either adjacent or some specified distance away. The curves in this figure tend to fluctuate randomly for slab separations greater than three indicating that for most projects slabs have similar crack counts with neighboring slabs up to about three slabs away or about 300 feet. When the broken lines fall near zero, we infer no relationship between a slab and other slabs the indicated distance away. The shaded area in Figure 8 shows the error in estimating the transition frequency distribution for joint deterioration. It is obvious that small shaded areas represent a good fit of the model.

Since we defined four states of joint condition, it is interesting to know how the transition probability changes for the different states over time. This is shown in Figure 9. The probability of a joint being in any of the four states can be seen by locating the desired service time on the horizontal axis and noting the corresponding probability on the vertical axis. Since State IV is so important (mostly blowups), we would like to know the chance that a given slab in State III (highly but not completely deteriorated) as time t_i , will deteriorate to State IV (blowup) as time t. Figure 10 gives this information for three values of τ .

Figure 11 shows the trend of expected (average) state of joint condition over time. Again, the three actual survey points were plotted to show how well the model fit the data.

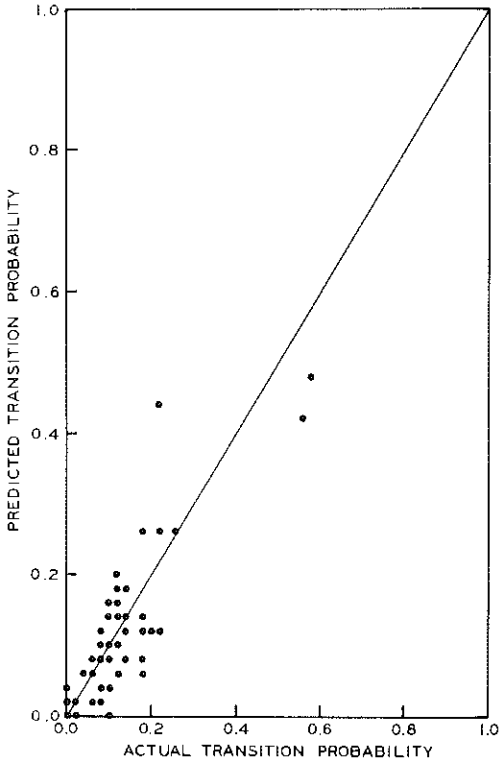

Figure 1. Relationship between actual and estimated cracking probability.

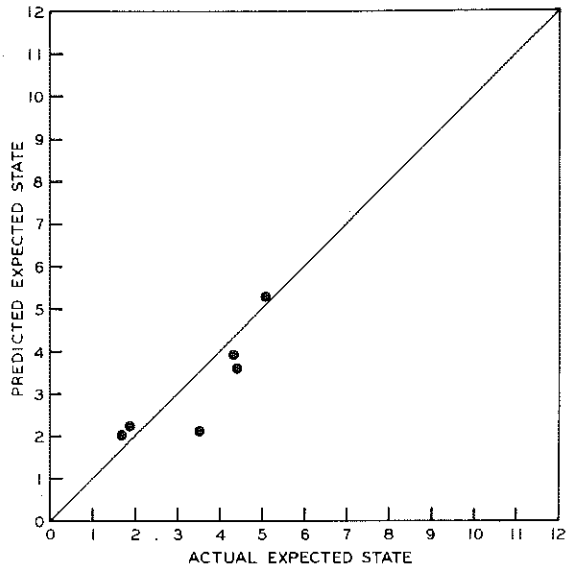

Figure 2. Relationship between actual and estimated average crack count.

Figure 3. Probability of crack States 1 and C over time.

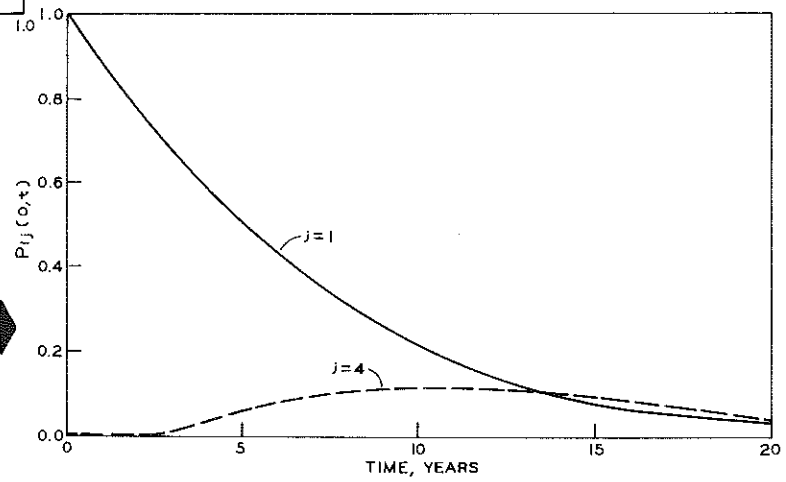

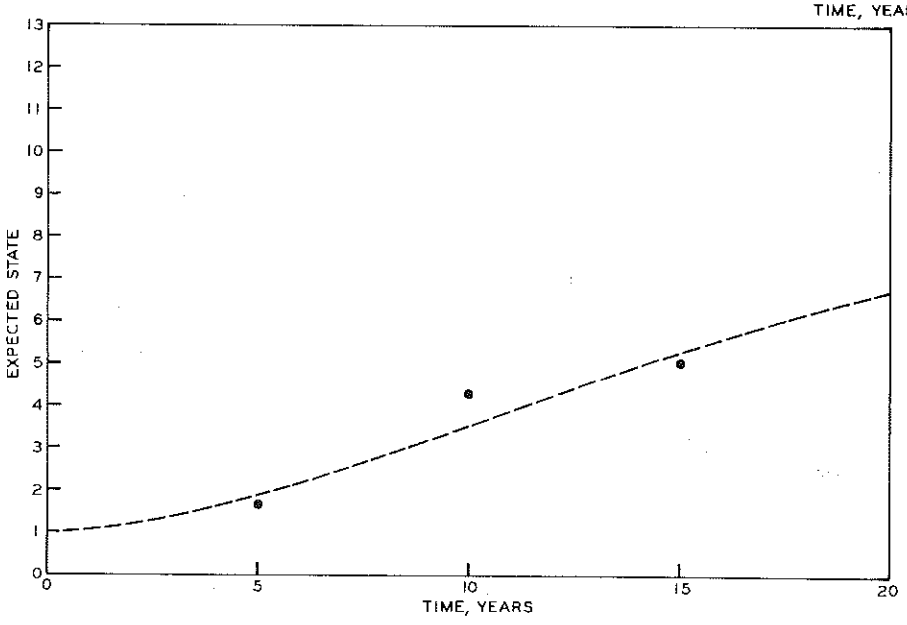

Figure 4. Average crack state over time.

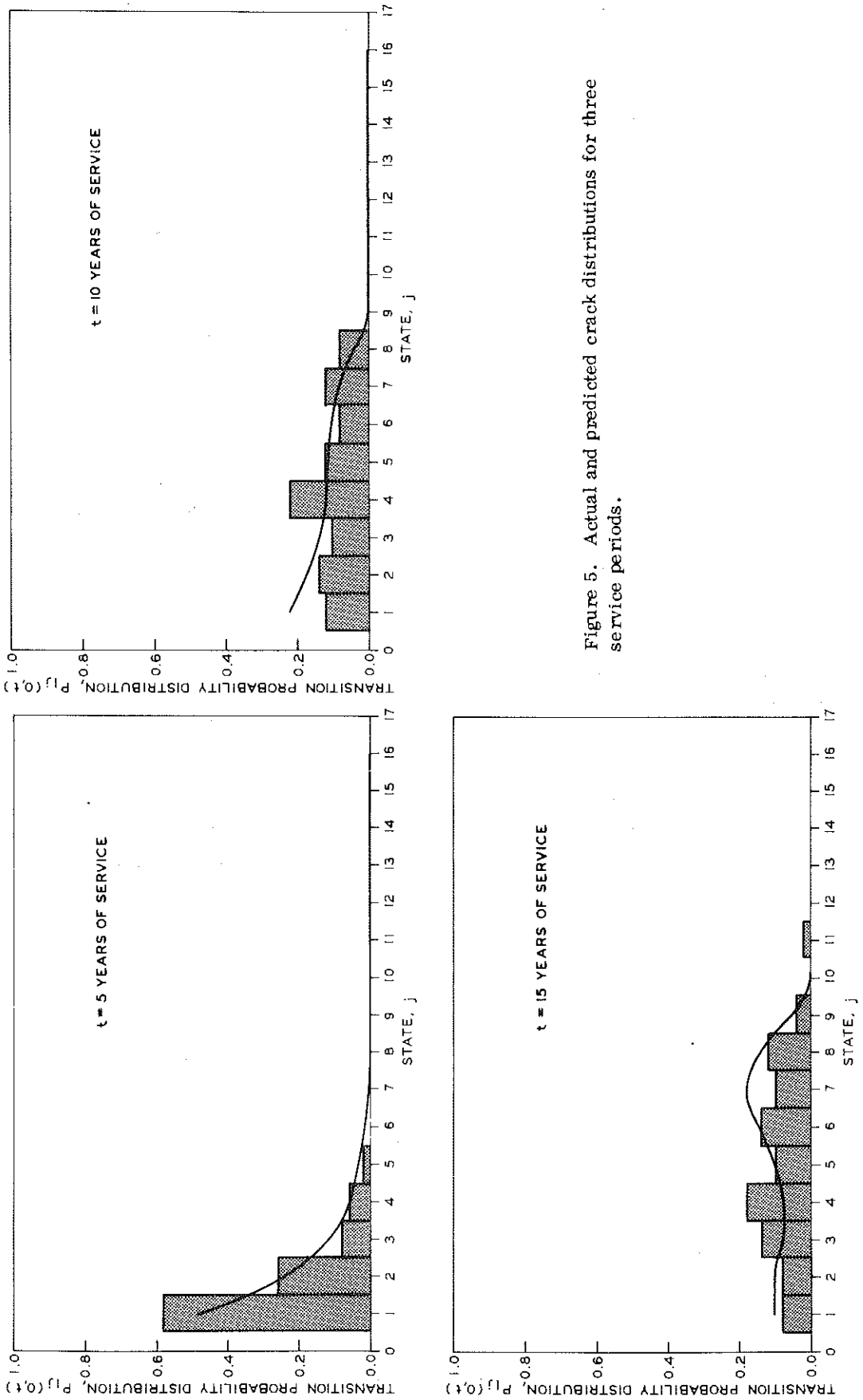

Figure 5. Actual and predicted crack distributions for three service periods.

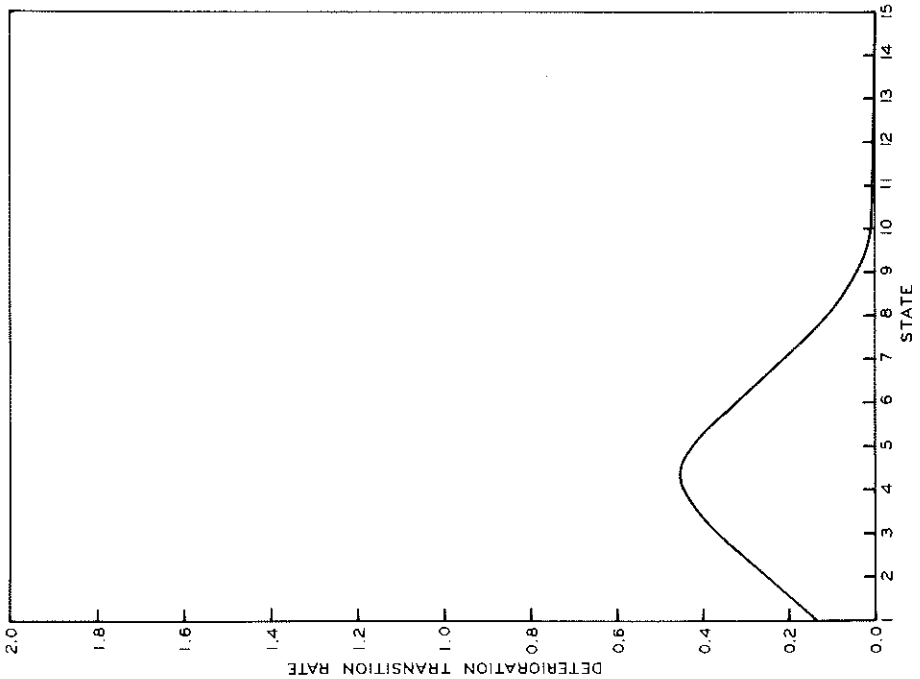

Figure 6. Crack state transition function.

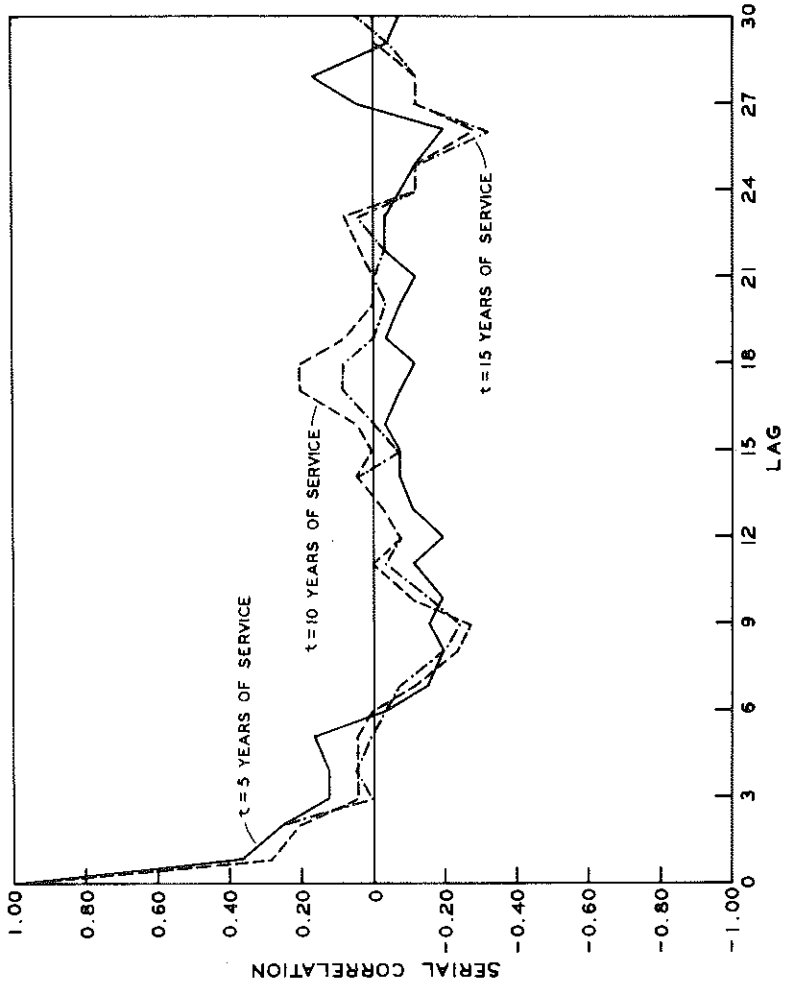

Figure 7. Crack autocorrelation plot for three service periods.

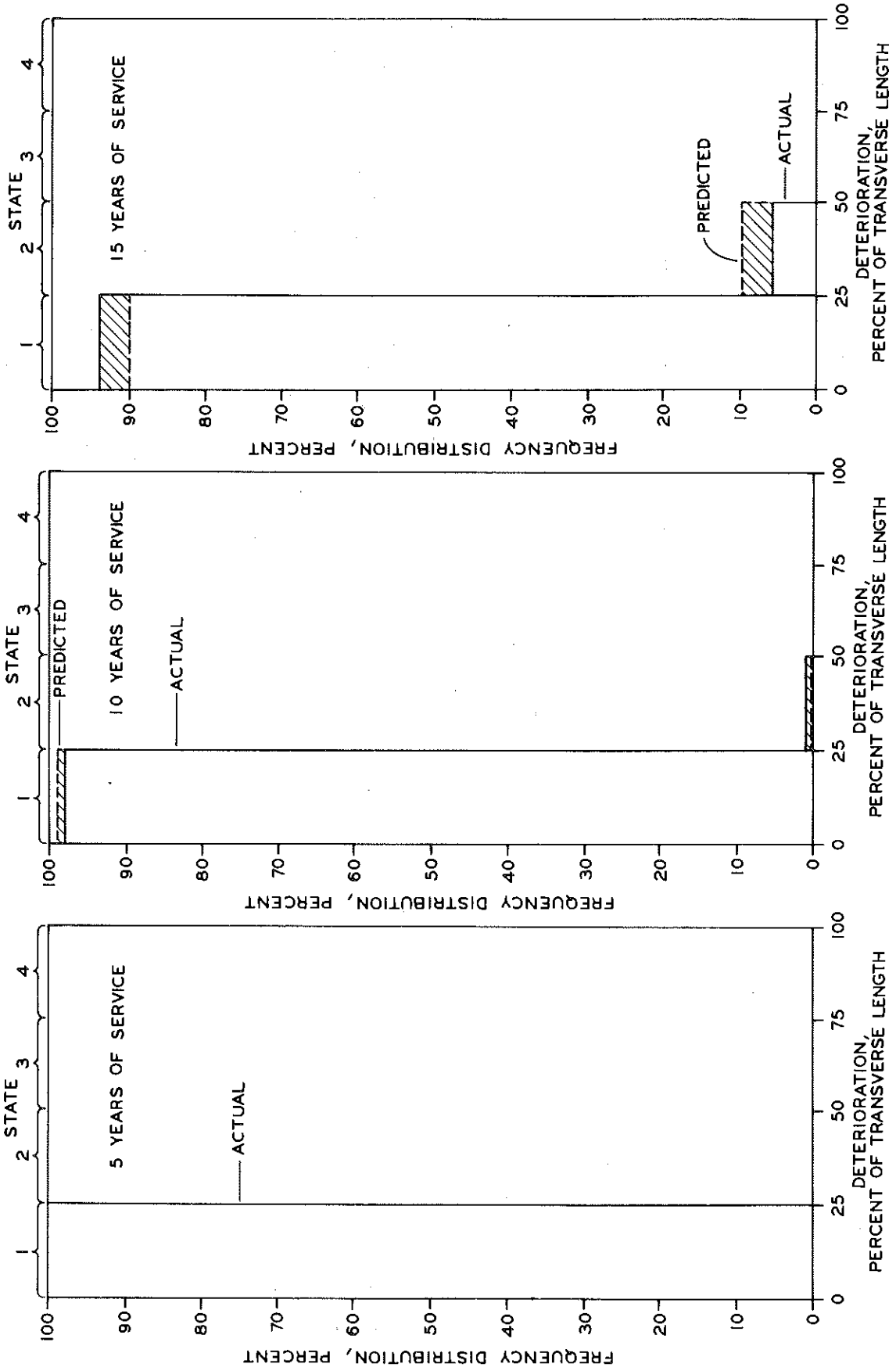

Figure 8. Joint deterioration histograms for three service periods.

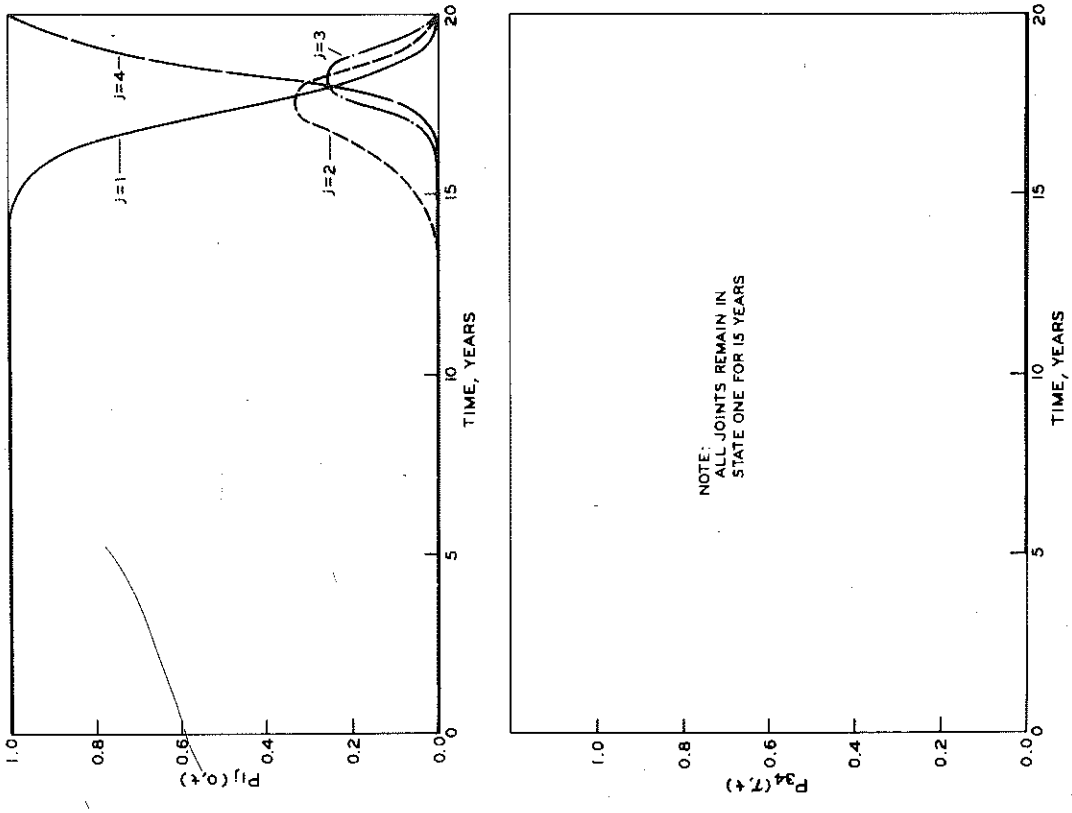

Figure 10. Probability of a joint passing from State 3 at time τ to State 4 at time t.

Figure 9. Joint deterioration state transition probability as a function of time.

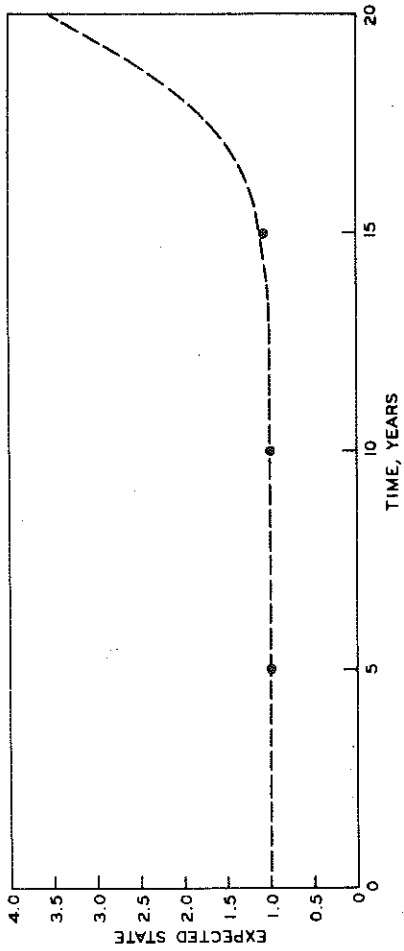

Figure 11. Joint deterioration, average state over time.

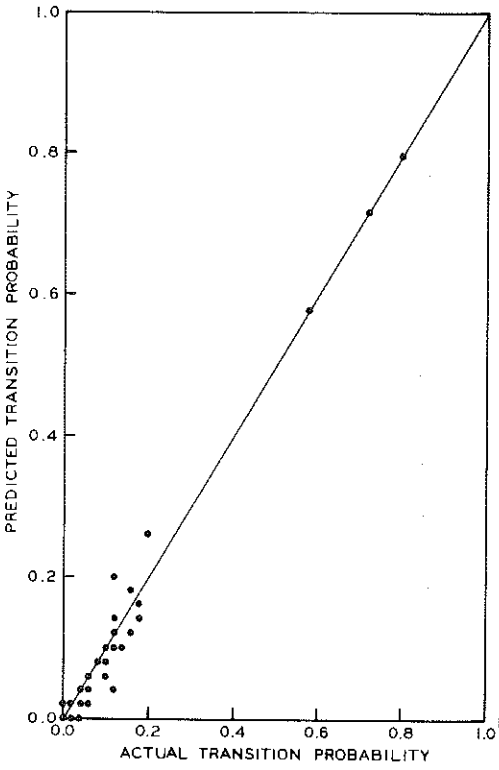

Figure 1. Relationship between actual and estimated cracking probability.

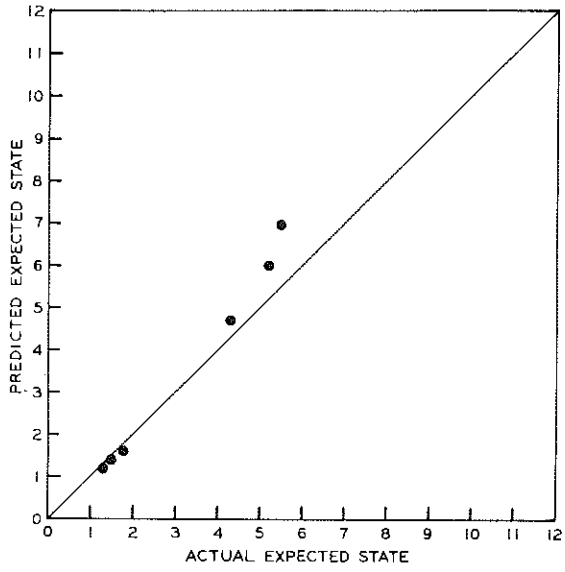

Figure 2. Relationship between actual and estimated average crack count.

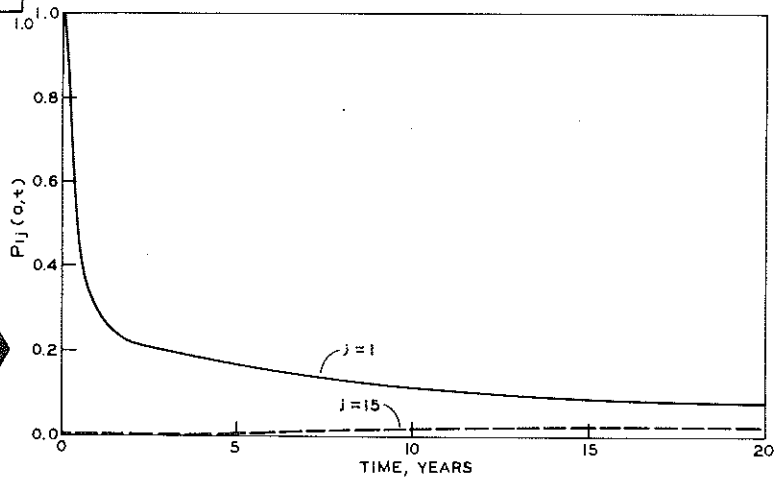

Figure 3. Probability of crack States 1 and C over time.

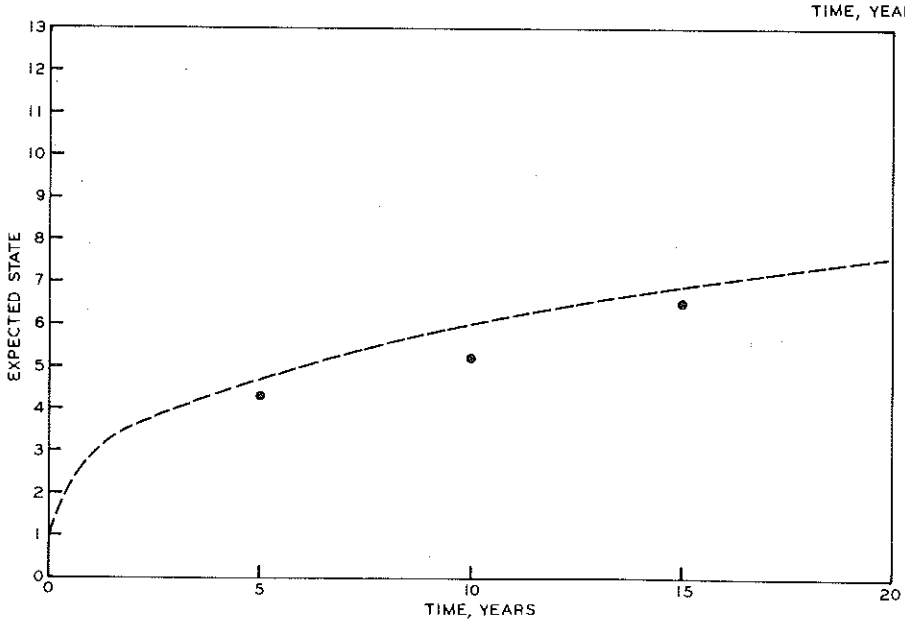

Figure 4. Average crack state over time.

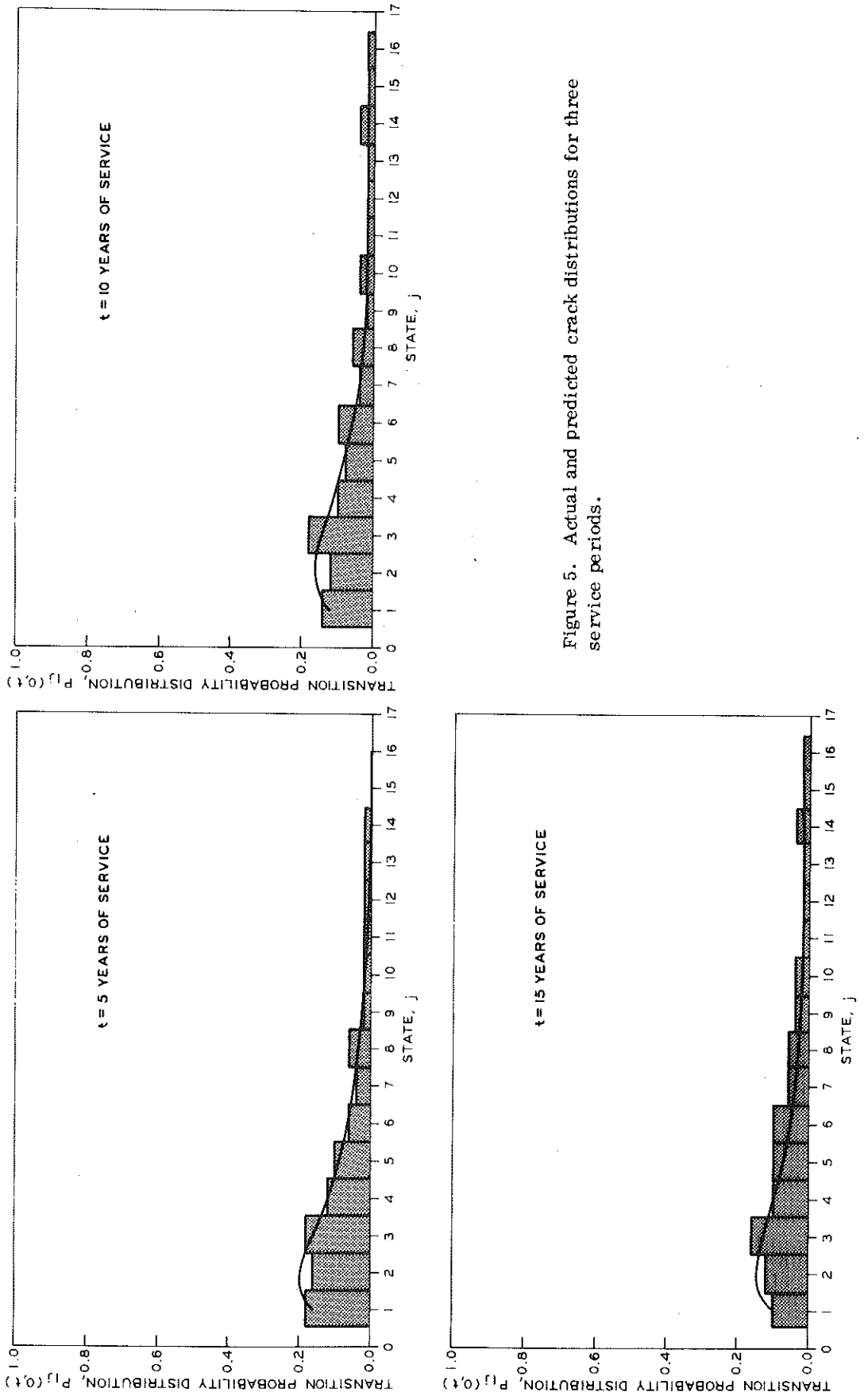

Figure 5. Actual and predicted crack distributions for three service periods.

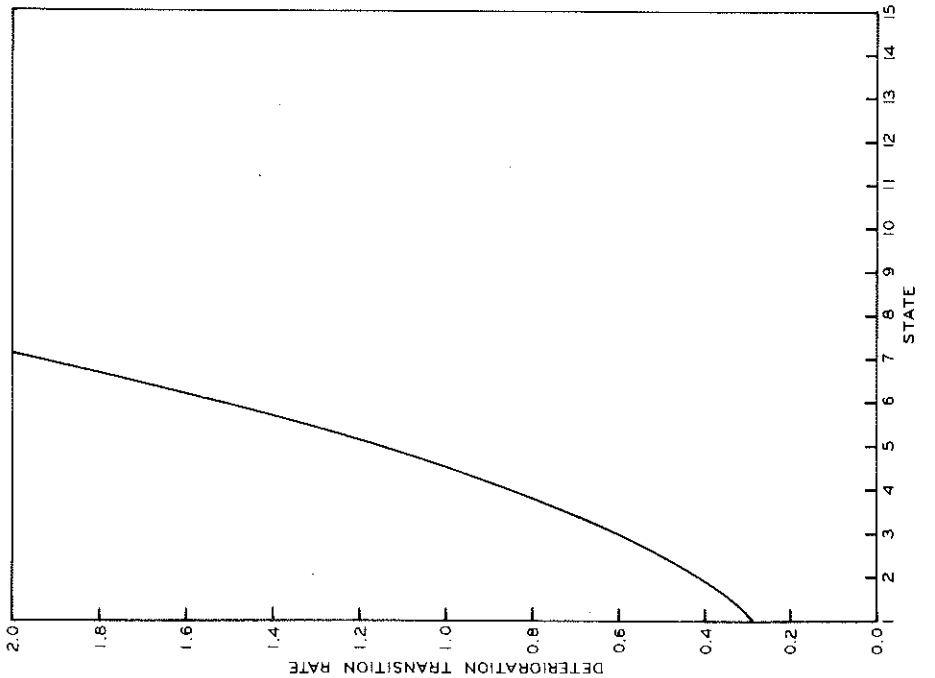

Figure 6. Crack state transition function.

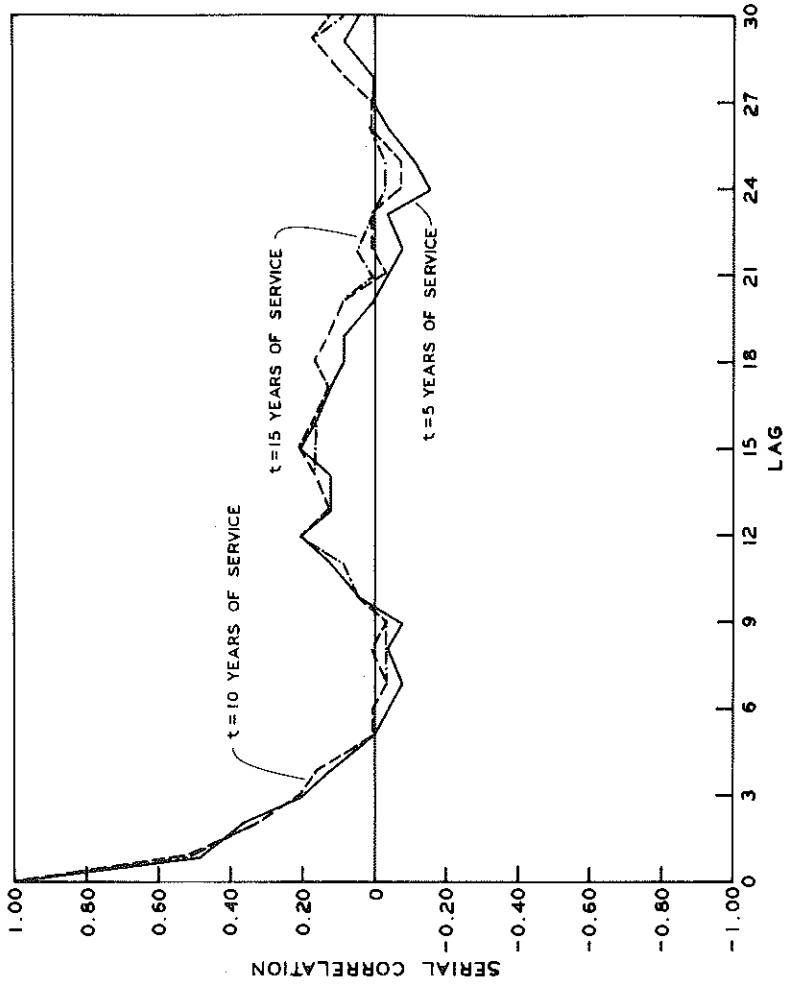

Figure 7. Crack autocorrelation plot for three service periods.

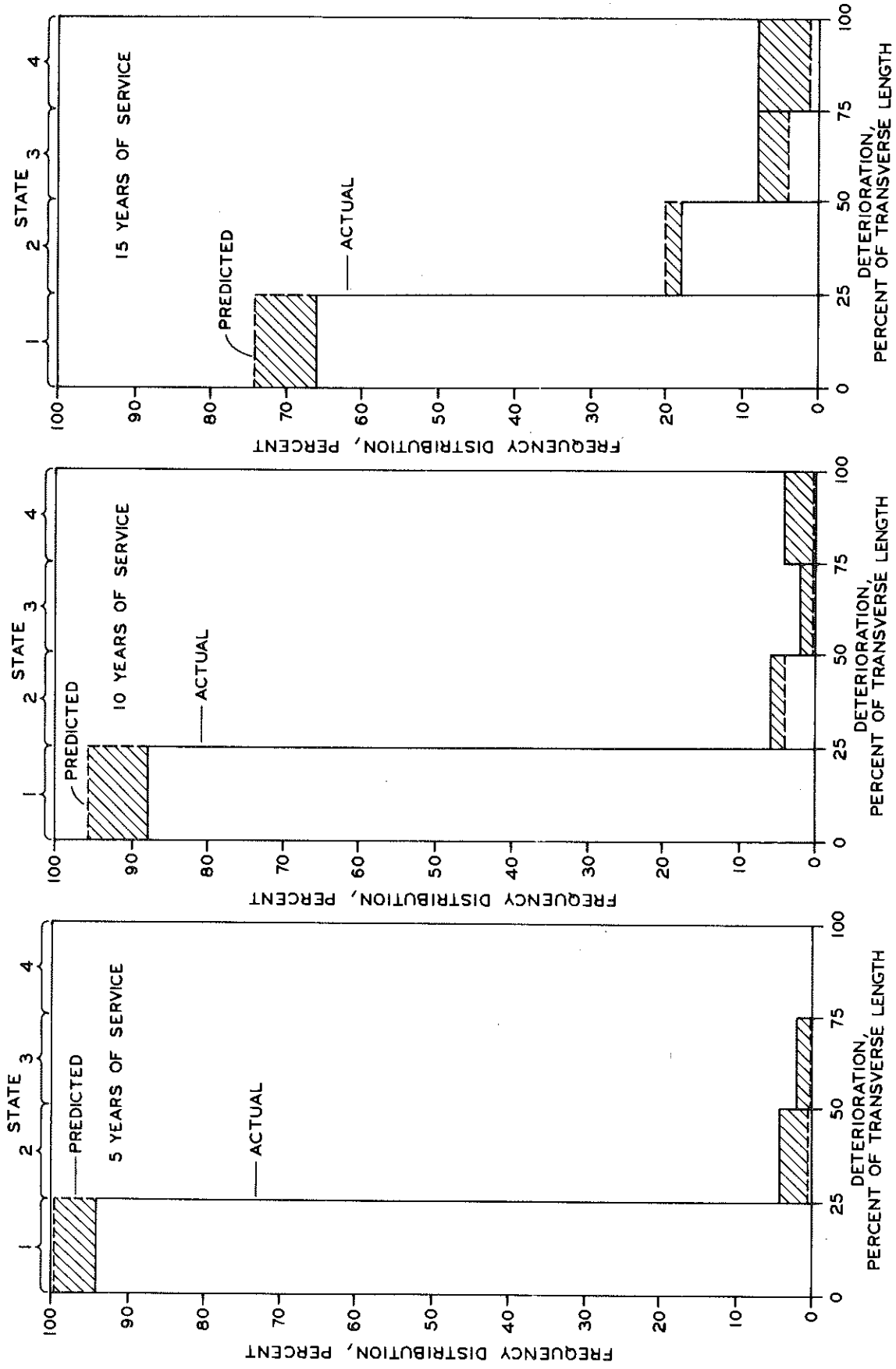

Figure 8. Joint deterioration histograms for three service periods.

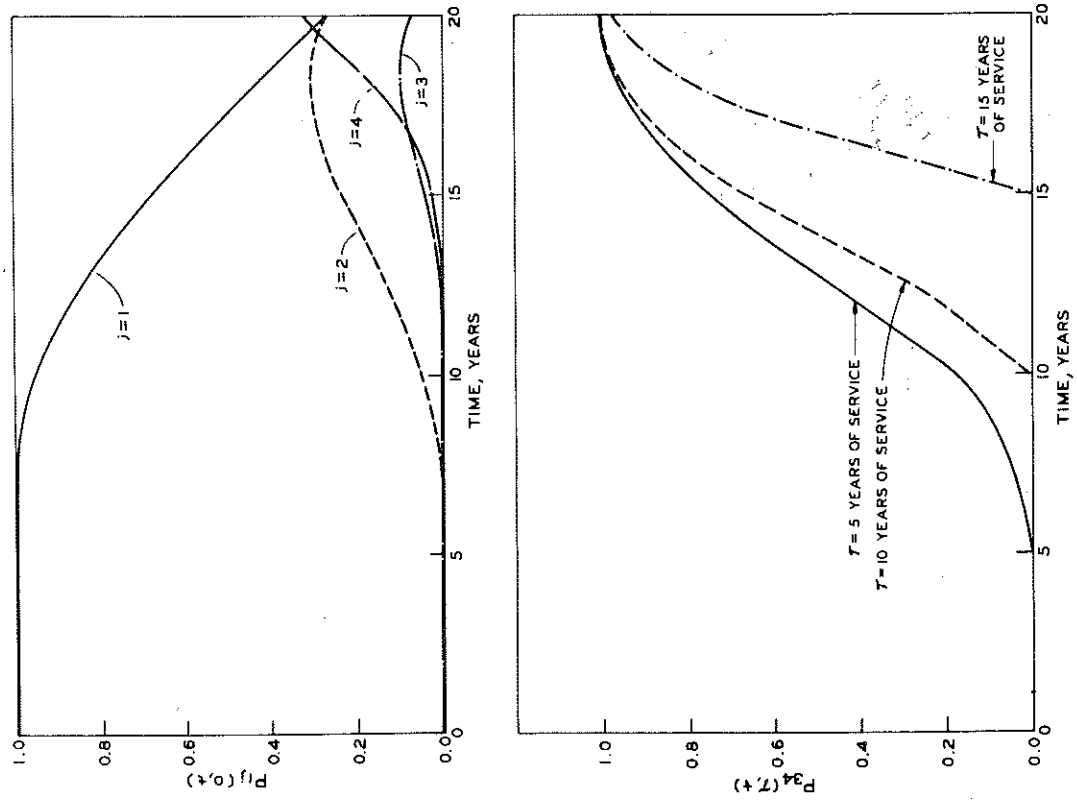

Figure 10. Probability of a joint passing from State 3 at time τ to State 4 at time t.

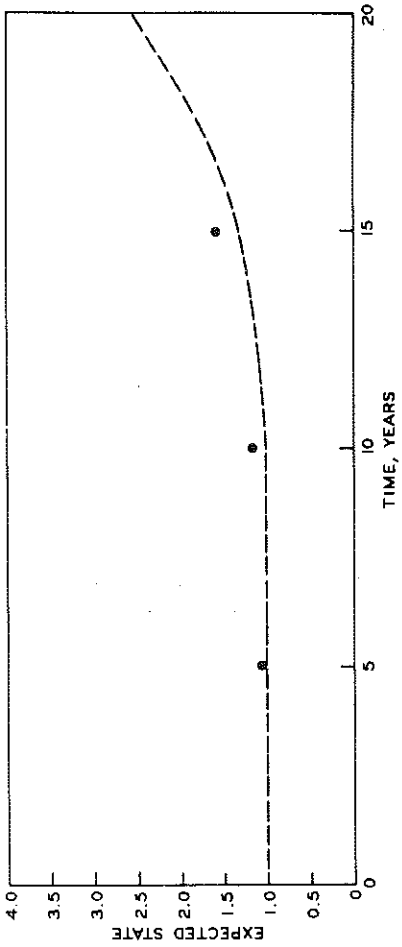

Figure 11. Joint deterioration, average state over time.

Figure 9. Joint deterioration state transition probability as a function of time.

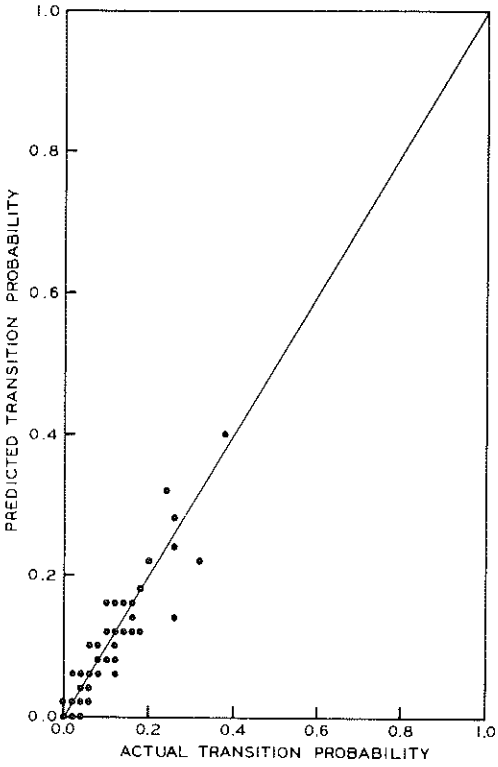

Figure 1. Relationship between actual and estimated cracking probability.

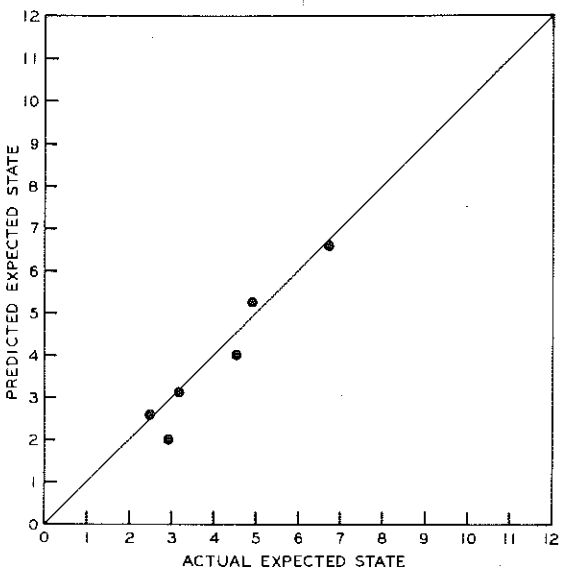

Figure 2. Relationship between actual and estimated average crack count.

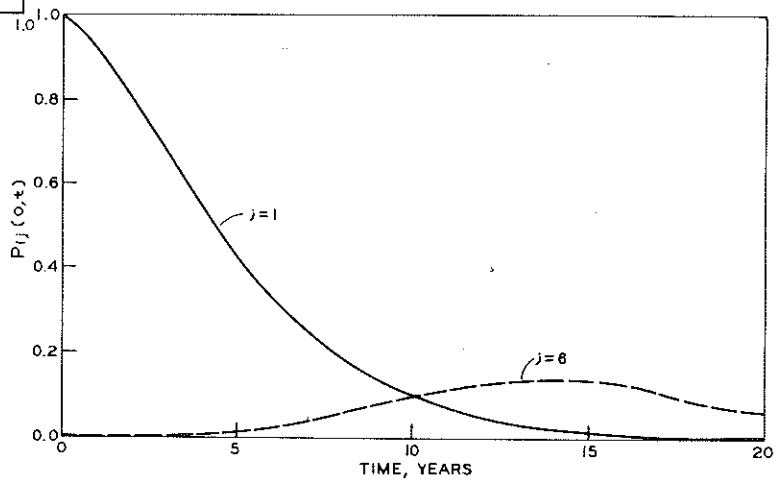

Figure 3. Probability of crack States 1 and C over time.

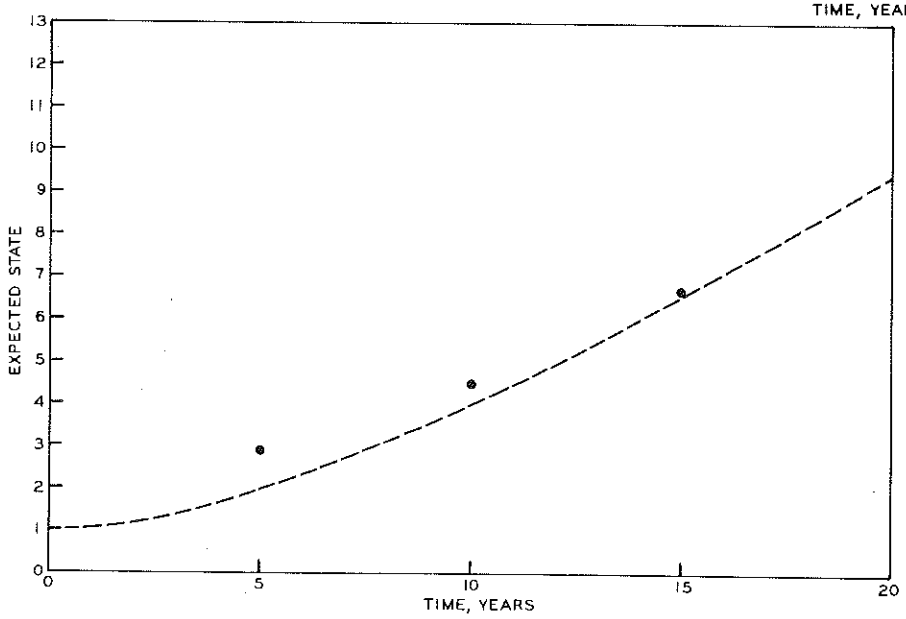

Figure 4. Average crack state over time.

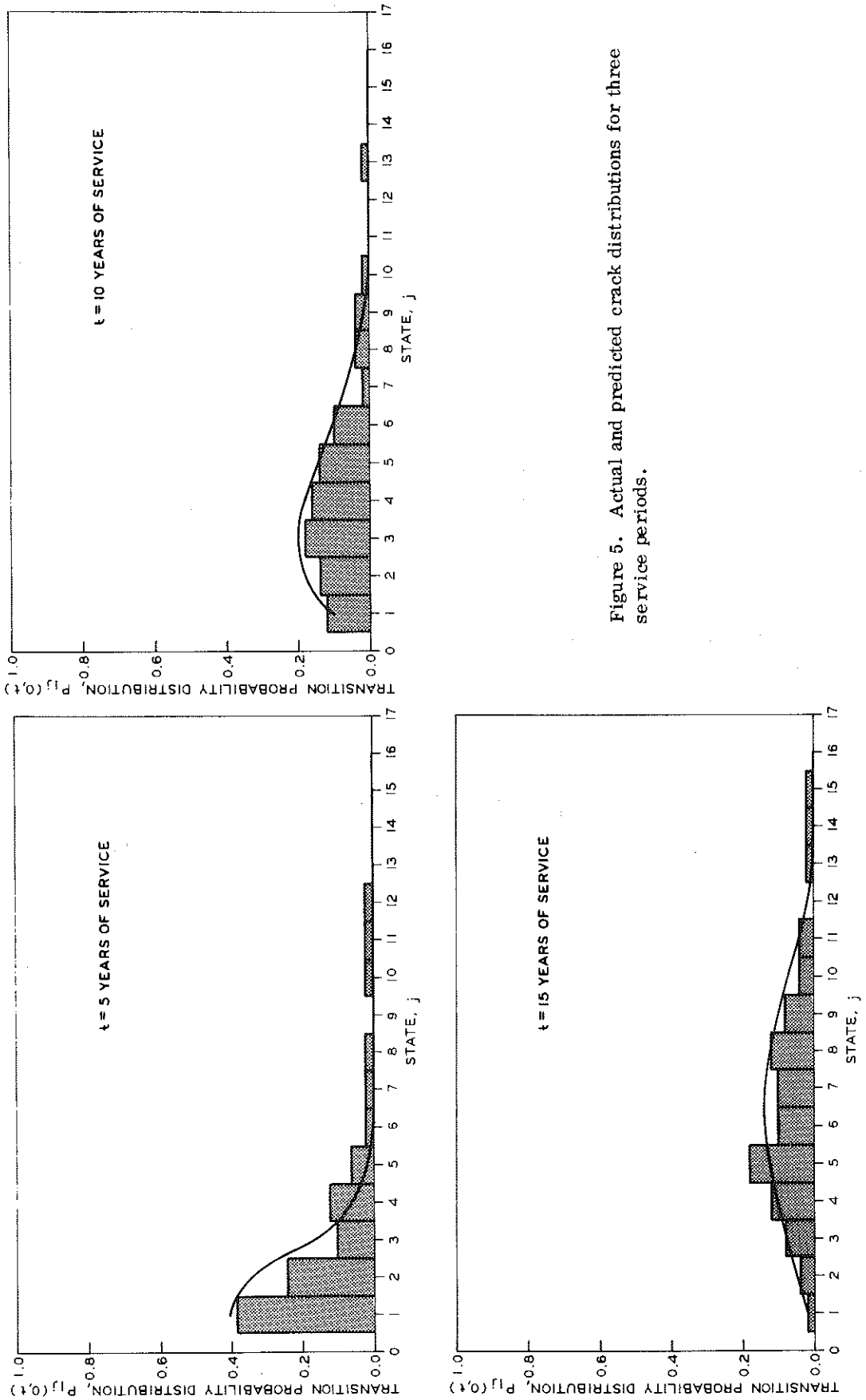

Figure 5. Actual and predicted crack distributions for three service periods.

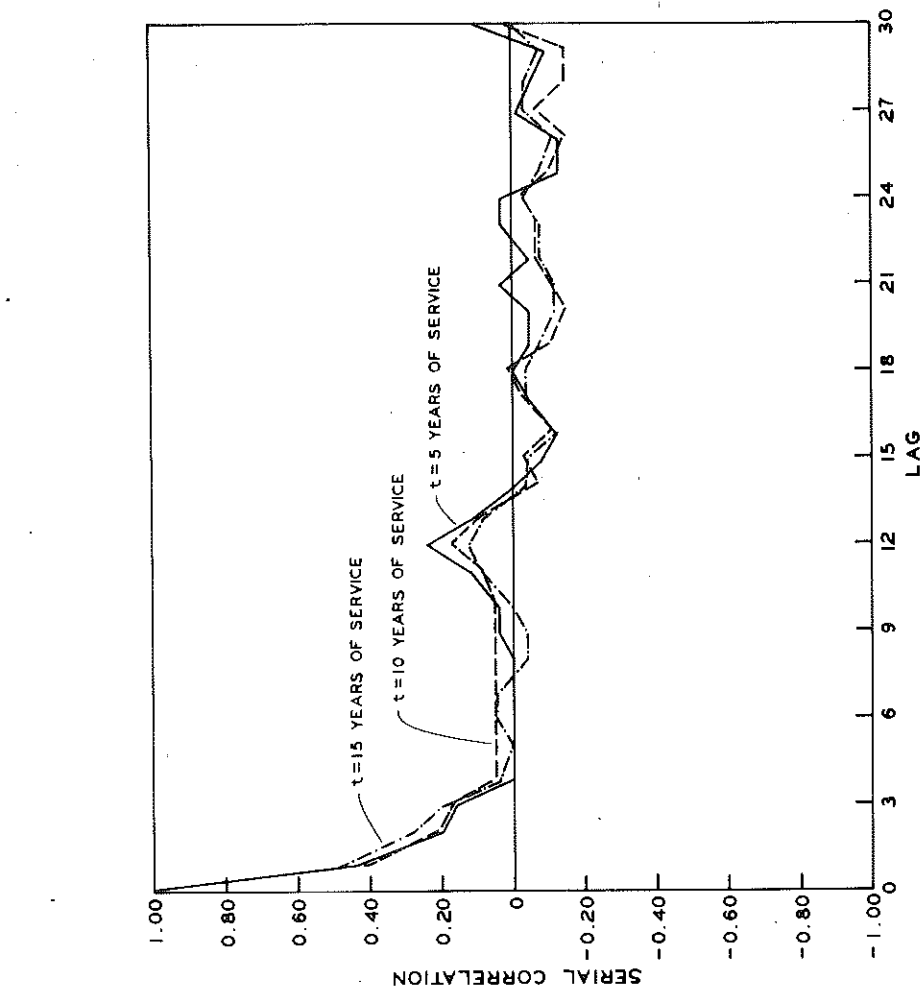

Figure 7. Crack autocorrelation plot for three service periods.

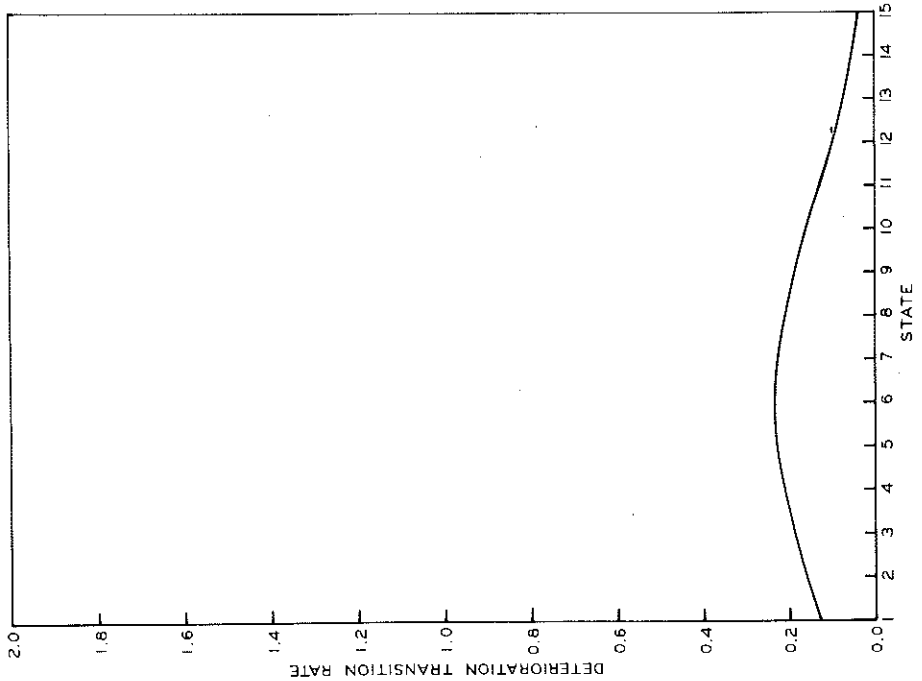

Figure 6. Crack state transition function.

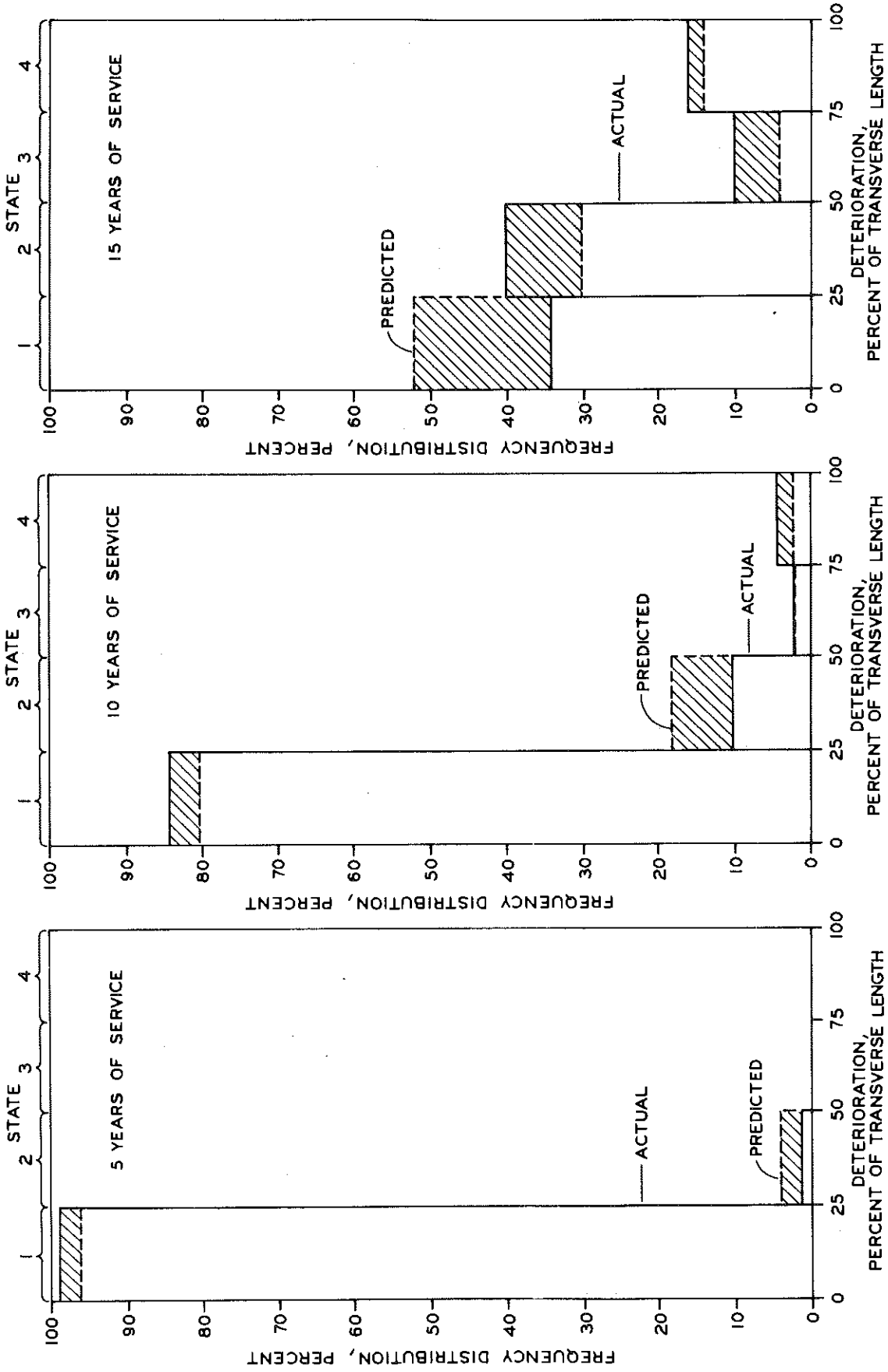

Figure 8. Joint deterioration histograms for three service periods.

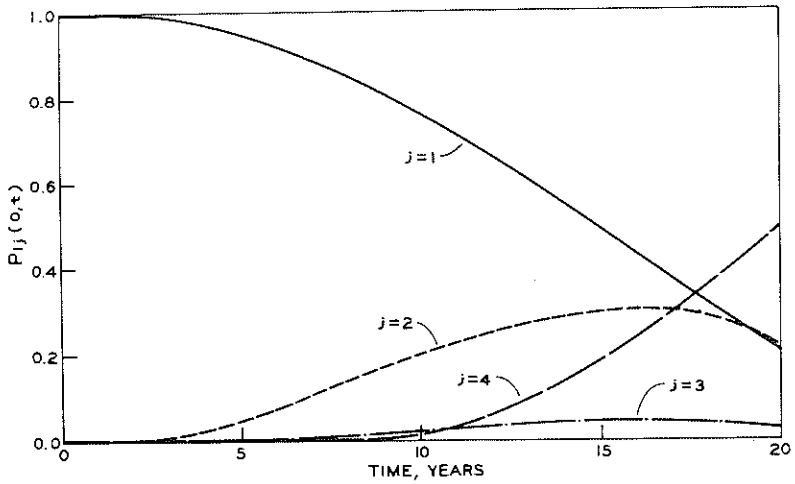

Figure 9. Joint deterioration state transition probability as a function of time.

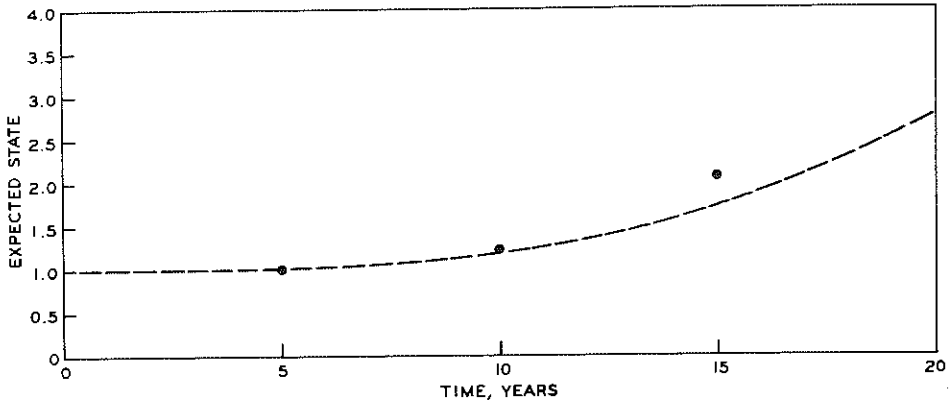

Figure 11. Joint deterioration, average state over time.

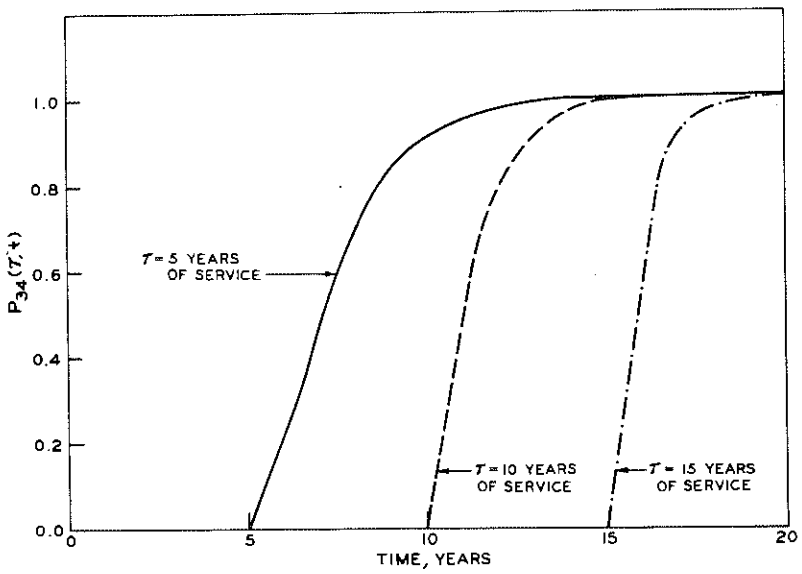

Figure 10. Probability of a joint passing from State 3 at time τ to State 4 at time t.

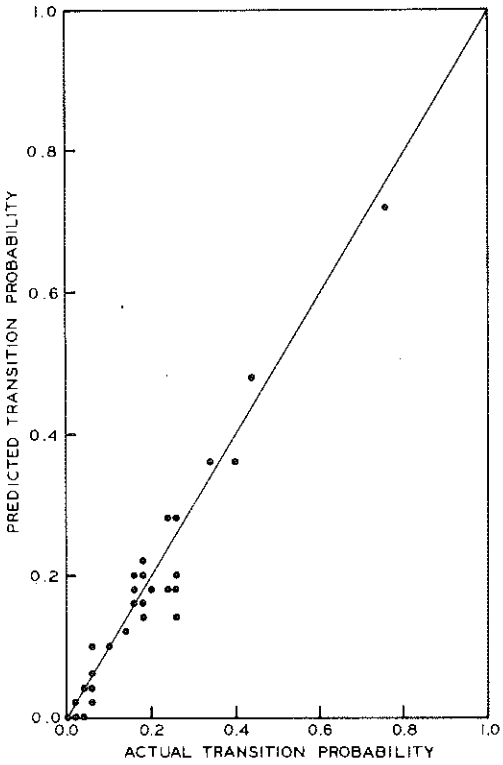

Figure 1. Relationship between actual and estimated cracking probability.

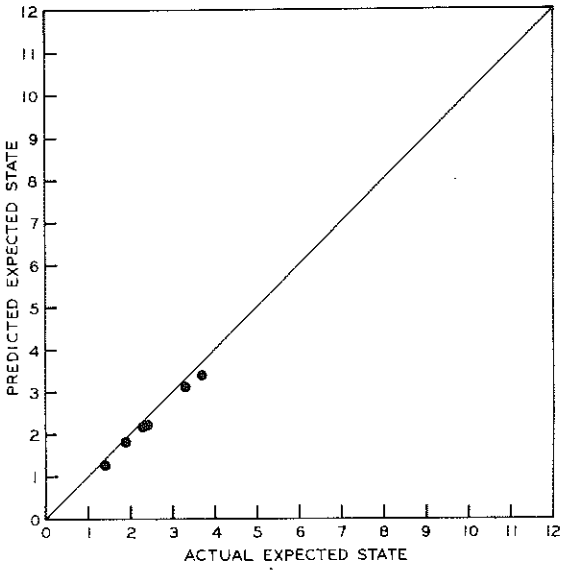

Figure 2. Relationship between actual and estimated average crack count.

Figure 3. Probability of crack States 1 and C over time.

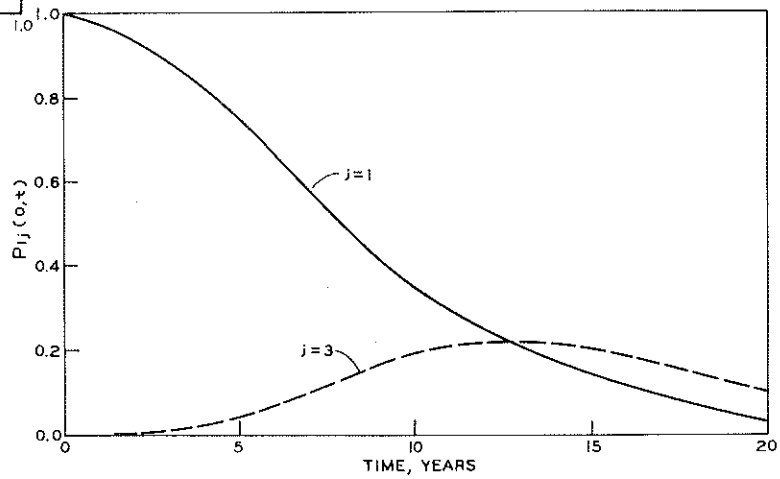

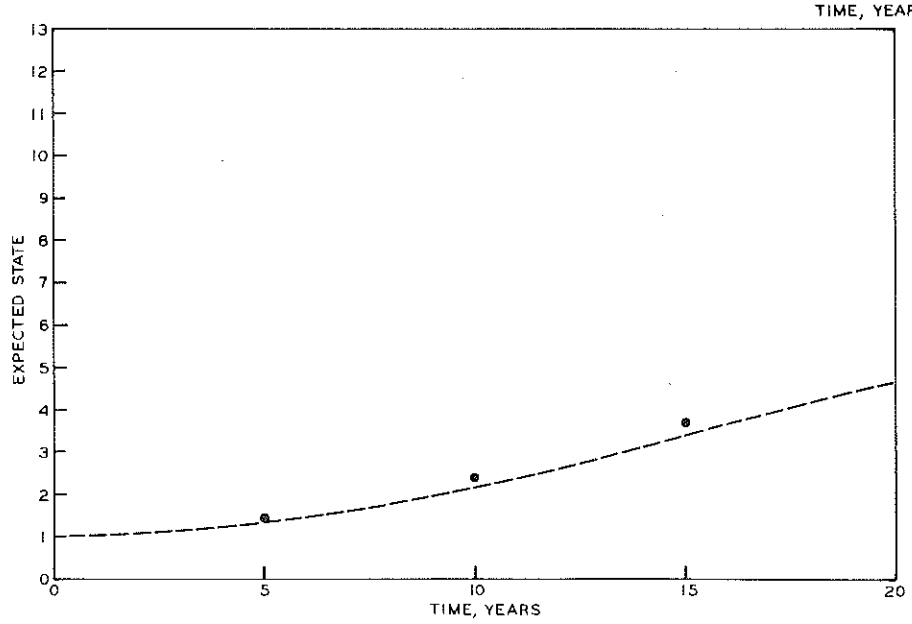

Figure 4. Average crack state over time.

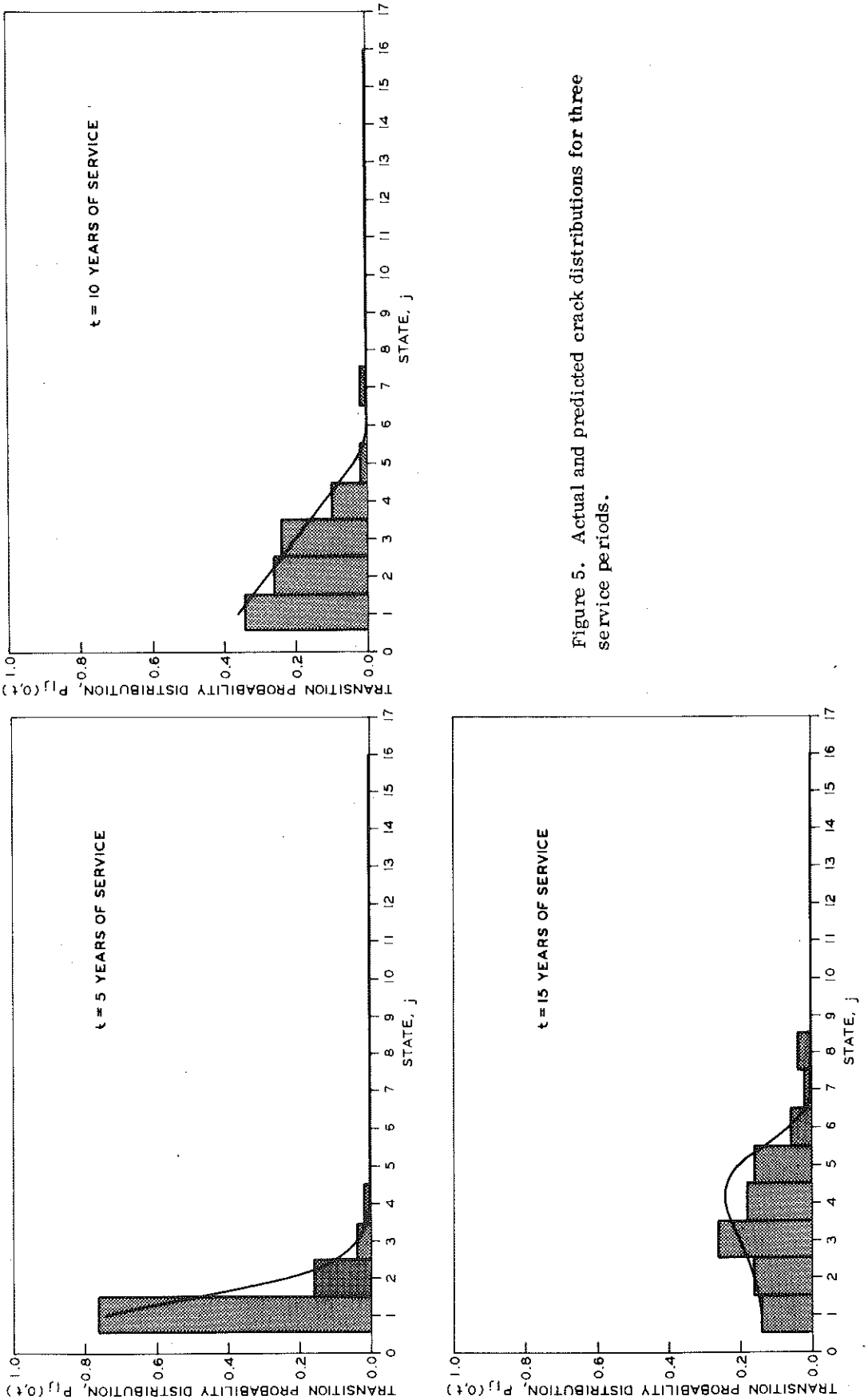

Figure 5. Actual and predicted crack distributions for three service periods.

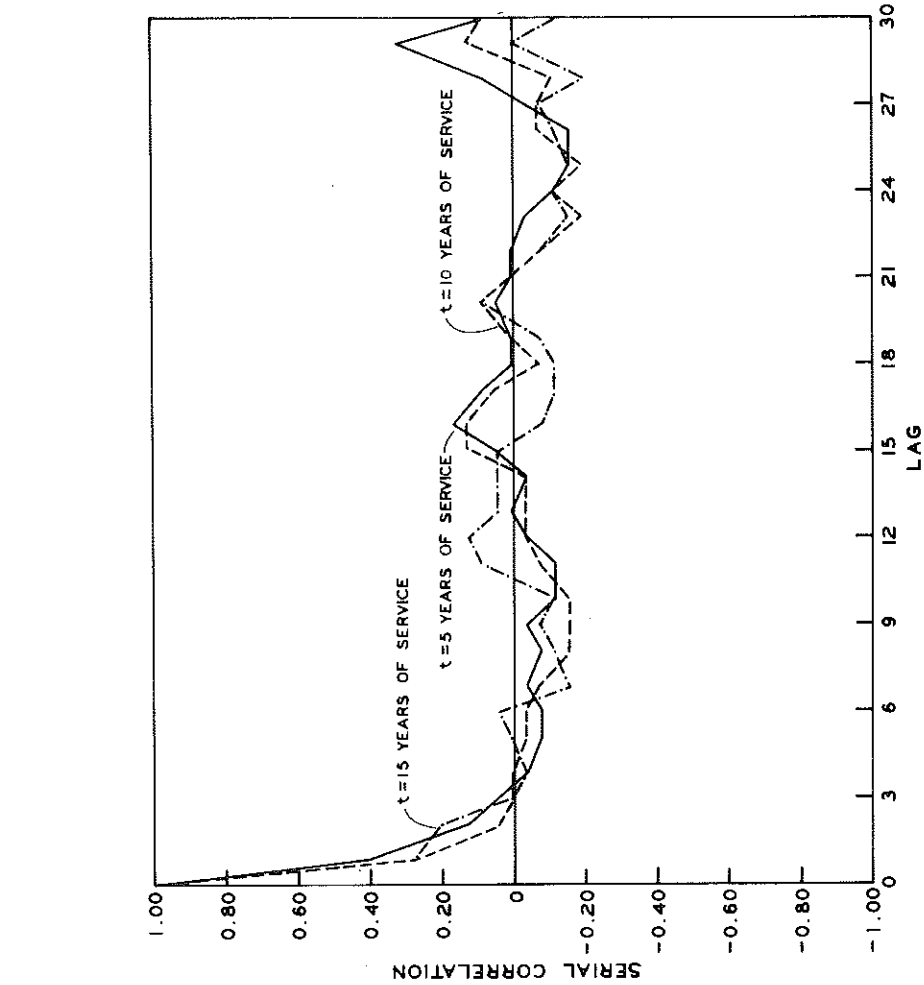

Figure 7. Crack autocorrelation plot for three service periods.

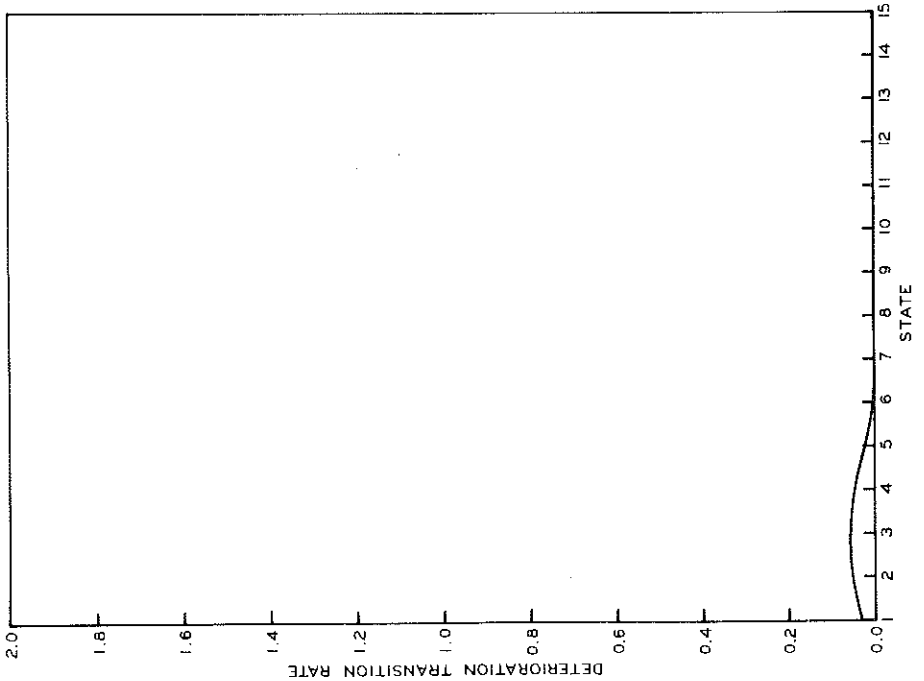

Figure 6. Crack state transition function.

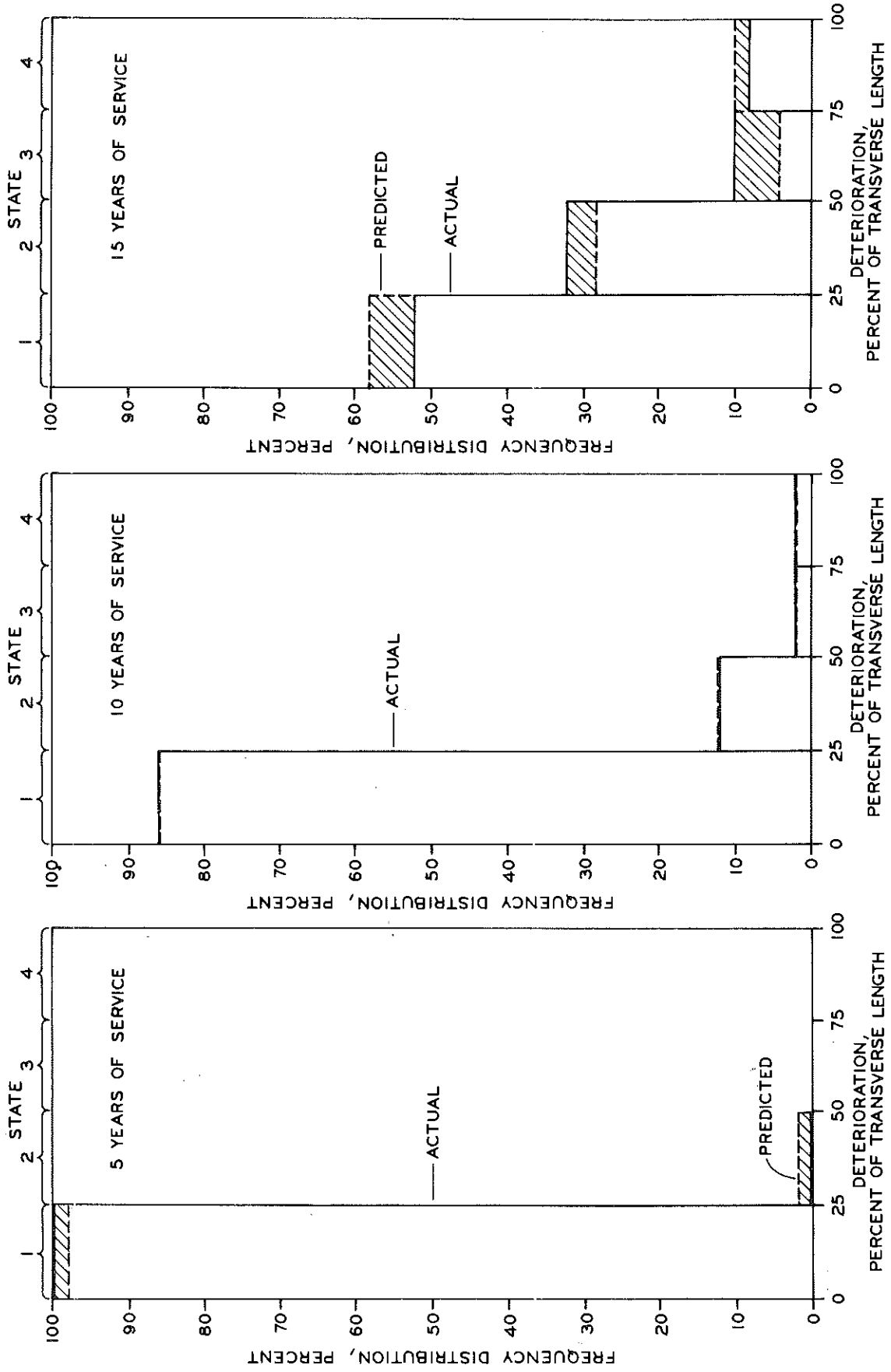

Figure 8. Joint deterioration histograms for three service periods.

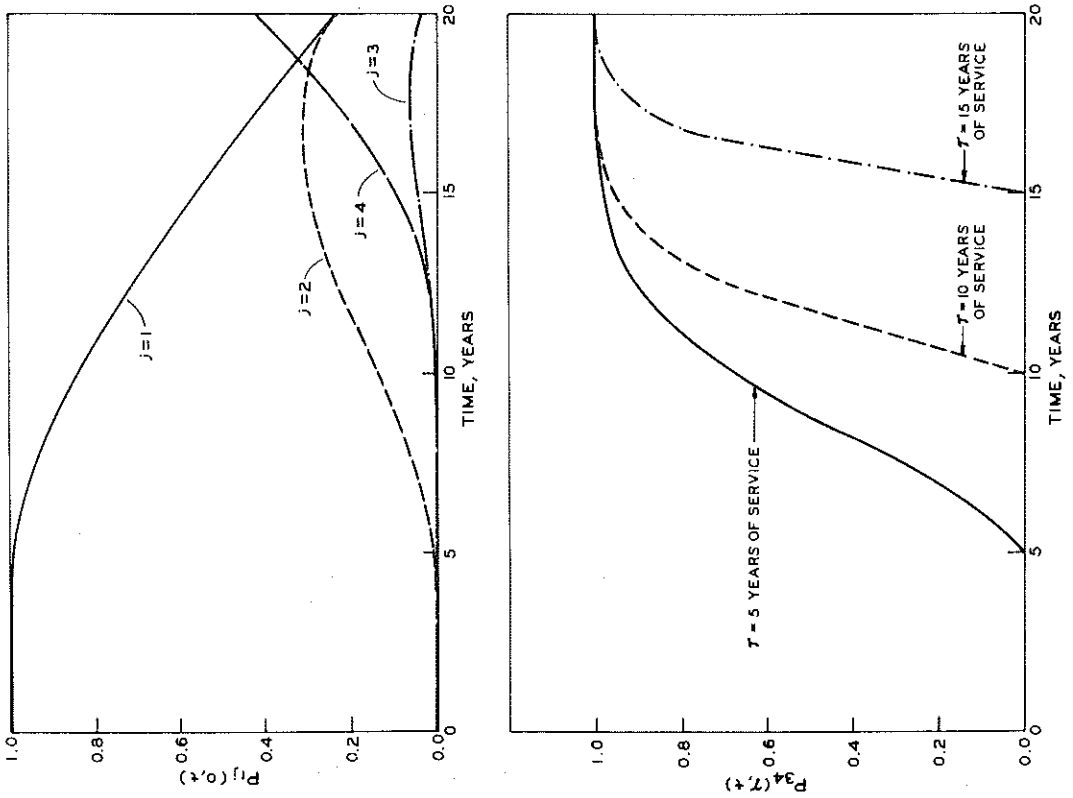

Figure 10. Probability of a joint passing from State 3 at time τ to State 4 at time t.

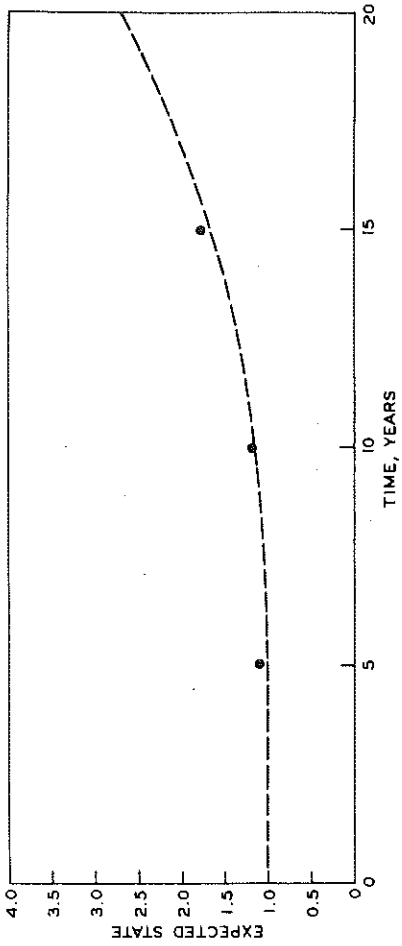

Figure 11. Joint deterioration, average state over time.

Figure 9. Joint deterioration state transition probability as a function of time.

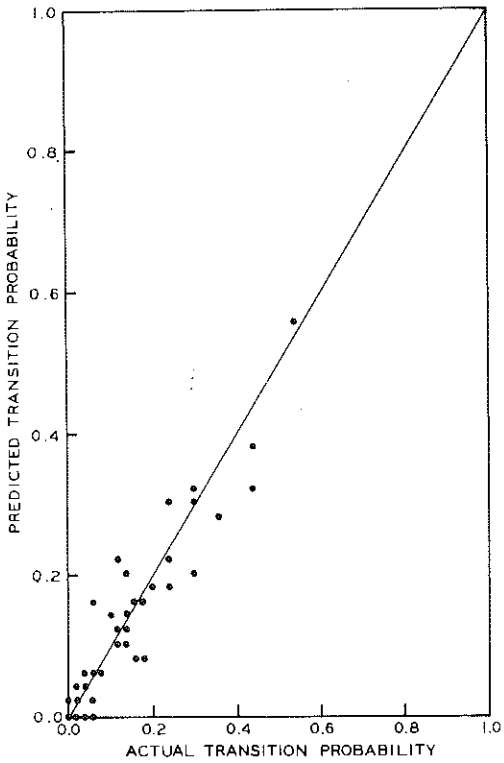

Figure 1. Relationship between actual and estimated cracking probability.

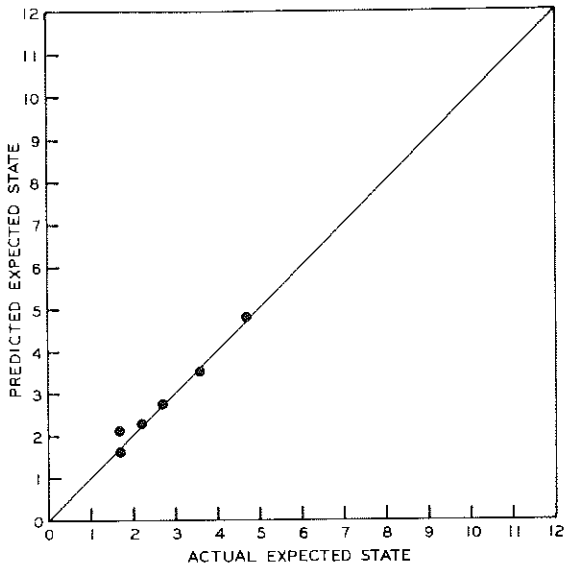

Figure 2. Relationship between actual and estimated average crack count.

Figure 3. Probability of crack States 1 and C over time.

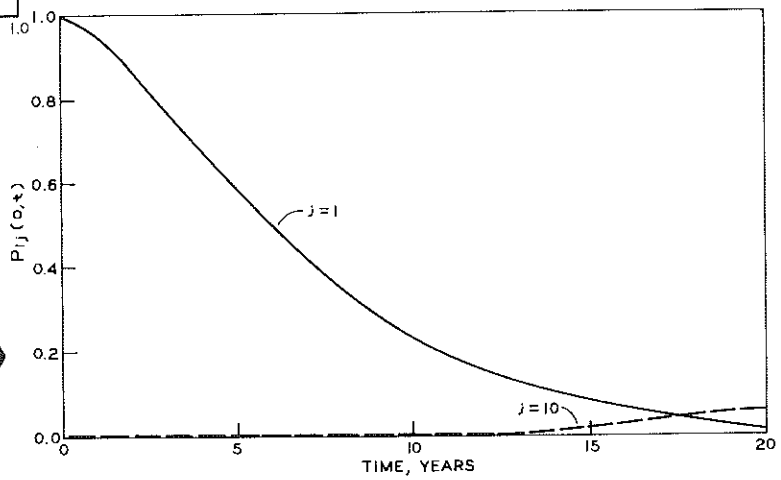

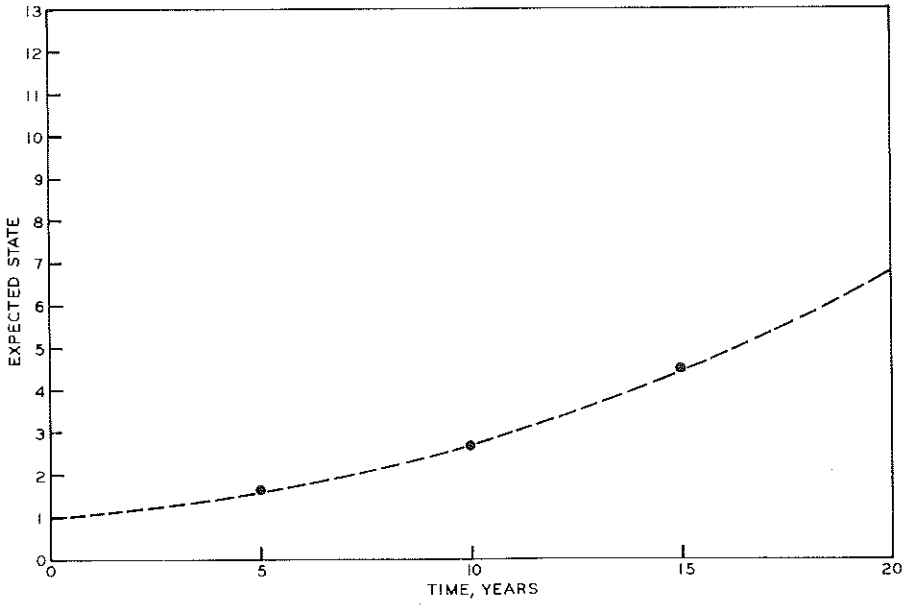

Figure 4. Average crack state over time.

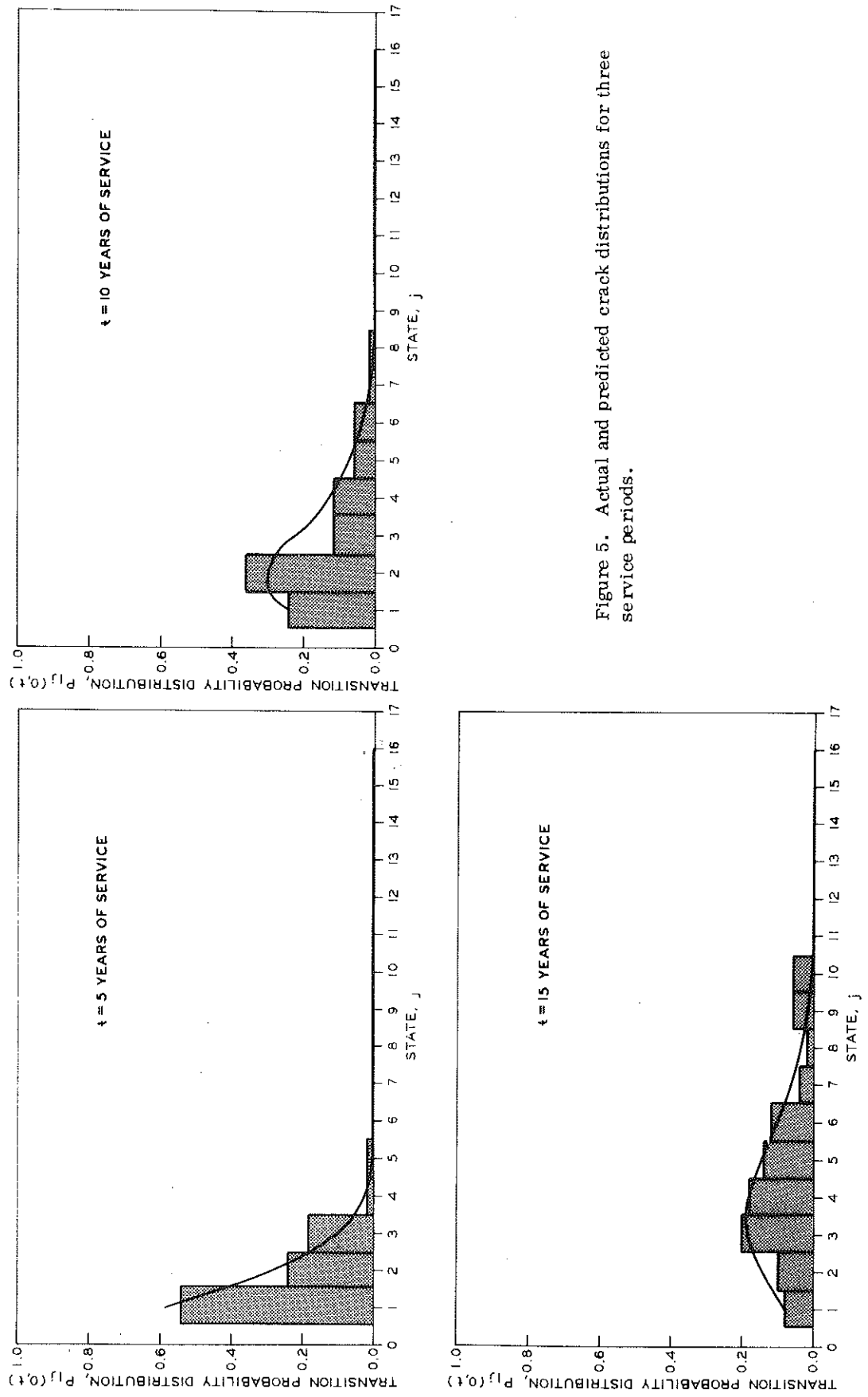

Figure 5. Actual and predicted crack distributions for three service periods.

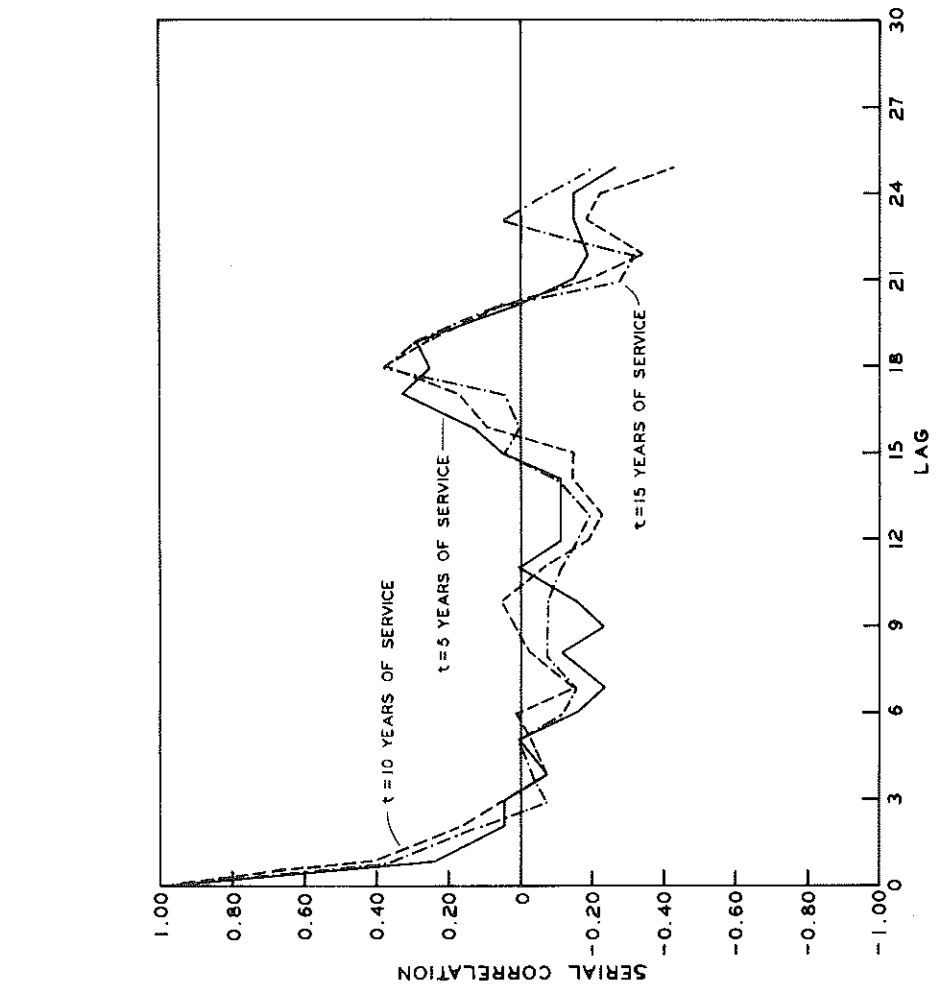

Figure 7. Crack autocorrelation plot for three service periods.

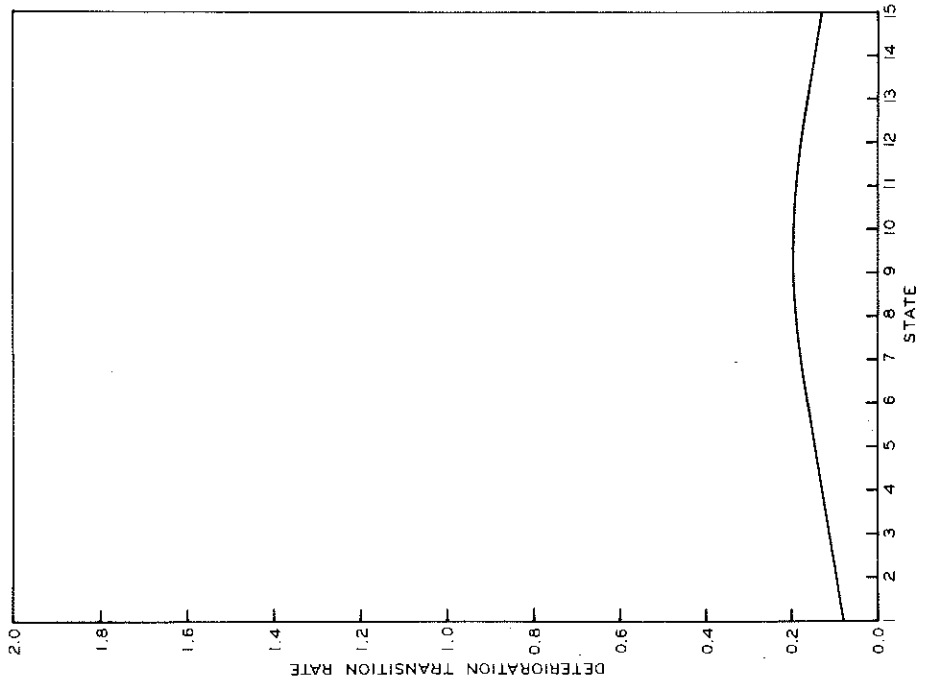

Figure 6. Crack state transition function.

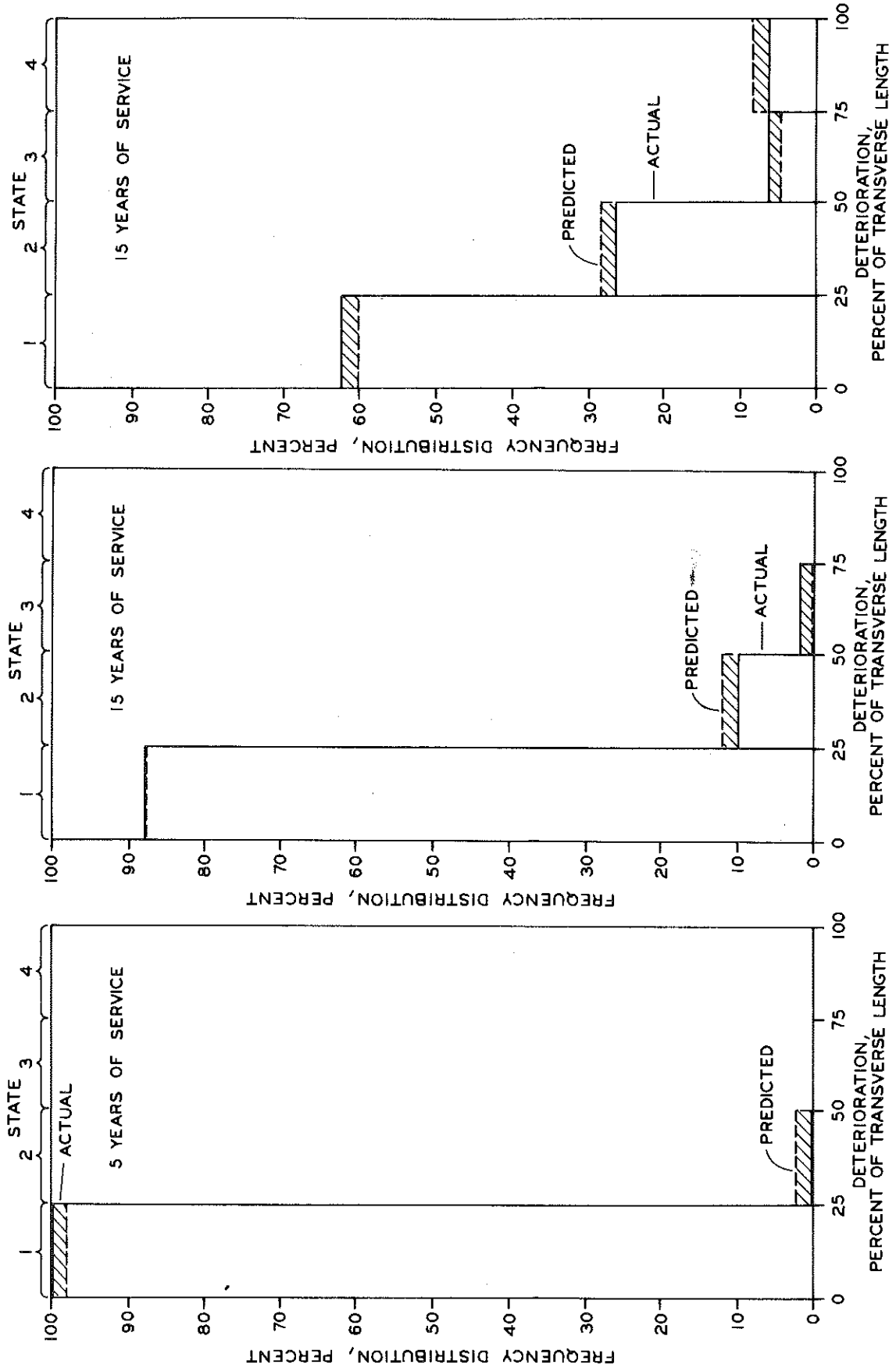

Figure 8. Joint deterioration histograms for three service periods.

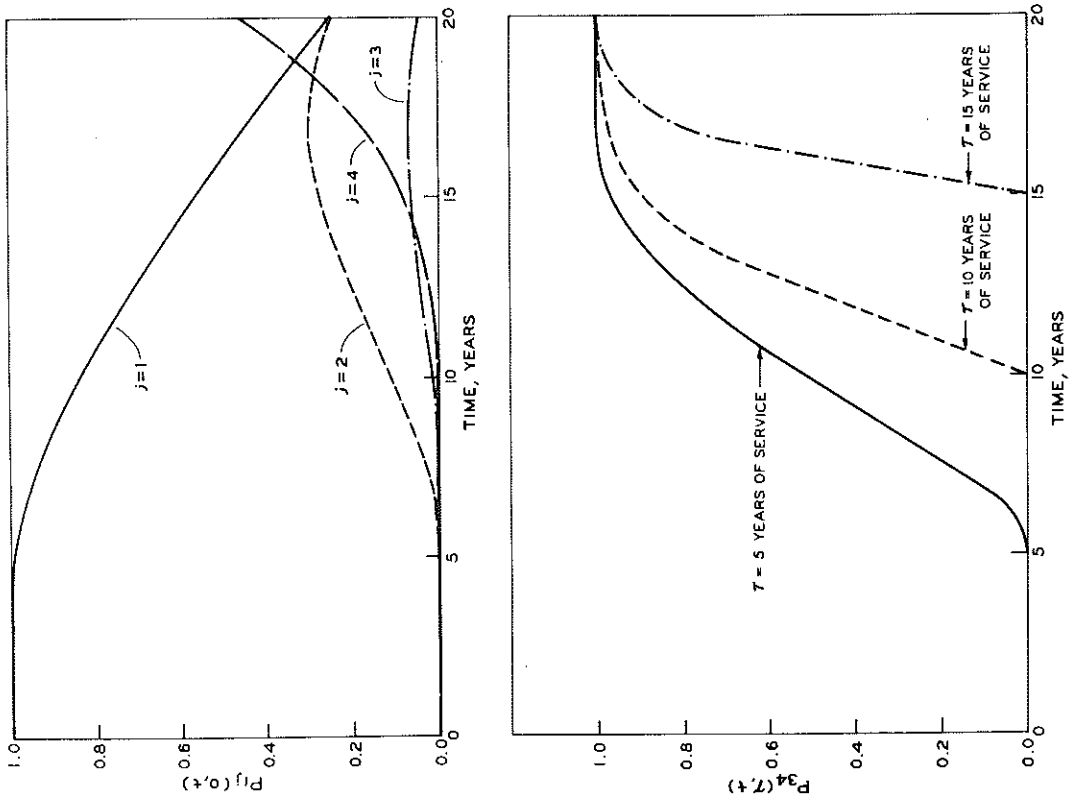

Figure 10. Probability of a joint passing from State 3 at time τ to State 4 at time t.

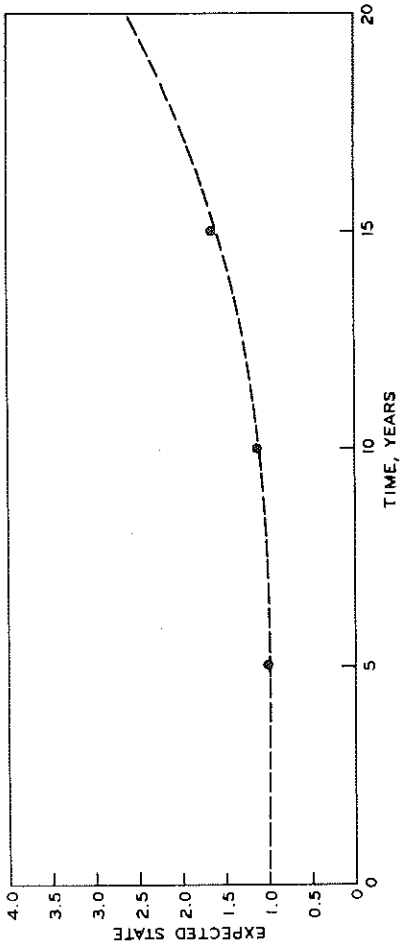

Figure 11. Joint deterioration, average state over time.

Figure 9. Joint deterioration state transition probability as a function of time.

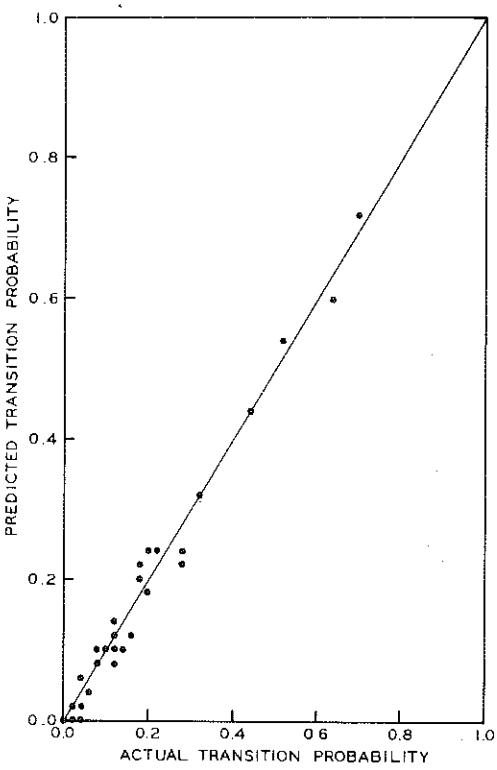

Figure 1. Relationship between actual and estimated cracking probability.

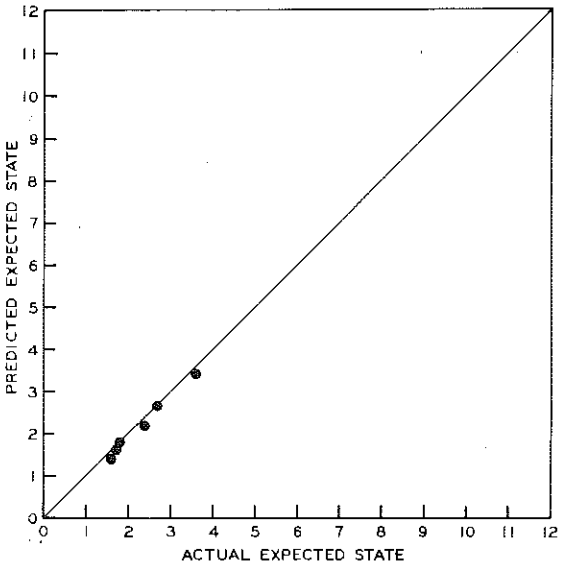

Figure 2. Relationship between actual and estimated average crack count.

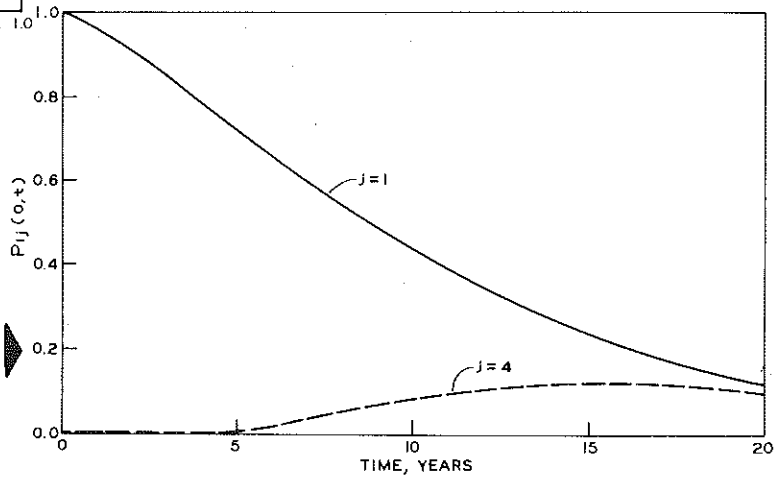

Figure 3. Probability of crack States 1 and C over time.

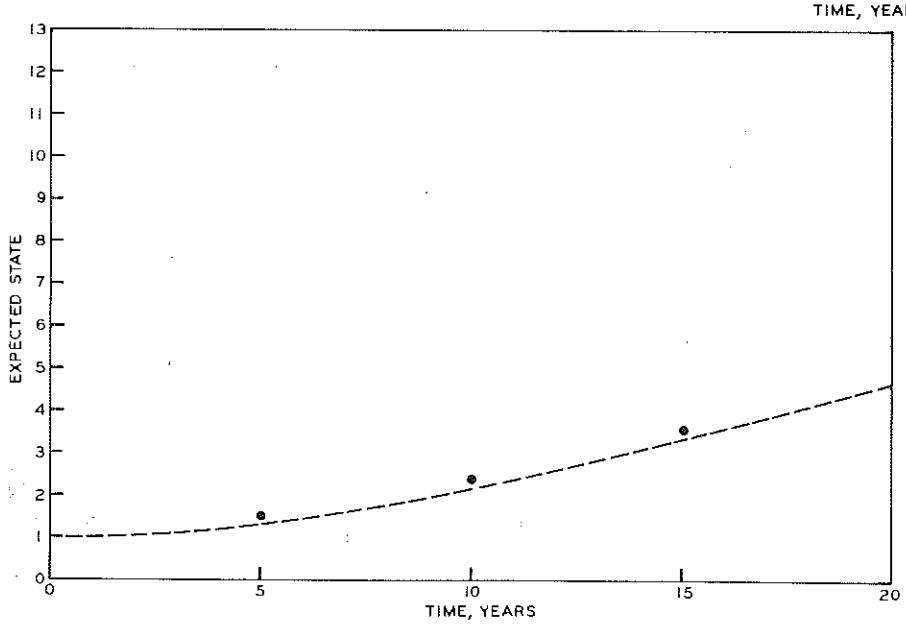

Figure 4. Average crack state over time.

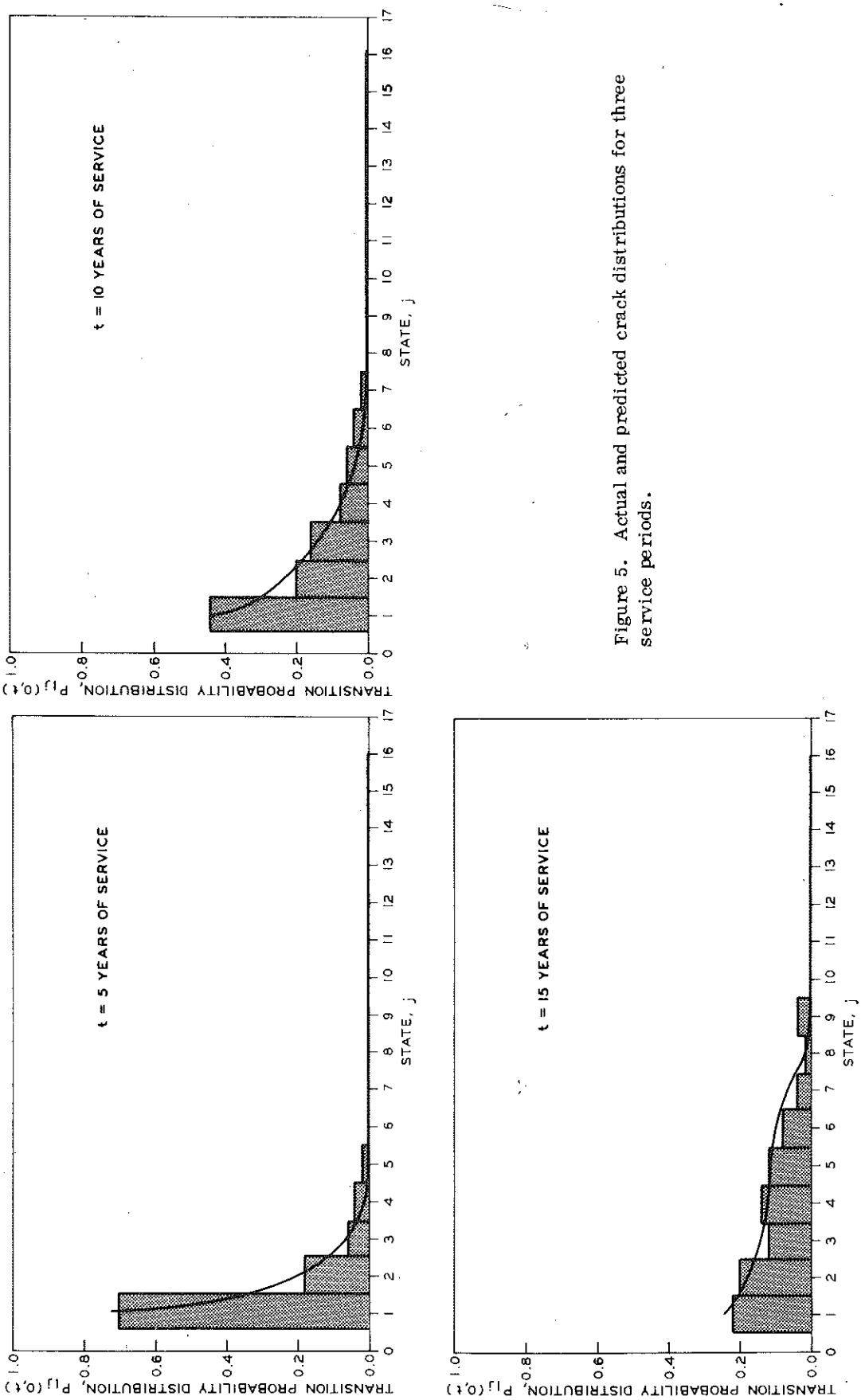

Figure 5. Actual and predicted crack distributions for three service periods.

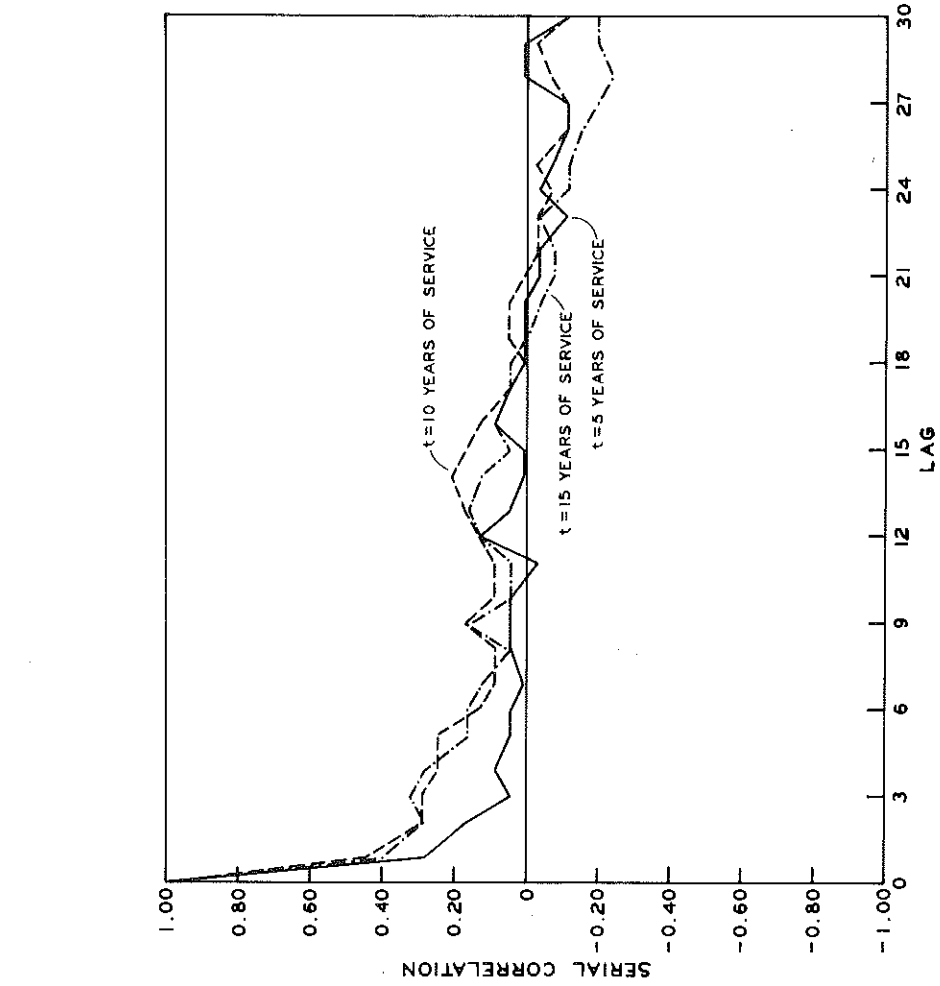

Figure 7. Crack autocorrelation plot for three service periods.

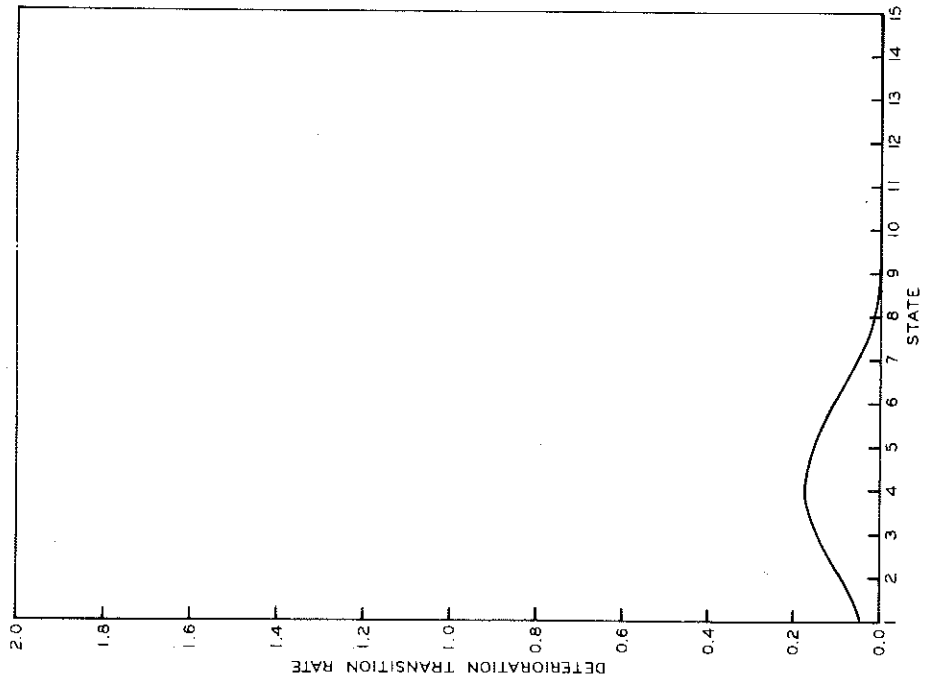

Figure 6. Crack state transition function.

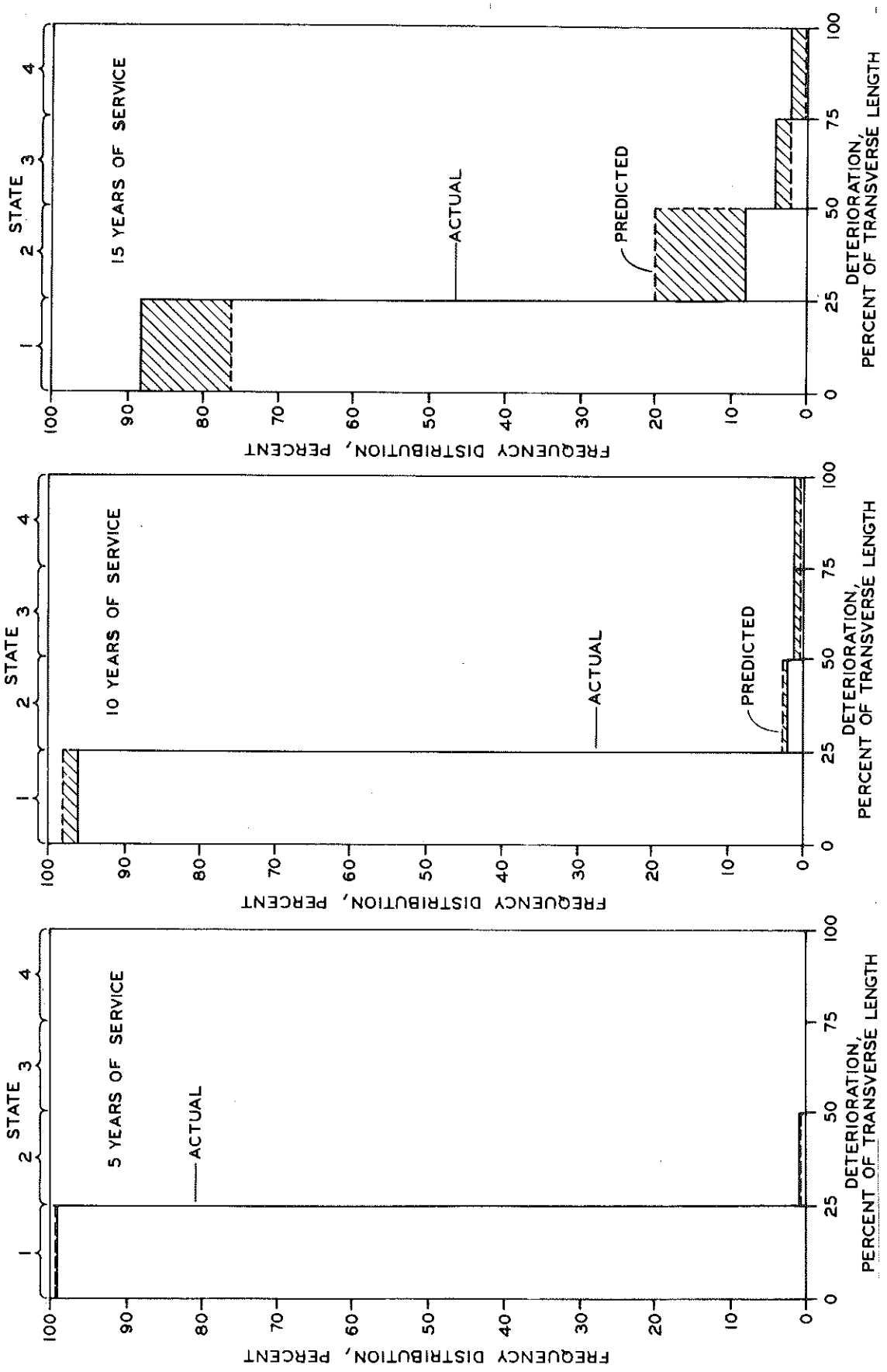

Figure 8. Joint deterioration histograms for three service periods.

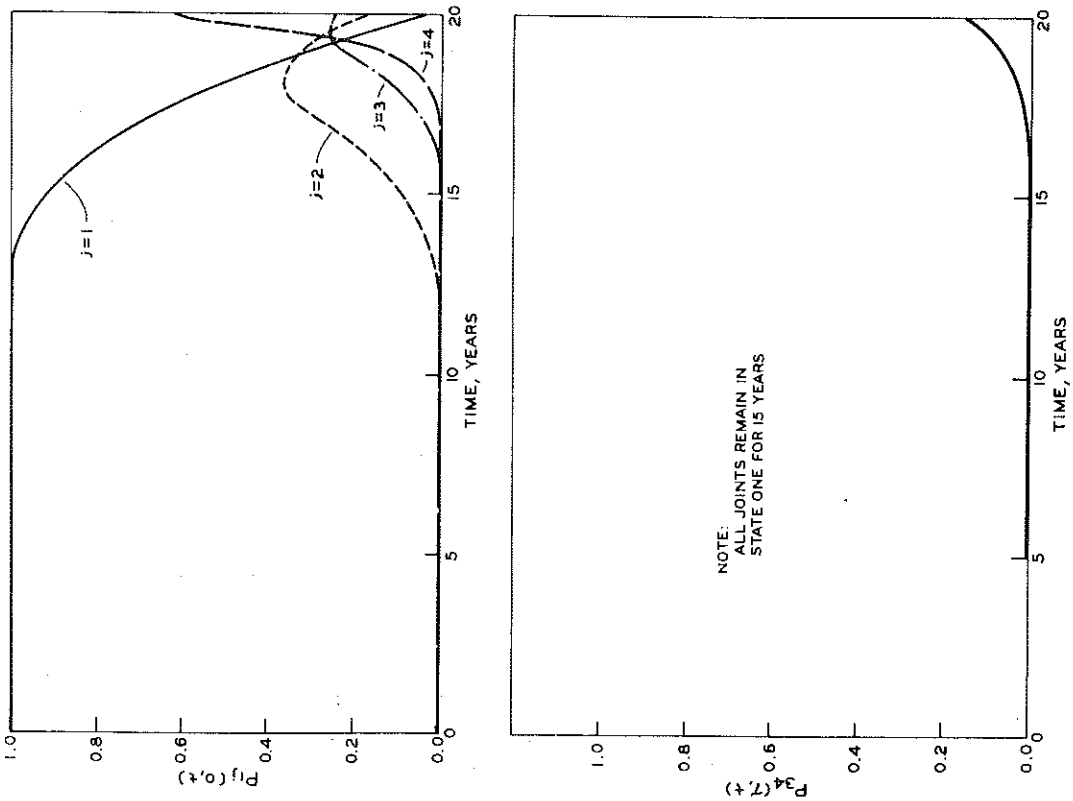

Figure 10. Probability of a joint passing from State 3 at time τ to State 4 at time t.

Figure 9. Joint deterioration state transition probability as a function of time.

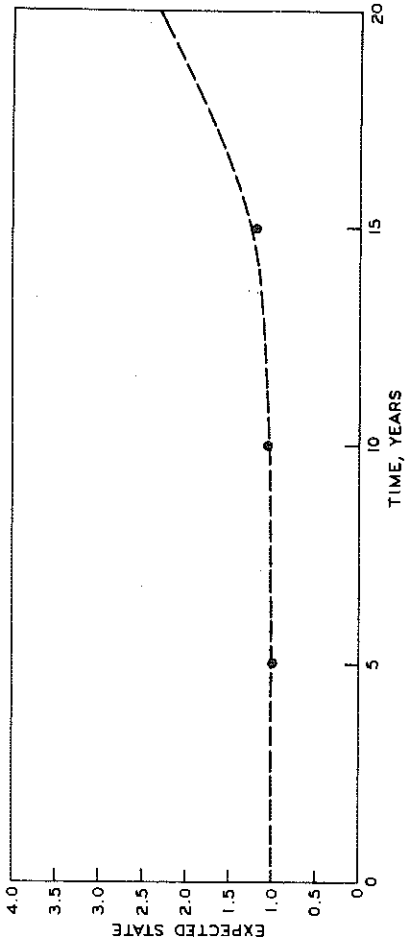

Figure 11. Joint deterioration, average state over time.